Hans Peter Dietz
Lennox P.J. Hoyte
Anneke B. Steensma

Atlas of Pelvic Floor Ultrasound

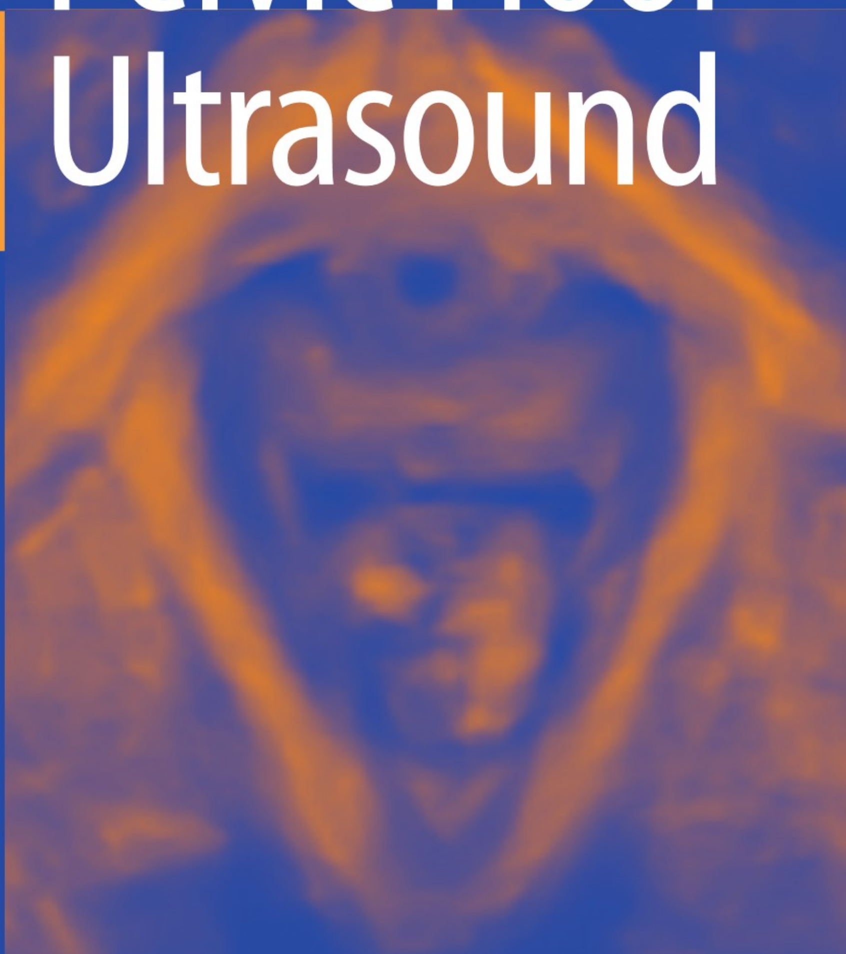

Springer

Atlas of Pelvic Floor Ultrasound

Hans Peter Dietz, Lennox P.J. Hoyte, and Anneke B. Steensma

Atlas of Pelvic Floor Ultrasound

Springer

Hans Peter Dietz, MD, PhD, FRANZCOG, DDU, CU
Associate Professor in Obstetrics and Gynaecology
University of Sydney
Nepean Clinical School
Penrith, NSW, Australia
http://www.med.usyd.edu.au/~pdietz/Site/Welcome.html

Anneke B. Steensma, MD
Gynaecologist
Department of Gynae-Oncology
Erasmus Medical Center
Rotterdam, The Netherlands

Lennox P.J. Hoyte, MD, MSEECS, FACOG
Assistant Professor of Obstetrics, Gynecology, and Reproductive Biology
Harvard Medical School
and
Staff Urogynecologist
Brigham and Women's Hospital
Boston, MA, USA

British Library Cataloguing in Publication Data
Dietz, Hans Peter
Atlas of pelvic floor ultrasound
1. Pelvic floor — Ultrasonic imaging — Atlases
I. Title II. Hoyte, Lennox P. J. III. Steensma, Anneke B.
617.5′507543′0222
ISBN-13: 9781846285202
ISBN-10: 1846285208

Library of Congress Control Number: 2006930109

Printed on acid-free paper

ISBN: 978-1-84628-520-2 eISBN: 978-1-84628-584-4

9 8 7 6 5 4 3 2 1

Springer Science+Business Media
springer.com

Foreword

Pelvic floor ultrasound is often described as a niche investigation within obstetrics and gynecology and even within gynecological ultrasound. After reading this book, I am convinced that it should be a mainstream investigation taught to all fellows and subspecialty trainees. Nothing should be of more importance to obstetricians and gynecologists than the protection of the pelvic floor of their patients and effective treatment when disorders arise. These disorders cause more prolonged and disruptive misery to patients than many of the conditions that clog up the waiting list in obstetrical and gynecological departments.

This book is more than an "atlas"; it is an education in the anatomy and dynamics of the lower urinary tract and pelvic floor and the investigation of disorders that occur, such as incontinence and prolapse. Ultrasound, despite its preeminence as an investigative tool in obstetrics and gynecology, has been slow to achieve such status in urogynecology, principally because the transvaginal ultrasound probe which is the standard tool in gynecologic scanning distorts the pelvic floor anatomy. This makes interpretation of prolapse impossible. It was the realization that perineal or translabial ultrasound provided equally good and artefact-free information on bladder dynamics and the integrity of the pelvic floor that a change in attitude occurred. However, many urogynecologists are still reluctant to supplement their multichannel recorders for urodynamic testing and X-ray video-cine-urethrography which were part of their training as junior doctors. The convincing images in this book must surely hasten the day when ultrasound becomes the standard technique in the investigation of pelvic floor problems.

Although this book contains an excellent chapter and images of MRI of the pelvic floor, it is the ultrasound techniques and images that predominate. This is not surprising because ultrasound has several advantages over competing imaging techniques; the equipment is readily available and most trainee gynecologists have experience in its use. Ultrasound is inexpensive, causes minimal discomfort to the patient, and can be used to study the dynamics of the pelvic floor in real time, for example bladder neck mobility. Furthermore, ultrasound is now entering an exciting new era of 3D imaging, which provides access to the axial plane, to study the levator hiatus and also, can create stunning tomographic 3D-rendered images of the complete pelvic floor.

Hans Peter Dietz has been working in this field for twenty years. He is one of the pioneers of transperineal/translabial ultrasound and is now the acknowledged expert in 3D/4D imaging of the pelvic floor. The images and text in this book are therefore based on his considerable experience in urogynecological investigation. Indeed, an invaluable chapter is a series of cases in which he presents the case history and report of fifteen patients, all with different clinical presentations of pelvic floor complications. It is in this section that the strength of ultrasound in investigation of incontinence and prolapse is convincingly demonstrated. Perhaps just one example (case number 10) will convince the reader that this is the technique of the present and future for such abnormalities. The case is of a woman referred nine months after a rotational forceps delivery, complaining of urgency, urge incontinence, sensation of prolapse and incomplete bowel emptying. Dr. Dietz's report is given below.

Findings:

2D: There was a postvoid residual of approximately 70 mL. The urethra appeared normal. We saw 44 mm of bladder neck descent on Valsalva, with the retrovesical angle opening up to 180°, 80° of urethral rotation, but no funneling. A cystocele descended to about 15 mm, below the symphysis; the uterus to 13 mm below. Detrusor wall thickness was normal at 3.5 mm. There was no defect of the rectovaginal septum.

3D: There was a major bilateral avulsion injury of the pubovisceral muscle, worse on the right, with complete loss of paragainal tenting. The hiatus measured more than 6 cm in the coronal plane, and the defects measured almost 3 cm in width. Although dimensions in the sagittal plane remained reasonable, the severe damage to levator insertions bilaterally caused marked ballooning of the hiatus to 43 cm squared.

Interpretation: Moderate cystocele with open RVA but no funnelling. Moderate uterine prolapse. Normal posterior compartment. Major bilateral avulsion defect of the pubovisceral muscle and severe ballooning. Marked risk of prolapse recurrence. . . . Her anterior compartment prolapse is probably incurable unless one uses mesh interposition. . . .

The case highlights several of the important advantages of ultrasound in the assessment of the pelvic floor. Ultrasound alone was able to identify the damage to the levator hiatus thus providing information on the risk of prolapse recurrence and the most appropriate treatment. Axial plane imaging has the potential to revolutionise our approach to pelvic floor problems. Dr. Dietz has established that if the levator hiatus enlarges to more than 35 cm^2 on Valsalva, (i.e., ballooning) then the degree of distention is associated with prolapse. Not only this, but ballooning is probably associated with recurrence after repair hence his advice on mesh interposition. It has been estimated that up to 50% of women have some degree of pelvic floor damage after vaginal birth. Dr. Dietz believes antenatal pelvic floor ultrasound will help to identify women at high risk of operative deliveries and significant pelvic floor damage. Ultrasound also provides audit of new surgical procedures to assess their effectiveness in providing for example durable and effective elevation of the bladder neck, and there is an excellent chapter on imaging of implant materials. Ultrasound is challenging conventional wisdom in many areas such as the need for hysterectomy as part of pelvic floor repair and the value of clinical examination in the assessment of prolapse.

Dr. Dietz and his colleagues must be congratulated for producing an instructive and challenging book that will be of value not just to trainees in urogynecology but to obstetricians, gynecologists, midwives, colorectal surgeons indeed all professionals concerned with the prevention and management of pelvic floor disorders. The stunning 3D images will I hope convince even the most conservative of professionals that ultrasound has a unique and important part to play in the investigation of pelvic floor disorders. In a way this book is just a start; the next step is to develop training programmes and obtain the latest equipment so that women can benefit from these recent advances. This book, however, is an important and necessary first step.

Stuart Campbell, DSc, FRCPEd, FRCOG

Preface

The increasing availability of ultrasound and magnetic resonance (MR) imaging equipment has, over the last decade in particular, triggered a renewed interest in diagnostic imaging in female urology and urogynecology. Although MR provides excellent resolution and contrast and is a wonderful tool for describing anatomy (as Lennox Hoyte will show), ultrasound has found more widespread use. This is attributable to cost and access issues, but also because ultrasound offers a degree of dynamic imaging that is not currently achievable by MR. Ultrasound, at least in the form of two-dimensional (2D) B mode real-time sonography, is almost universally available and provides for real-time observation of maneuvers such as Valsalva and pelvic floor muscle contraction. This is of great importance when assessing pelvic floor anatomy and function because maneuvers enhance the visibility of structures and help uncover defects.

A number of different sonographic approaches have been used for lower urinary tract and pelvic floor imaging. From the 1980s onward, transabdominal,[1,2] perineal,[3,4] transrectal,[5] and transvaginal ultrasound[6] have been investigated for use in women with urinary incontinence and prolapse. Because of its noninvasive nature, ready availability, and the absence of distortion, perineal or translabial ultrasound is currently used most widely. However, most of the text in this volume (and many of the images) will also apply and be useful to colleagues more familiar with introital ultrasound, a method that generally uses transducers designed for intravaginal use, by placing them in the vestibule of the vagina.

One of the advantages of translabial or perineal ultrasound is that it allows the use of standard curved array transducers designed for abdominal and obstetric imaging. Another is the fact that the characteristics of such transducers usually permit imaging of the entire levator hiatus. This includes the anorectum, allowing us to finally see beyond the confines of our respective specialties. Pelvic floor morbidity encompasses urologic, gynecologic, and colorectal abnormalities, and modern imaging may well come to be a factor that leads to a closer integration of those three specialties. Colorectal pelvic floor imaging is still in its infancy, with sphincter assessment the only area that has developed beyond the experimental stage at present, but hopefully Anneke Steensma's chapter will help demonstrate the potential of sonography in this field.

The development of 3D ultrasound has opened up entirely new diagnostic possibilities in pelvic floor imaging, not the least because it has given us access to the axial plane, i.e., the plane of the levator hiatus. First attempts at producing 3D-capable systems go back to the 1970s when the processing of a single volume of data would have required 24 hours of computer time on a system large enough to fill a small room. Such data processing is now possible on a laptop computer, and in real time. The advent of volume ultrasound has also allowed the use of rendering techniques for contrast enhancement and speckle reduction. As a result, resolutions in all potential planes have improved markedly over the last few years and we have made great progress in evaluating pelvic floor function and trauma. Transvaginal and translabial techniques of 3D ultrasound allow higher frequencies, and although they suffer from a restricted field of view, resolution can potentially be much higher. It is likely that there will be significant development of this field in the next few years.

We have no evidence that modern imaging techniques improve patient outcomes in pelvic floor medicine, and it would be a major challenge to try to conduct a trial to prove or disprove such a hypothesis. However, this is also the case for the other main diagnostic method in urogynecology, i.e., multichannel urodynamics. In the meantime, it is evident that any diagnostic method is only as good as the operator behind the machine, and we all know that diagnostic ultrasound is particularly operator dependent. We all carry a responsibility to ensure that diagnostic methods are used appropriately, and for a field as recent as pelvic floor ultrasound, this implies that teaching is of paramount importance.

The volume you hold in your hands is designed with these thoughts in mind. We would like it to be a resource for all those using or intending to use ultrasound in the investigation of women with pelvic floor and lower urinary tract dysfunction, i.e., with urinary incontinence, voiding dysfunction, recurrent urinary tract infections, and prolapse, and it may also be of interest to those dealing with anorectal dysfunction. Its original purpose was to provide a companion volume for courses in pelvic floor imaging. The integration of 4D View software and volume data for offline analysis, made possible by the support of GE Medical Ultrasound, should provide the beginner with a simple and convenient means to train pattern recognition and quantitative analysis.

We have taken great care to provide as much original imaging material as was possible within the limits of the format, but it is recognized that this field is in rapid development. There is no doubt that we will be able to do much better in the future, and the authors would like to invite all readers to accompany us on this journey.

Hans Peter Dietz
Sydney

References

1. White RD, McQuown D, McCarthy TA, Ostergard DR. Real-time ultrasonography in the evaluation of urinary stress incontinence. Am J Obstet Gynecol 1980;138(2):235–237.

2. Bernaschek G, Spernol R, Wolf G, Kratochwil A. Comparative determination of the vesico-urethral angle in incontinence via ultrasound and lateral urethrocystogram (author's transl). Geburtshilfe Frauenheilkd 1981;41(5):339–342.
3. Grischke EM, Dietz HP, Jeanty P, Schmidt W. A new study method: the perineal scan in obstetrics and gynecology. Ultraschall Med 1986;7(4):154–161.
4. Kohorn EI, Scioscia AL, Jeanty P, Hobbins JC. Ultrasound cystourethrography by perineal scanning for the assessment of female stress urinary incontinence. Obstet Gynecol 1986;68(2):269–272.
5. Bergman A, McKenzie CJ, Richmond J, Ballard CA, Platt LD. Transrectal ultrasound versus cystography in the evaluation of anatomical stress urinary incontinence. Br J Urol 1988;62(3):228–234.
6. Quinn MJ, Beynon J, Mortensen NJ, Smith PJ. Transvaginal endosonography: a new method to study the anatomy of the lower urinary tract in urinary stress incontinence. Br J Urol 1988;62(5):414–418.

Contents

1

Live Anatomy of the Pelvic Floor: An MRI Perspective

Lennox P.J. Hoyte

The pelvic floor consists of a set of soft tissue structures, supported by a group of muscles, which are in turn attached to a bony framework. The soft tissues are attached to each other and the bony framework by condensations of fascial and fibromuscular tissues. This chapter will briefly review contemporary understanding of these structures and their anatomic relationships.

Following this review, the magnetic resonance (MR)-based two-dimensional (2D) and three-dimensional (3D) anatomy of the pelvic floor structures will be presented and reviewed.

Pelvic Floor Anatomy: Overview

An overview of the 3D pelvic anatomy is shown in Figure 1.1, where lithotomy, sagittal, and posterior views of the pelvic structures are demonstrated. These images were derived from a single, T2-weighted isotropic MR acquisition, with the individual structures manually segmented and rendered. The subject was a 24-year-old asymptomatic nullipara who was scanned in the supine position. These images demonstrate the levator ani muscle complex supporting the rectum, vagina, and bladder and urethra. The most caudal portion of the levator ani muscle (the puborectalis portion) attaches to the pubis near the lateral aspects of the symphysis bilaterally. The more cranial aspects of the levator ani (the iliococcygeus portion) attaches bilaterally to the obturator internus fascia, up to the level of the ischial spines. The most inferior part of the levator ani (puborectalis portion) merges with the external anal sphincter. The most dorsal part of the levator ani (the pubococcygeus portion) attaches to the distal sacrum at the coccyx. These soft tissues are all enclosed within the framework of the bony pelvis, which forms a scaffold from which the muscles and organs are suspended. The specific anatomic relationships will now be reviewed in more detail.

Bony Pelvis

The bony pelvis consists of four bones: the ilium, ischium, pubis, and sacrum. These are connected by three principal joints, namely, the symphysis pubis, and two sacroiliac joints, further held in place by several

A

B

Figure 1.1. Multiple views of the MR-based 3D anatomy of the female pelvic floor structures. Pelvic bones, white; obturator internus, rose; levator ani, brown; urethra, dark yellow; bladder, light yellow; vagina, pink; rectum, blue; symphysis and coccyx, gray. **A** Dorsal lithotomy view: The pelvic bones enclose the obturator internus muscles, and the urethra, vagina, and rectum can be seen exiting from the levator hiatus anteriorly. **B** A left lateral view, bones and obturator internus removed: The levator ani muscles can be seen supporting the rectum, vagina, and urethra/bladder.

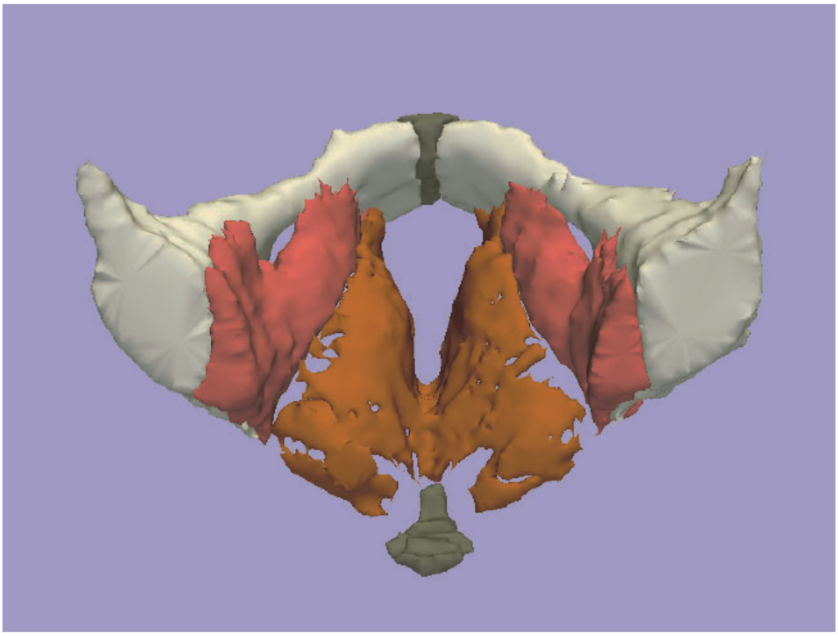

C

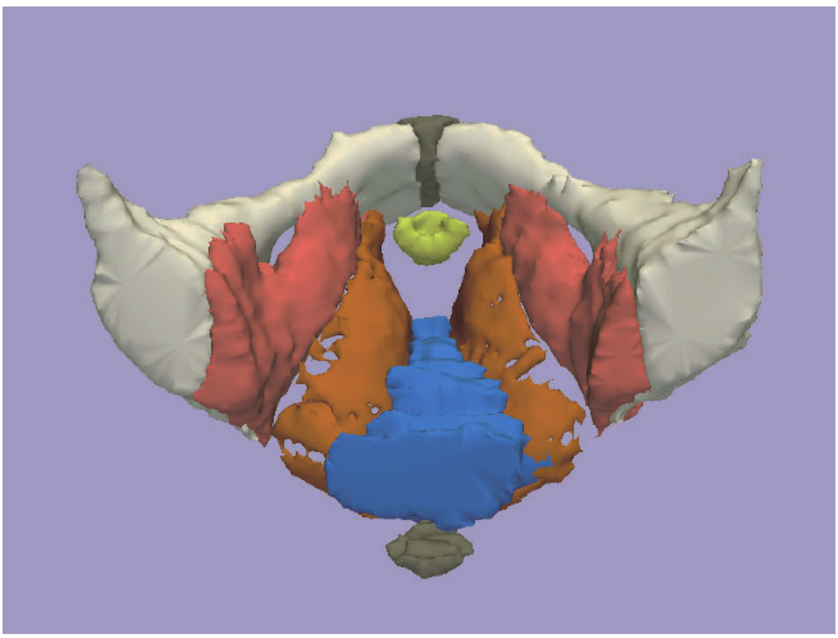

D

Figure 1.1. C A posterior-superior view: The pelvic bones are lined medially by the obturator internus muscles, which overlie the obturator foramen. The anteriormost portion of the levator is the puborectalis portion, and it attaches bilaterally to the pubic bones. The posterior portion of levator ani is the iliococcygeus, and it is suspended from the obturator internus fascia bilaterally, along a condensation called the arcus tendineus levator ani, which courses from the anterior pelvis to the ischial spines bilaterally. Both halves of the levator ani come together in the midline to form a "sling" which supports the pelvic structures. **D** Posterior-superior view: The rectum rests in a midline groove in the levator ani complex.

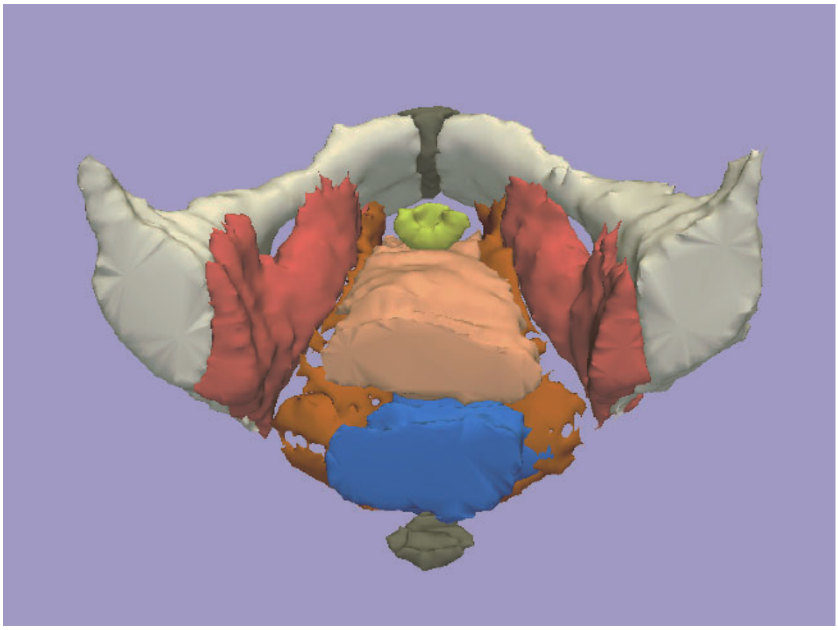

E

F

Figure 1.1. E Posterior-superior view: The vagina is suspended across the midline, attached partly to the levator ani anteriorly, and to the obturator internus fascia posteriorly. The attachment is called the arcus tendineus fascia pelvis. The apex of the vagina is supported by the uterine cervix and the uterosacral ligaments (not shown). The urethra is fully supported by the anterior vaginal wall. **F** Posterior-superior view: The vagina is seen supporting the bladder. Defects in the vaginal supports can lead to descent of the bladder and urethra.

ligaments, including the sacrospinous, sacrotuberous, posterior sacrococcygeal, and sacroiliac ligaments. In the standing position, the bony pelvis is oriented such that the pelvic brim is obliquely oriented, and the inferior pubic rami are parallel to the ground.

Muscular Pelvis

The bony pelvis is lined bilaterally by the obturator internus muscles, which overlie the obturator foramina, inserting distally into the superior and inferior pubic rami, and exiting the pelvis posteriorly proximal to the sacrospinous ligament, to attach to the greater trochanter of the femurs bilaterally. The obturator internus muscles are lined medially by the obturator internus fascia.[1] The iliococcygeus portions of levator ani attach bilaterally to the obturator internus fascia, along a connective tissue condensation called the arcus tendineus levator ani, which goes from the pubic bone anteriorly to the ischial spine posteriorly.[1,2] The medial portions of the iliococcygeus muscles meet in the midline to form the proximal part of the levator plate. The puborectalis and pubococcygeus portions of levator ani (also termed the "pubovisceral muscle") attach anteriorly to the pubic bones bilaterally, and course around the bladder, vagina, and rectum in a sling-like manner to converge in the distal posterior midline as the distal levator plate.[2–4] The distal aspect of the levator plate merges with fibers from the external anal sphincter, whereas the proximal part of the levator plate attaches to the distal sacrum and coccyx in the midline. Thus, the puborectalis forms a sling near the junction of the rectum and external anal sphincter, and will pull this junction anteriorly when it is contracted, thus sharpening the anorectal angle. The levator ani complex is itself covered by a fascial layer superiorly and inferiorly, known as the superior and inferior fascia of levator ani, respectively.

The Soft Tissue Pelvis

The organs of the female pelvic floor include the bladder and urethra, the vagina, the rectum, and the uterus.

Bladder/Urethra

The bladder/urethra complex rests on top of the vagina. The bladder is a muscular reservoir that stores urine for later emptying at appropriate times. It consists of the detrusor smooth muscle, whose outer lining is composed of an adventitia and serosa, which covers its dome. Outer and inner layers of the detrusor muscle are generally longitudinal, with an intervening circular layer. The inner lining of the bladder is made up of a submucosa and transitional epithelium. Near the bladder neck, some fibers of the distal detrusor loop around and attach to the pubic bones and pelvic walls, forming the pubovesical muscles.[5] In the distal posterior aspect of the bladder, the trigone can be seen as a visible triangular area, bounded by the bilateral ureteric orifices proximally, and the bladder neck distally. The muscle fibers in this area are from a specific group, of a separate embryologic origin to the rest of the detrusor. These fibers merge above with the ureteric musculature, and below with the dorsal smooth muscle of the urethra.[6,7] The urethra is a complex multilayered muscular tube, responsible for controlling the storage and emptying functions of the bladder. The proximal third of the urethra is easily separable from the underlying vagina, but the distal portion is fused with the anterior vaginal wall.[5] The urethral components are organized in such a way as to allow its lumen to be closed or opened according to the need to store urine or to void. The outermost layer of the urethra consists of circular striated muscle from the urogenital sphincter. In its proximal aspect, this muscle is oriented in a circular manner around the urethra. More distally, this muscle is present over the anterior aspect of the urethra, but travels posteriorly and laterally to reach around the vagina (the urethrovaginal sphincter) and to the inferior pubic rami (compressor urethrae), respectively. This muscle consists primarily of slow twitch fibers,[8] ideally suited to maintaining resting closure tone to the urethra. Voluntary constriction can further increase closure pressure to compensate for periods of increased intravesical pressures, as can occur during a cough or Valsalva. Muscle blockade studies suggest that this muscle is responsible for up to one third of total urethral closure pressure.[9] The urethra also has a layer of smooth muscle, consisting of an inner longitudinal portion contiguous with, but embryologically distinct from, the detrusor and trigone, as well as an outer circular portion. This smooth muscle lies inside of the circular striated layer, and covers the proximal four fifths of the urethra. The urethra also contains an inner mucosal lining together with a rich, hormone-sensitive submucosal vascular plexus, which contains specialized arterio-venous anastomoses,[7] with venules that can be inflated or deflated depending on blood flow, thus influencing the coaptation of the urethral lumen. The urethral tissues are held together with a network of connective tissue, consisting primarily of collagen and elastin fibers, suggested by some to also contribute to the urethral closure mechanism.[7]

Vagina

The vagina is a fibromuscular tube that is suspended across the midline from the pelvic sidewalls, where it is attached on each side by a condensation of connective tissue called the arcus tendineus fasciae pelvis.[10] The most proximal aspect (or apex) of the vagina is suspended in a superio-posterior direction by the cervix in the midline, and the uterosacral ligaments bilaterally. Delancey[10] identified three levels of support for the vagina, which he named Levels I, II, and III. Level I consists of the apical or proximal support which attaches the upper vagina to the ischial spines and the uterosacral ligaments. Level II comprises the lateral, or paravaginal supports, in which the vagina attaches laterally to the puborectalis fascia anteriorly, and the obturator internus fascia posteriorly. Level III is the distal support, where the vagina is attached laterally to the puborectalis, and perineal body. The vaginal supports at each level combine to keep the vagina suspended across the midline, allowing it to support the organs anterior to it. The bladder and urethra lie on, and are supported by, the anterior wall of the vagina. In its undamaged state, the vagina can be thought of as a trampoline upon which rests the urinary bladder and urethra. Vaginal support is integral to maintaining the position of the bladder and urethra, and is thought to be a key component of the urinary continence mechanism. The distal rectum lies behind the posterior vaginal wall. It is separated from the vaginal wall by a fibromuscular layer called Denonvilliers fascia. The innermost mucosal layer of the vagina is a nonkeratinized squamous epithelium, and this is overlaid by a fibromuscular layer.

Rectum

The rectum rests on the levator plate, in a hollowing in the midline. The distal rectum feeds into the sphincter complex of the anal canal, formed by the smooth muscle of the internal sphincter, and the striated muscle of the external anal sphincter. The puborectalis portion of the levator ani muscle loops around the anorectal junction, and contraction of the intact puborectalis muscle can markedly sharpen the angle of the anorectal junction.

Connective Tissue Attachments in the Pelvis

The "investing" layer of the pelvic floor structures is called the "endopelvic fascia," and it attaches the pelvic organs to the pelvic sidewalls. This tissue is not a fascia in the sense of the anterior rectus sheath, but instead consists of a combination of blood vessels, nerve bundles, and fibrous connective tissues that provide mechanical support, as well as blood and nerve supply to the organs of the pelvic floor.[10–12] On either side, the endopelvic fascia can be thought of as a sheet, which drapes over the uterus and vagina, and attaches these organs to the pelvic sidewall. That portion of the tissue that attaches the uterus is called the parametrium, and the part that attaches the vagina is called the paracolpium. The cardinal, Mackenrodt's, and uterosacral ligaments are the familiar terms used to describe the condensations of this tissue that invest and connect the uterus and upper portions of the endopelvic fascia.[13,14] The structure referred to as the uterosacral ligament is but the most medial aspect of this condensation of the endopelvic fascia. This endopelvic fascia contains an elastic component, which can be readily appreciated by the movement engendered by placing downward traction on the cervix in a healthy woman. Upon release of the traction, the cervix returns to its original position. The inelastic component is appreciated as the resistance to further stretch at the limits of elasticity.

Disruption in this endopelvic fascia is said to lead to prolapse of the different parts of the vagina.[15] Defects in the anterior vaginal wall may lead to anterior wall prolapse (also called cystocele), whereas posterior wall defects may lead to posterior wall prolapse (rectocele). Apical defects (i.e., in the uterosacral ligaments or upper paracolpium) may lead to vaginal vault or uterine prolapse.

MR Anatomy of the Female Pelvis

The remainder of this chapter will review the 2D MR anatomy in different planes, and at different levels in the pelvis. The subject was a 24-year-old asymptomatic nullipara, who was scanned in the supine position, using the isotropic, T2-weighted protocol discussed at the beginning of the chapter. Nulliparous anatomy will be shown in the axial, sagittal, and coronal planes, after which examples of anatomic changes in the primiparas will be presented.

Nullipara: Axial Plane

The axial MR anatomy is presented in Figures 1.2–1.6. Figure 1.2A shows the 2D MR axial image at the level of the distal urethra. Figure 1.2B shows the labeled outlines of the structures visible at this level. The next MR image was taken more cephalad, showing the MR anatomy at the mid urethra (Figure 1.3A,B), in a similar sequence from left to right. At this level, the thickened, periurethral striated muscle is seen, more pronounced anteri-

A

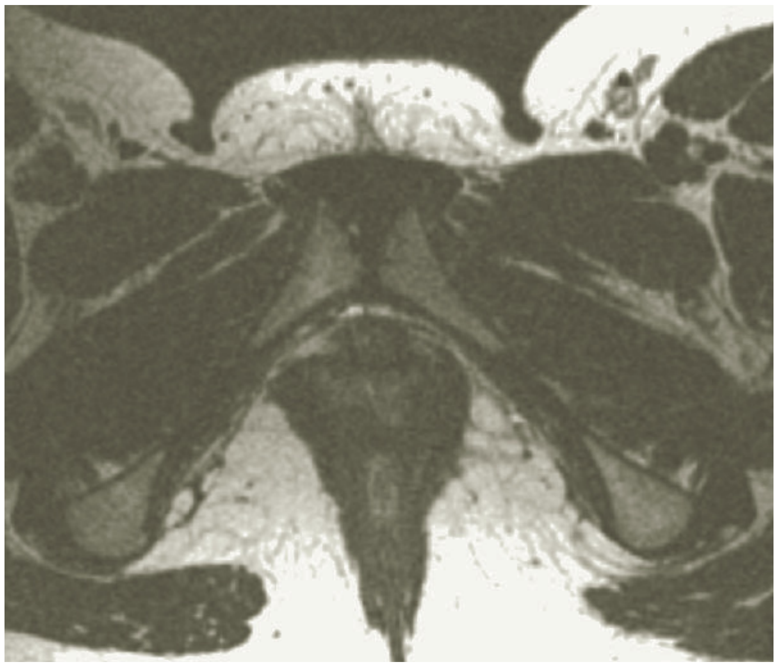

B

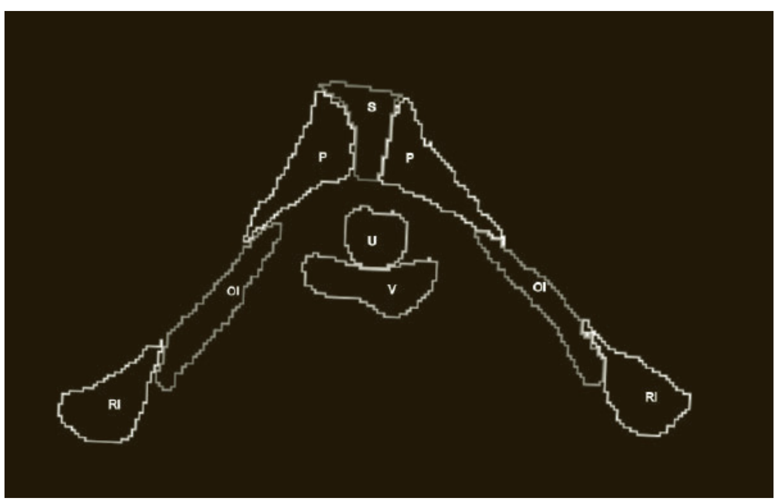

Figure 1.2. Axial MR view of the female pelvic floor structures at the level of the distal urethra. *Note:* For Figures 1.2–1.15, the labels represent the following: P, pubis; S, symphysis; U, urethra; V, vagina; OI, obturator internus; RI, ramus of the ischium; R, rectum; I, ischium; B, bladder; C, coccyx.

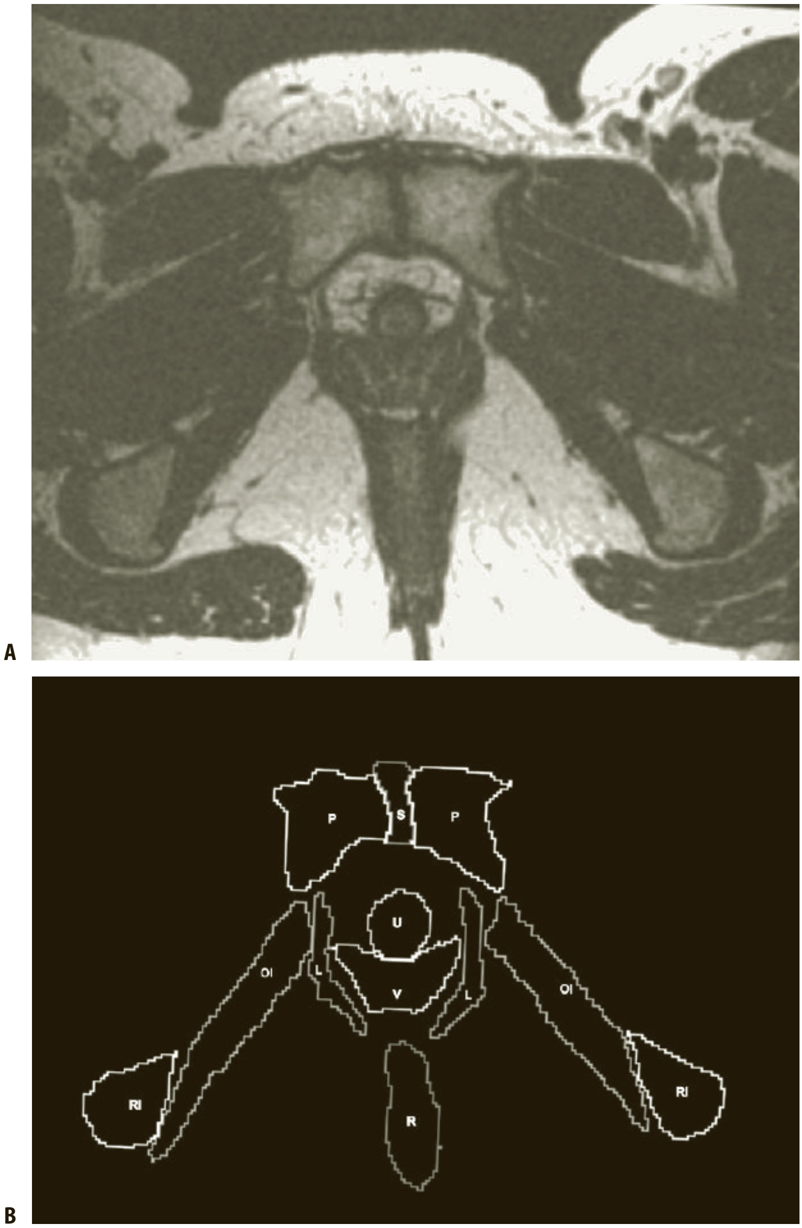

Figure 1.3. Axial MR views of the female pelvic floor structures at the mid urethra. The urethra can be seen centrally under the symphysis (yellow outline). The thickened anterior aspect of the urethra represents the circumferential striated urethral sphincter muscle, which is thickest at mid urethra. The inferior aspect of the puborectalis muscle is seen as it attaches bilaterally to the pubic bone at the level of the symphysis anteriorly, and merges with the fibers of the external anal sphincter posteriorly. The vagina is attached bilaterally to the medial puborectalis muscle, along the arcus tendineus fascia pelvis.

orly, and the vagina is seen supporting the urethra. The bladder neck anatomy is shown next (Figure 1.4A,B). At this level, the bladder is seen being supported by the anterior vaginal wall, itself pulled bilaterally to the pelvic sidewalls. The bladder and mid vaginal anatomy is shown next

Figure 1.4. Axial MR views of the female pelvic floor structures at the level of the bladder neck. The bladder neck (yellow outline) can be seen centrally under the symphysis. The area just above the bladder neck is the muscle wall of the anterior bladder. The junction of the puborectalis and iliococcygeus muscles is seen attaching partially to the superior pubic bone, and laterally to the obturator internus. Posteriorly, the puborectalis portion merges with fibers of the external anal sphincter. At this level, the levator ani complex cradles and supports the attachment of the vagina, which in turn supports the bladder neck.

(Figure 1.5A,B). Here, the bladder can be seen supported by the vagina, itself pulled bilaterally toward the pelvic sidewall. The anatomy at the level of the ischial spines is given in Figure 1.6, demonstrating the attenuation of the iliococcygeus as it moves posteriorly and cranially.

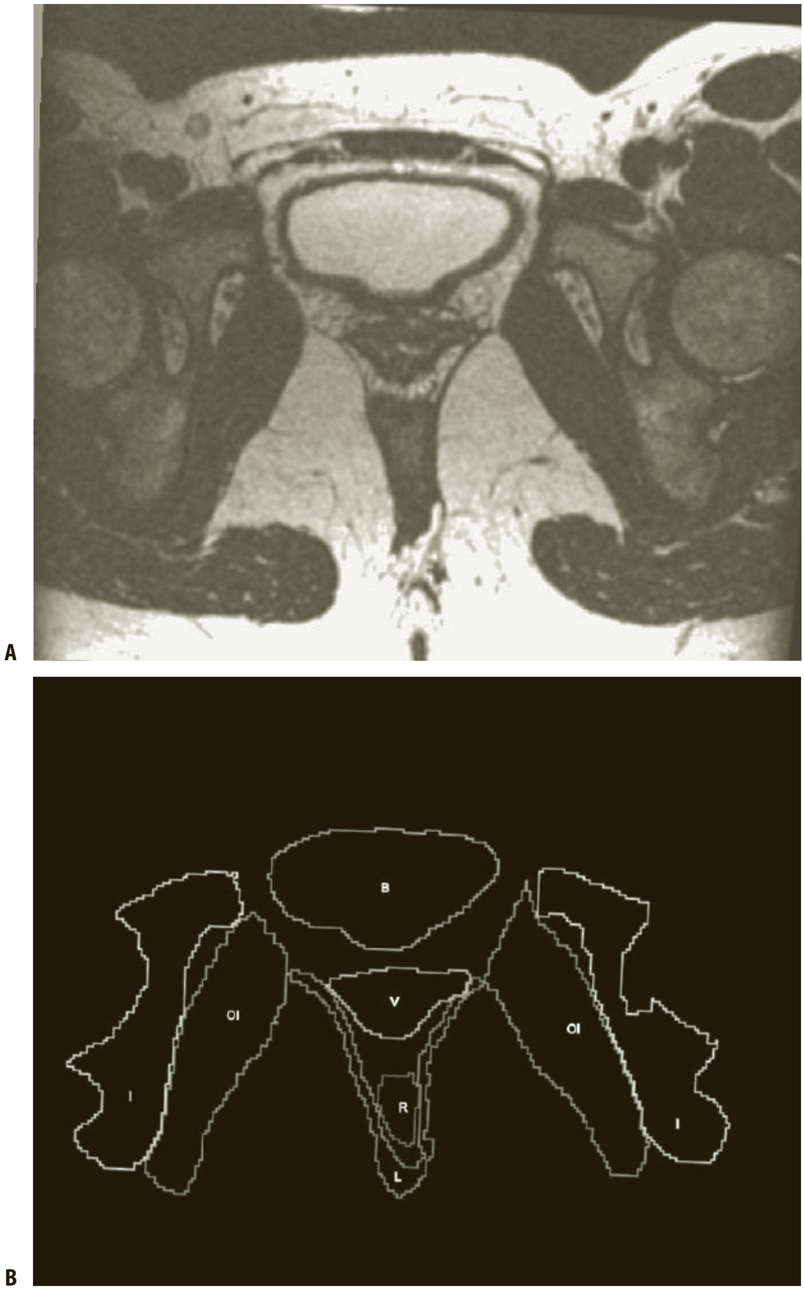

Figure 1.5. Axial MR views of the female pelvic floor structures at the level of the bladder at mid vagina. The bladder can be seen anteriorly (yellow outline). The iliococcygeus muscles are seen attaching bilaterally to the obturator internus. Posteriorly, the puborectalis portion of levator ani wraps around the rectum, in the manner of a "sling." At this level, the levator ani complex cradles and supports the attachment of the vagina, which in turn supports the bladder. Note the thinning of the iliococcygeus as it curves posteriorly toward the sacrum and coccyx.

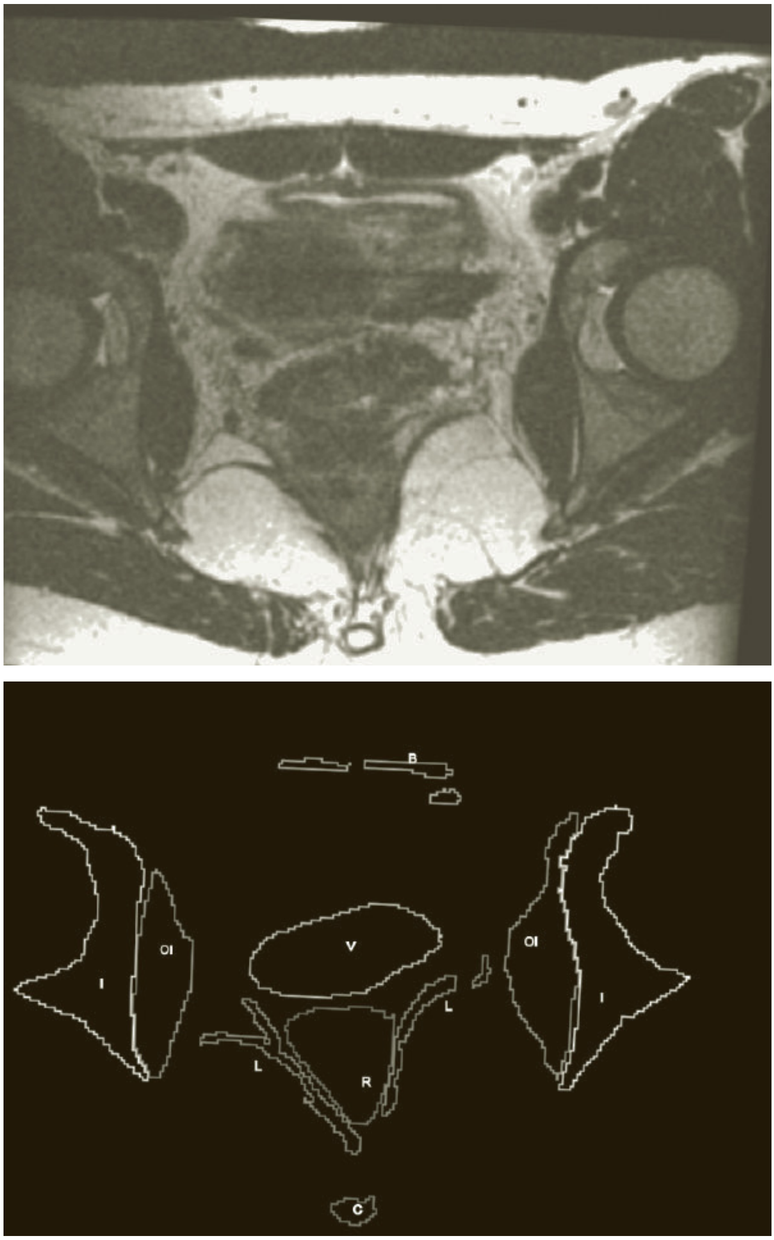

A

B

Figure 1.6. Axial MR views of the female pelvic floor structures at the level of the ischial spines and proximal vagina. The iliococcygeus muscles are seen attaching bilaterally to the obturator internus, near the ischial spines. At this level, the levator ani complex cradles and supports the vagina, which is now pulled bilaterally toward its attachment along the obturator internus fascia. The rectum rests in a groove in the midline of the iliococcygeus. Note the thinning of the iliococcygeus as it curves posteriorly toward the sacrum and coccyx.

Nullipara: Sagittal Plane

The midsagittal pelvic MR anatomy at rest is reviewed in Figure 1.7. In this figure, a resting midsagittal view of the female pelvic floor anatomy is given, with and without the 3D midline structures superimposed for orientation.

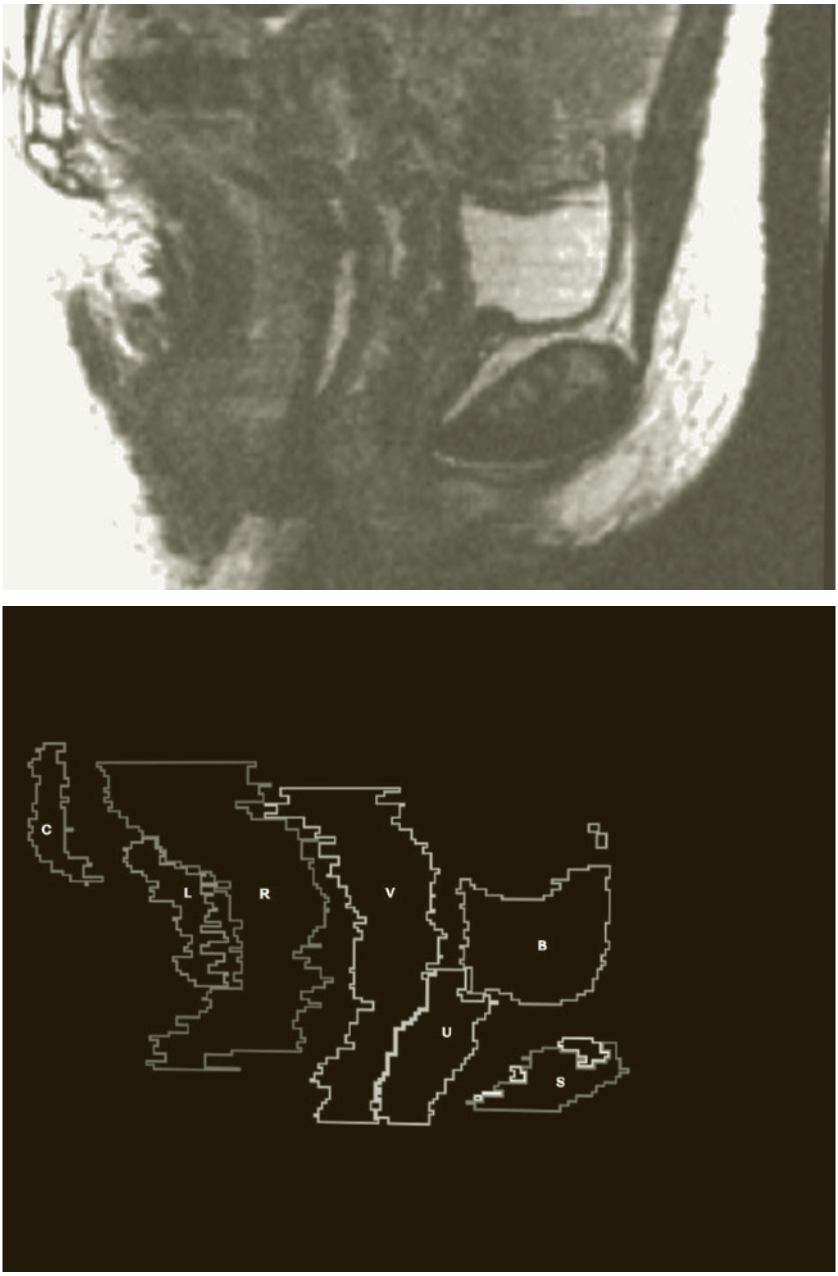

Figure 1.7. Midsagittal MR views of the female pelvic floor structures. The bladder and urethra are seen just posterior to the symphysis. The vagina is seen curving superiorly and posteriorly, undergirding the urethra and bladder. The rectum sits behind the vagina. Just under the rectum, midline fibers from the levator complex can be seen in brown, extending from the coccyx posteriorly, toward the perineal body.

Here, the levator ani is seen posterior and inferior to the rectum and vagina, acting as support for both structures.

Nullipara: Coronal Plane

The coronal pelvic MR anatomy is reviewed in Figures 1.8–1.15, each of which demonstrates a different depth within the pelvis. In these figures, a coronal view of the female pelvic floor anatomy is given, at a level at the anteriormost aspect of the symphysis (Figure 1.8). Successively deeper

A

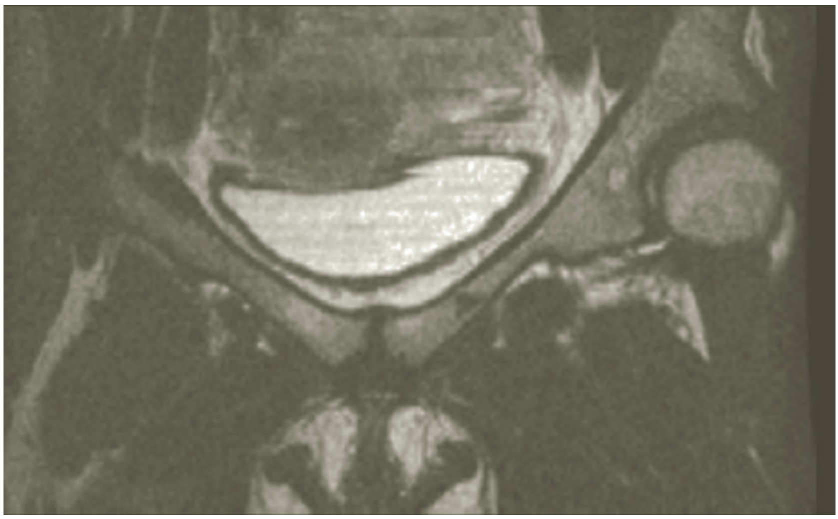

B

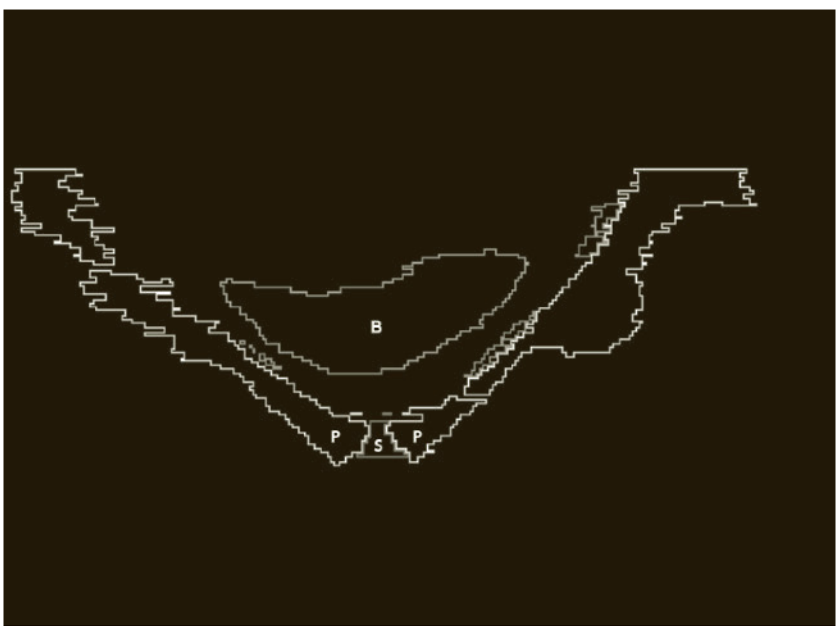

Figure 1.8. Coronal MR views of the female pelvic floor structures. The bladder, superior pubic rami, symphysis, and the anteriormost aspect of the obturator internus are seen in this coronal view.

A

B

Figure 1.9. Coronal MR views of the female pelvic floor structures, at the level of the inferior symphysis. The bladder, superior pubic rami, symphysis, the anteriormost aspect of the obturator internus, and the anteriormost arms of the puborectalis muscle are seen in this coronal view.

coronal views (Figures 1.9–1.15) demonstrate the position of the arms of the puborectalis as they move from their anterior location near the pubic rami, coursing back around the vagina and rectum posteriorly. From these MR images, it can be readily appreciated that the puborectalis forms a "sling-like" structure, attached anteriorly to the pubic rami, encircling the rectum, vagina, and urethra.

Figure 1.10. Coronal MR views of the female pelvic floor structures, at the level of the bladder neck. The belly of the obturator internus is seen overlying the obturator foramen. The arms of the puborectalis muscle are more developed in this view.

Figure 1.11. Coronal MR views of the female pelvic floor structures, at the level posterior to the bladder neck. The vagina is seen bounded by the puborectalis and iliococcygeus portions of levator ani.

A

B

Figure 1.12. Coronal MR views of the female pelvic floor structures, at the level of the posterior vaginal wall. The iliococcygeus portions of levator ani are seen attaching to the obturator internus along the arcus tendineus levator ani.

Figure 1.13. Coronal MR views of the female pelvic floor structures, at the level of the interface between the posterior vaginal wall and the mid rectum. The iliococcygeus portions of levator ani are seen attaching to the obturator internus along the arcus tendineus levator ani. The rectum is also enclosed by the iliococcygeus bilaterally.

Figure 1.14. Coronal MR views of the female pelvic floor structures, at the level of the interface between the posterior vaginal wall and the mid rectum. The iliococcygeus portions of levator ani form the bilateral boundaries of the rectum, and give way to the fibers of the external anal sphincter in the lower part of the image.

A

B

Figure 1.15. Coronal MR views of the female pelvic floor structures, at the level of the posterior mid rectum. The posteriormost aspect of the iliococcygeus is seen moving bilaterally toward the ischial spines. The external anal sphincter is seen in the lower part of the image.

Conclusion

The MR appearance of the pelvic floor structures in nulliparas and new primiparas was reviewed. The levator ani is seen as a main support of the pelvic floor structures.

References

1. Agur AMR, Dalley AF. Grants Atlas of Anatomy. Vol 1. Philadelphia: Lippincott Williams & Wilkins; 2005.
2. Strohbehn K, Ellis J, Strohbehn JA, Delancey JOL. Magnetic resonance imaging of the levator ani with anatomic correlation. Obstet Gynecol 1996;87:277–285.
3. DeLancey JO. Anatomy and physiology of urinary continence. Clin Obstet Gynecol 1990;33:298–307.
4. Delancey JOL. Three dimensional analysis of urethral support: "the hammock hypothesis." Neurourol Urodyn 1992;11:306–308.
5. Delancey JOL. Anatomy. In: Cardozo L, Staskin D, eds. Textbook of Female Urology and Urogynecology. Vol 1. Abingdon, UK: Martin Dunitz; 2000.
6. Woodburne RT. The ureter and ureterovesical junction and the vesical trigone. Anat Rec 1965;151:243–249.
7. Huisman AB. Aspects on the anatomy of the female urethra with special relation to urinary incontinence. Obstet Gynecol 1983;10:1–31.
8. Gosling JA, Dixon JS, Critchley HOD, Thompson SA. A comparative study of the human external sphincter and periurethral levator ani muscles. Br J Urol 1981;53:35–41.
9. Rud T, Andersson KE, Asmussen M, Hunting A, Ulmsten U. Factors maintaining the urethral pressure in women. Invest Urol 1980;17:343–347.
10. DeLancey JO. Anatomic aspects of vaginal eversion after hysterectomy. Am J Obstet Gynecol 1992;166:1717–1724; discussion 1724–1728.
11. Ricci JV, Thom CH. The myth of a surgically useful fascia in vaginal plastic reconstructions. Q Rev Surg 1954;2:261–263.
12. Uhlenhuth E, Nolley GW. Vaginal fascia a myth? Obstet Gynecol 1957;10:349–358.
13. Range RL, Woodburne RT. The gross and microscopic anatomy of the transverse cervical ligament. Am J Obstet Gynecol 1964;90:460–467.
14. Campbell RM. The anatomy and histology of the sacrouterine ligaments. Am J Obstet Gynecol 1950;59:1–12.
15. Richardson AC, Lyon JB, Williams NL. A new look at pelvic relaxation. Am J Obstet Gynecol 1976;126:568–573.

2

Pelvic Floor Ultrasound: Basic Physics, Instrumentation, and Examination Technique

Hans Peter Dietz

Diagnostic ultrasound produces images by way of registration of echoes arising in insonated tissues. The ultrasound signal, of a frequency between 2 and 20 MHz, i.e., above the audible range by a factor of 100–1000, is produced by piezoelectric crystals which can act as both transmitters and receivers. The elements have to go through at least 15 cycles of sending and listening per second in order to produce a flicker-free image; B mode frame rates are often set at half the AC power supply frequency, i.e., between 25 and 30 frames per second, but frame rates may be higher for some systems. The sending phase is much shorter, e.g., 1 ms, followed by, e.g., 39 ms of listening. The timing of arrival of any returning echoes defines the depth at which the reflection has occurred. Once the crystal has converted a returning ultrasound signal to a voltage, this voltage can be displayed on a cathode ray tube, or processed electronically.

Decades of technologic development stand between this basic concept and the reality of current diagnostic imaging systems. Multiple elements are integrated to form arrays, and steering of outgoing beams allows focusing. Frequency shifts resulting from wavefronts being reflected from moving reflectors such as red blood cells (the "Doppler effect") allow the representation of blood (or urine) flow with color Doppler, power/energy Doppler, and other techniques. Speckle reduction algorithms (such as speckle reduction imaging) and crossbeam techniques, such as compound resolution imaging (CRI), help to distinguish true echoes from random noise, and harmonic imaging techniques utilize the fact that echoes are not exclusively returned in the original frequency (e.g., 4 MHz) but at many other "harmonic" frequencies. Most recently, fast mechanical oscillation of a transducer array has been used to produce volume datasets that allow reconstruction of imaging data in any potential plane, and "matrix arrays" have moved from strips of elements to blocks of further and further miniaturized piezoelectric transmitters. Systems currently in use rely heavily on modern computer technology familiar from consumer electronics, and many modern machines use Windows-type user interfaces. Data volumes obtained with latest-generation four-dimension (4D)-capable systems may reach more than 130 MB with one acquisition, and more than 1 GB per patient. A DVD burner and a large-capacity hard disk (preferably more than 400 GB) have become indispensable.

Clearly, the technical side of ultrasound imaging is well beyond the scope of this manual. The interested reader is referred to recent literature on the subject.[1]

The use of transabdominal ultrasound in the evaluation of lower urinary tract and pelvic floor dysfunction was first documented in the early 1980s,[2] with translabial,[3,4] transrectal,[5] and transvaginal[6] techniques developed somewhat later. In this volume, we intend to limit ourselves to translabial (transperineal, introital) imaging as first described in 1986.[3,4] This modality is the most widespread because of wide availability of suitable equipment and its noninvasive nature, and has the advantage of reducing tissue distortion compared with transvaginal techniques.[7]

For translabial pelvic floor imaging, the most basic requirement is a small, portable real-time B mode–capable system. This implies that the monitor is capable of displaying a 2D grayscale image in real time. For documentation, a videoprinter is the most convenient solution. The standard transducers used for abdominal or obstetric imaging (e.g., 3.5- to 5-MHz curved arrays) are virtually perfect for pelvic floor diagnosis, allowing visualization of all three compartments. A cineloop function is useful for capturing the effect of maneuvers such as a pelvic floor muscle contraction or a Valsalva maneuver, but not essential. The same holds true for the option of splitting the screen into two adjacent images, and image inversion (top-bottom, left-right). On-screen calipers have been standard since the early 1980s. In essence, any older, surplus-to-requirement ultrasound imaging system you may locate in a regional hospital anywhere in the developed world is going to be suitable. Used equipment including a printer and abdominal/obstetric-type transducer should not require an investment of more than the equivalent of USD 10,000/Eur 8000, but could certainly be obtained much cheaper.

To image a midsagittal view of the pelvic floor, the transducer (ideally a curved array of a footprint of 5–8 cm) is placed on the perineum, after covering the transducer with a glove or thin plastic wrap for hygienic reasons (see Figure 2.1A–D). Powdered gloves can markedly impair image quality because of reverberations and should be avoided. Imaging can be performed in dorsal lithotomy, with the hips flexed and slightly abducted, or in the standing position. The latter is sometimes necessary in women who find it difficult to perform an effective Valsalva maneuver. Bladder filling should be specified; for some applications, prior voiding is preferable. The presence of a full rectum may impair diagnostic accuracy and sometimes necessitates a repeat assessment after bowel emptying.

Tissue discrimination is best in pregnancy and poorest in menopausal women with marked atrophy, likely because of varying hydration of tissues. The symphysis pubis should appear <1 cm from the transducer surface which signifies that the labia have been displaced laterally by the transducer, improving imaging conditions. Manual parting of the labia before transducer placement may be necessary, especially if they are hypertrophic or particularly hirsute. The transducer can generally be placed quite firmly against the symphysis pubis without causing significant discomfort, unless there is marked atrophy. Gain is adjusted, focal zones are set to the region of interest (at a depth of 2–5 cm), and harmonic imaging or software options such as speckle reduction algorithms may be used to optimize image quality.

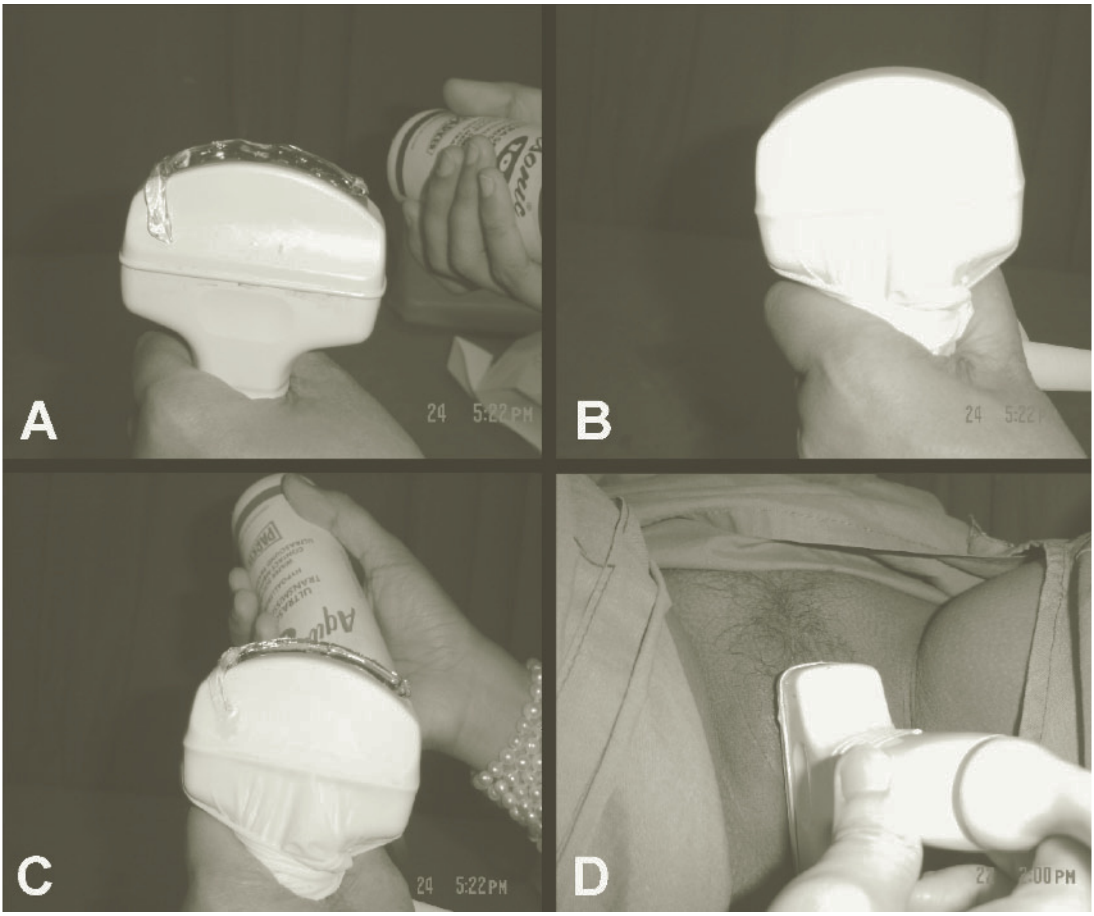

Figure 2.1. Preparation of a curved array transducer for translabial ultrasound. After covering the transducer with gel **(A)**, it is covered with a powder-free glove **(B)**. More gel is applied **(C)**, and the transducer is placed on the perineum, between the labia majora **(D)**. (Images courtesy of Dr Nelinda Pangilinan, Manila, Philippines.)

The standard midsagittal field of vision includes the symphysis pubis anteriorly, the urethra and bladder neck, the vagina, cervix, rectum, and anal canal (see Figure 2.2). Posterior to the anorectal junction, a hyperechogenic area indicates the central portion of the levator plate, i.e., the puborectalis/pubococcygeus or pubovisceral muscle. The cul-de-sac may also be seen, filled with a small amount of fluid, echogenic fat, or peristalsing small bowel. Larger amounts of free fluid in the pouch of Douglas will of course require further investigation unless the cause is known. Parasagittal or transverse views may yield additional information, e.g., enabling assessment of the puborectalis muscle and its insertion on the arcus tendineus of the levator ani, and for imaging of transobturator implants.

A basic fact to remember is that the echogenicity of a given tissue depends largely on the presence of interfaces between areas of different acoustic impedance, and on the angle between the incident beam and the interfaces in question. This implies that striated muscle or tubular structures such as the urethra may appear hypo- or iso-hyperechoic

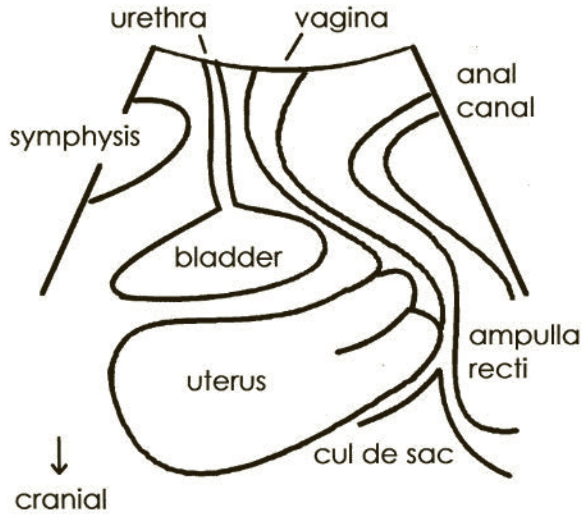

Figure 2.2. Field of view in the midsagittal plane when using a curved array transducer designed for abdominal or obstetric applications. (From Dietz HP, Ultrasound Imaging of the pelvic floor: 2D aspects. Ultrasound Obstet Gynaecol 2004; 23: 80–92, with permission.)

depending on transducer orientation.[8] In practice, this is most relevant as regards the urethral rhabdosphincter which appears hyperechoic on translabial ultrasound and partly hypoechoic on transvaginal scanning. In fact, the urethral rhabdosphincter may appear hypoechoic *and* hyperechoic in the same plane or image obtained by transvaginal ultrasound, giving rise to misunderstandings regarding its shape and extent[9,10] (see also Chapter 4).

There has been some disagreement regarding image orientation in the midsagittal plane. Some prefer orientation as in the standing patient facing right[11,12] which requires image inversion on the ultrasound system, a facility that is not universally available. Others (including the author) prefer an orientation as on conventional transvaginal ultrasound (cranioventral aspects to the left, dorsocaudal to the right).[13] The latter also seems more convenient when using 3D/4D systems. As any image reproduced in one of the above orientations can be converted to the other by rotation through 180°, formal standardization may be unnecessary.

Translabial ultrasound of the lower urinary tract, even if limited to B mode imaging in the midsagittal plane, yields information equivalent or superior to the lateral urethrocystogram (shown in Figure 2.3, rotated by 180° for comparison) or fluoroscopic imaging. Comparative studies have mostly shown good correlation between radiologic and ultrasound data.[5,14–19] Figure 2.4 demonstrates appearances on standard midsagittal view, the left image taken at rest, the right one on maximal Valsalva.

The one remaining advantage of X-ray fluoroscopy may be the ease with which the voiding phase can be observed although some investigators have used specially constructed equipment to document voiding with ultrasound.[20] It even seems possible, at least in principle, to observe voiding while using handheld B mode transducers, with the patient seated on a commode.[21] Because of psychological factors, however, it seems unlikely

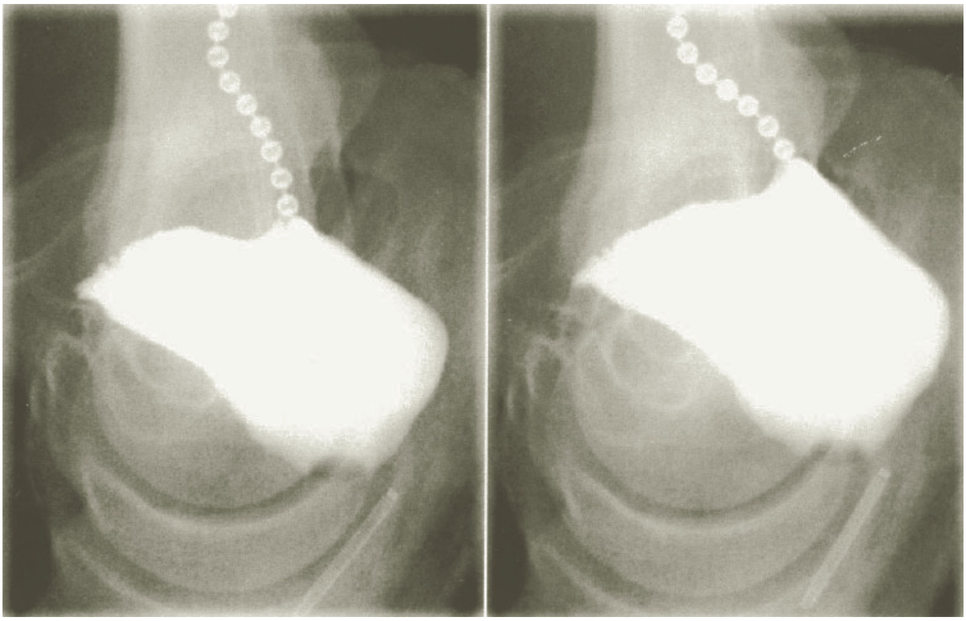

Figure 2.3. Lateral bead-chain urethrocystography, at rest (left) and on Valsalva (right), rotated and combined to allow for easier comparison with translabial ultrasound images. (From Dietz HP, Ultrasound Imaging of the pelvic floor: 2D aspects. Ultrasound Obstet Gynaecol 2004; 23: 80–92, with permission.)

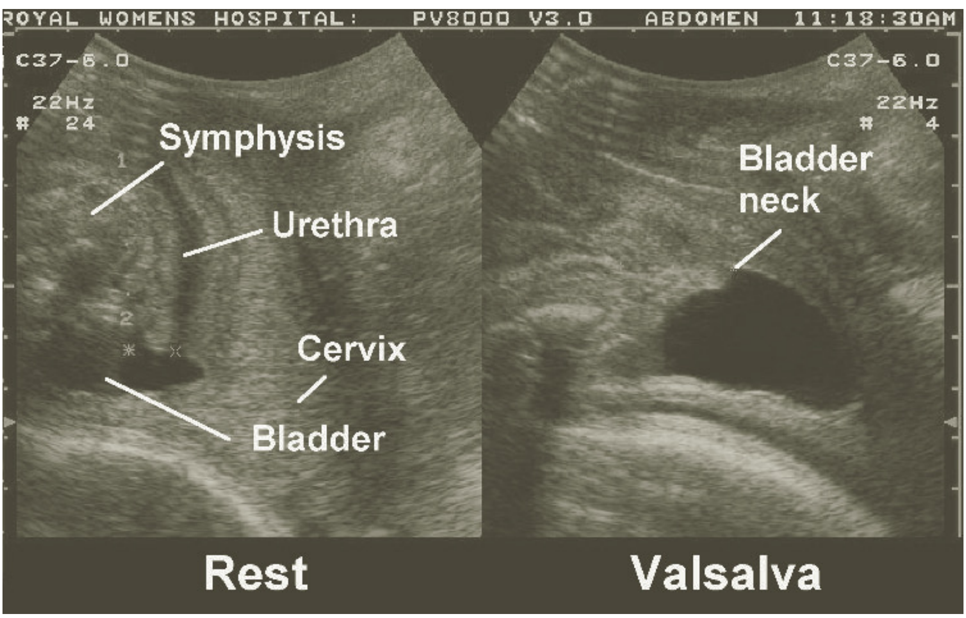

Figure 2.4. Translabial midsagittal view demonstrating the symphysis pubis, urethra and bladder neck at rest (left) and maximal Valsalva (right).

that any imaging method requiring the presence of staff (or even just a significant amount of unfamiliar machinery) could reproducibly document normal voiding, especially in females.

For colorectal imaging, contrast medium has been used in an attempt to replicate defecation proctography (DP), with good agreement found between ultrasound and fluoroscopy.[22,23] Because anismus, rectocele, rectal prolapse, and other causes of obstructed defecation can be imaged during a Valsalva maneuver and without resorting to invasive manipulation or contrast (own unpublished observations), one wonders whether there is any need to try to reproduce the exact process of an investigation such as DP, which is quite unlikely to bear much resemblance to normal defecation. This issue will be discussed in more detail in Chapter 5.

References

1. Kremkau FW. Diagnostic Ultrasound: Principles and instruments. St. Louis: WB Saunders; 2005.
2. White RD, McQuown D, McCarthy TA, Ostergard DR. Real-time ultrasonography in the evaluation of urinary stress incontinence. Am J Obstet Gynecol 1980;138(2):235–237.
3. Kohorn EI, Scioscia AL, Jeanty P, Hobbins JC. Ultrasound cystourethrography by perineal scanning for the assessment of female stress urinary incontinence. Obstet Gynecol 1986;68(2):269–272.
4. Grischke EM, Dietz HP, Jeanty P, Schmidt W. A new study method: the perineal scan in obstetrics and gynecology [article in German]. Ultraschall Med 1986; 7(4):154–161.
5. Bergman A, McKenzie CJ, Richmond J, Ballard CA, Platt LD. Transrectal ultrasound versus cystography in the evaluation of anatomical stress urinary incontinence. Br J Urol 1988;62(3):228–234.
6. Quinn MJ, Beynon J, Mortensen NJ, Smith PJ. Transvaginal endosonography: a new method to study the anatomy of the lower urinary tract in urinary stress incontinence. Br J Urol 1988;62(5):414–418.
7. Wise BG, Burton G, Cutner A, Cardozo LD. Effect of vaginal ultrasound probe on lower urinary tract function. Br J Urol 1992;70(1):12–16.
8. Rahmanou P, Chaliha C, Khullar V. Role of imaging in urogynaecology. Br J Obstet Gynaecol 2004;111(S1):24–32.
9. Toozs-Hobson P, Khullar V, Cardozo L. Three-dimensional ultrasound: a novel technique for investigating the urethral sphincter in the third trimester of pregnancy. Ultrasound Obstet Gynecol 2001;17(5):421–424.
10. Robinson D, Toozs Hobson P, Cardozo L, Digesu GA. Correlating structure and function: three-dimensional ultrasound of the urethral sphincter. Ultrasound Obstet Gynecol 2004;23:272–276.
11. Schaer GN, Koelbl H, Voigt R, et al. Recommendations of the German Association of Urogynecology on functional sonography of the lower female urinary tract. Int Urogynecol J 1996;7(2):105–108.
12. Tunn R, Petri E. Introital and transvaginal ultrasound as the main tool in the assessment of urogenital and pelvic floor dysfunction: an imaging panel and practical approach. Ultrasound Obstet Gynecol 2003;22:205–213.
13. Dietz HP. Ultrasound imaging of the pelvic floor. Part 1. 2D aspects. Ultrasound Obstet Gynecol 2004;23:80–92.
14. Grischke EM, Anton HW, Dietz HP, Schmidt W. Perinealsonographie und roentgenologische Verfahren im Rahmen der weiblichen Harninkontinenzdiagnostik. Geburtshilfe Frauenheilkd 1989;49:733–736.

15. Dietz HP, Wilson PD. Anatomical assessment of the bladder outlet and proximal urethra using ultrasound and videocystourethrography. Int Urogynecol J 1998;9(6):365–369.
16. Gordon D, Pearce M, Norton P, Stanton SL. Comparison of ultrasound and lateral chain urethrocystography in the determination of bladder neck descent. Am J Obstet Gynecol 1989;160(1):182–185.
17. Koelbl H, Bernaschek G, Wolf G. A comparative study of perineal ultrasound scanning and urethrocystography in patients with genuine stress incontinence. Arch Gynecol Obstet 1988;244(1):39–45.
18. Voigt R, Halaska M, Michels W, Martan A, Starker K, Voigt P. Examination of the urethrovesical junction using perineal sonography compared to urethrocystography using a bead chain. Int Urogynecol J 1994;5:212–214.
19. Ammann ME, Winkelbauer F, Fitzal P. The urethrocystogram and perineal sonography compared [article in German]. Rofo 1992;156(4):309–312.
20. Schaer GN, Siegwart R, Perucchini D, DeLancey JO. Examination of voiding in seated women using a remote-controlled ultrasound probe. Obstet Gynecol 1998;91(2):297–301.
21. Lim B. Voiding sonography: how do women void? 14th National Conference on Incontinence, Melbourne, 2005:54.
22. Beer-Gabel M, Teshler M, Barzilai N, et al. Dynamic transperineal ultrasound in the diagnosis of pelvic floor disorders: pilot study. Dis Colon Rectum 2002;45(2):239–245.
23. Beer-Gabel M, Teshler M, Schechtman E, Zbar AP. Dynamic transperineal ultrasound vs. defecography in patients with evacuatory difficulty: a pilot study. Int J Colorectal Dis 2004;19(1):60–67.

3

3D/4D Imaging: Technical Overview and Basic Methodology

Hans Peter Dietz

Technical Overview

Two main engineering solutions have been developed to allow integration of two-dimensional (2D) sectional images into 3D volume data: motorized acquisition and external electromagnetic position sensors. A simplified technique is the freehand acquisition of volumes without any reference to transducer position. In essence, this means that a cineloop of images is collated to form a volume dataset; because the system has no information on transducer position relative to the insonated tissues, measurements on volume data are impossible. Nevertheless, qualitative information may be obtained, and such systems have been used for clinical research in urogynecology.[1]

However, quantitative evaluation of volumes requires information on transducer position at the time of acquisition. If probe movement is achieved with the help of a motor, its characteristics will determine imaging data coordinates. Motorized acquisition may take the shape of automatic withdrawal of an endocavitary probe or motor action within the transducer itself. The first such motorized probe was developed in 1974, and by 1987 transducers for clinical use were developed that allowed motorized acquisition of imaging data.[2] The first commercially available system platform, the Kretz Voluson, was developed around such a "fan scan" probe. Endocavitary probes make a freehand acquisition technique impractical, which is why the company did not develop this alternative approach further[2] and instead concentrated on a technology reminiscent of (otherwise obsolete) mechanical sector transducers. The results have been the abdominal and endovaginal probes used in systems such as the GE Kretz Voluson 730 series. The widespread acceptance of 3D ultrasound in obstetrics and gynecology was helped considerably by this development because these transducers do not require any movement relative to the investigated tissue during acquisition. Most of the major suppliers of ultrasound equipment have now developed their own transducers along such lines, although it is widely recognized that this technology will probably be replaced by matrix array transducers within the next five years. Such transducers are already available for echocardiography and small parts ultrasound.[3]

With current mechanical 3D transducers, automatic image acquisition is achieved by rapid oscillation of a group of elements within the transducer. This allows the registration of multiple sectional planes that can be integrated into a volume as the location of a given pixel (or, to use the correct term for a pixel that has a defined location in space, a "voxel") is determined by transducer and insonation characteristics. Orientation within the volume is achieved by providing 2D image data in the three main axes of the volume, the "orthogonal planes" A (for our purposes, midsagittal), B (coronal), and C (axial or transverse) (see Figure 3.1).

Fortuitously, transducer characteristics on currently available systems for transabdominal use have been highly suitable for pelvic floor imaging. Acquisition is most conveniently performed with the main axis of the transducer in the midsagittal plane, because the urethra and bladder neck provide points of reference, ensuring symmetry. Provided this plane shows both the inferoposterior margin of the symphysis pubis and the pubovisceral muscle posterior to the anorectal junction, a single volume obtained

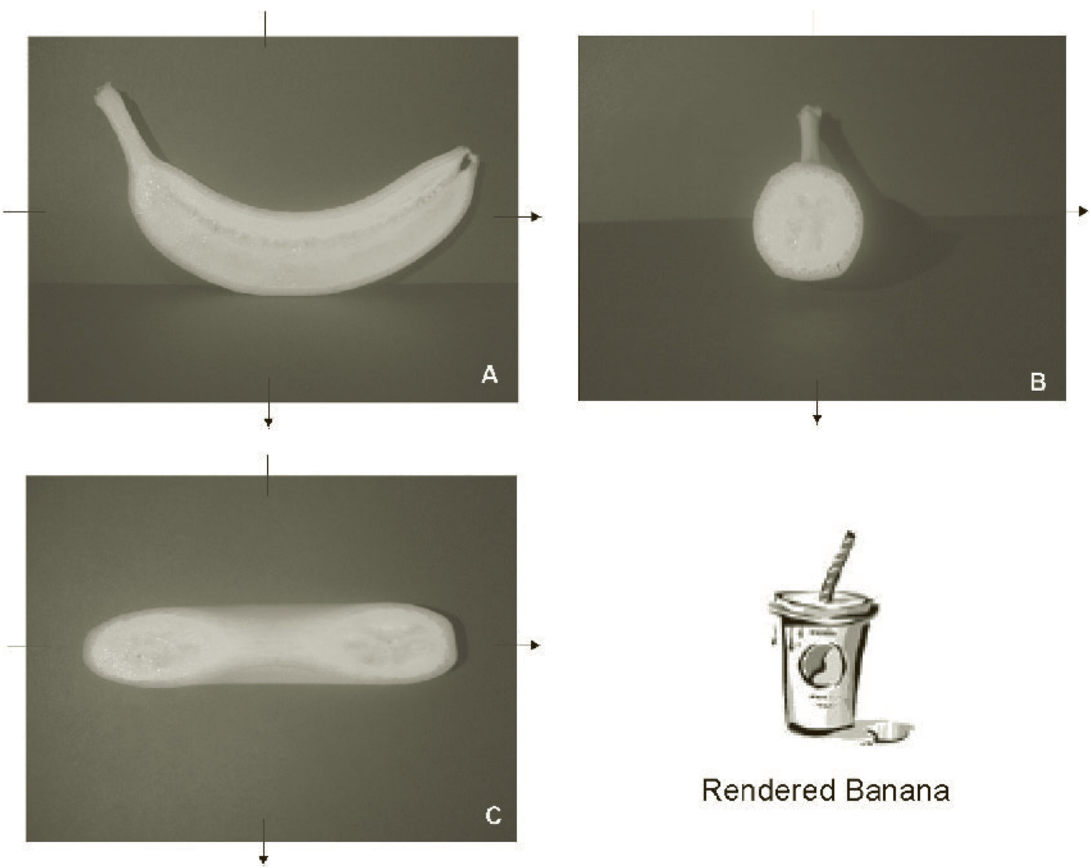

Figure 3.1. The three orthogonal planes used to represent volume data information on translabial ultrasound, illustrated by transection of a popular fruit. The A plane (top left) represents the midsagittal plane, B (top right) the coronal, and C (bottom left) the axial or transverse plane. By convention, the bottom right field is generally used to show semitransparent, "rendered" representations of volume data. (Banana split images courtesy of Dr Shawn Choong, Melbourne.)

Figure 3.2. The three orthogonal planes: midsagittal (A, top left), coronal (B, top right), and axial (C, bottom left) as well as a semitransparent rendering of all voxels in the region of interest (the boxed area evident in the orthogonal B planes) at the bottom right.

at rest with an acquisition angle of 70° or higher will comprise the entire levator hiatus as our area of interest.

The volume dataset will include part of the symphysis pubis, the inferior pubic rami, urethra, paravaginal tissues, the vagina, the cervix if present, the anorectum, and the pubovisceral (puborectalis/pubococcygeus part of the levator ani) muscle from the pelvic sidewall in the area of the arcus tendineus of the levator ani (ATLA) to the posterior aspect of the anorectal junction (see Figure 3.2 and the following). Depending on the anteroposterior dimensions of the pubovisceral muscle, it may also include the anal canal and even the external sphincter. This also holds true for volumes acquired on levator contraction because this shortens the hiatus. A Valsalva maneuver, however, may result in lateral or posterior parts of the puborectalis being displaced outside the field of vision, especially in women with significant prolapse (see Chapter 6).

The currently offered abdominal 8–4 MHz volume transducer for Voluson 730 expert systems allows acquisition angles of up to 85°, ensuring that the levator hiatus can be imaged in its entirety even in women with significant enlargement ("ballooning") of the hiatus on Valsalva. Higher acquisition angles come at a price: one will have to accept lower spatial or temporal resolutions. Gain, focusing, harmonic imaging, speckle reduction techniques, etc., may be used as for B mode imaging: as a rule, one should optimize image quality in the midsagittal plane before progressing to volume acquisition.

Display Modes

Figure 3.2 demonstrates the two basic display modes currently in use on 3D ultrasound systems. The multiplanar or orthogonal display mode shows cross-sectional planes through the volume in question. For pelvic floor imaging, this most conveniently means the midsagittal (top left), the coronal (top right), and the axial plane (bottom left).

One of the main advantages of volume ultrasound for pelvic floor imaging is that the method gives access to the axial plane. Up until recently, translabial pelvic floor ultrasound was limited to the midsagittal plane.[4–6] Parasagittal and coronal plane imaging have not been reported which may be attributable to the fact that there are no obvious points of reference, as opposed to the convenient reference point of the symphysis pubis on midsagittal views. The axial plane was accessible only on magnetic resonance imaging (MRI)[7–9] although some investigators used intracavitary ultrasound systems to assess the axial plane.[10] Pelvic floor MRI is an established investigational method, at least for research applications, with a multitude of papers published over the last 10 years.[11–18] Figure 3.3 shows a comparison of axial views of the levator hiatus on MRI and 3D ultrasound in a young nulliparous volunteer.

Imaging planes on 3D ultrasound can be varied in a completely arbitrary manner to enhance the visibility of a given anatomic structure, either at the time of acquisition or offline at a later time. The levator ani for example usually requires an axial plane that is tilted in a ventrocaudal to dorsocranial direction – by about 20° for a volume acquired at rest, more for volumes on pelvic floor muscle contraction, and less for volumes on Valsalva.

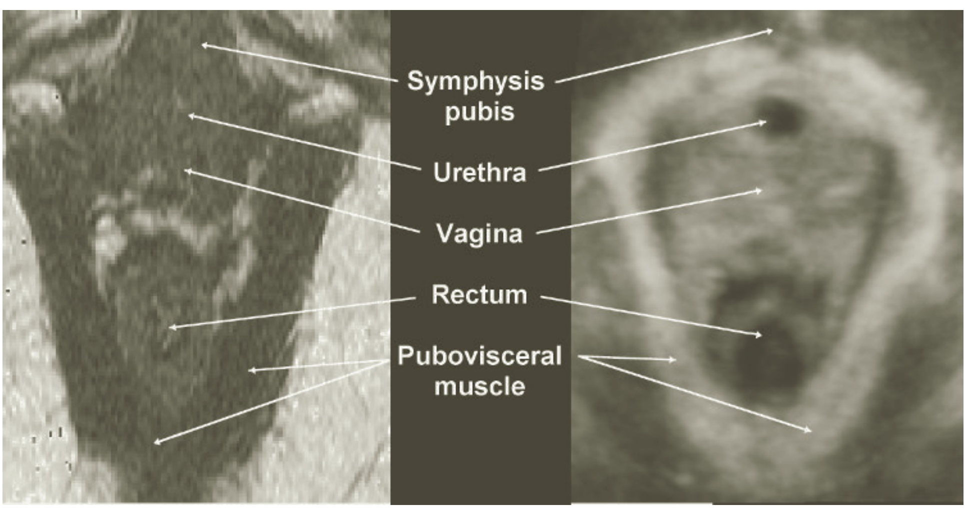

Figure 3.3. A comparison of magnetic resonance and 3D pelvic floor ultrasound imaging of the pubovisceral muscle in a 23-year-old nulliparous volunteer. (From Dietz HP and Lanzarone V: Levator trauma after vaginal delivery. Obstet Gynecol 2005; 106: 707–712, with permission.)

The three orthogonal images are complemented by a "rendered image," i.e., a semitransparent representation of all voxels in an arbitrarily definable "box." The bottom right-hand image in Figure 3.2 shows a rendered image of the levator hiatus, with the rendering direction set from caudally to cranially, which seems to be the most convenient setting for pelvic floor imaging. To allow for easy comparison with images obtained by MRI, it is suggested to orient the resulting axial plane image in such a way as to have the ventral aspect at the top of the image, and the patient's right on the left-hand side of the image. Incidentally, this orientation is the most intuitive for those used to clinical pelvic floor assessment, and is easily obtained as the default with 2D image orientation as suggested by the authors, i.e., with the symphysis pubis in the top left-hand corner of the B mode midsagittal plane.

The possibilities for postprocessing are restricted only by the software used for this purpose; programs such as GE Kretz 4D View (Kretztechnik GmbH, Zipf, Austria), at present in its fifth version and included in the DVD shipped with this manual, allow extensive manipulation of image characteristics and output of stills, cineloops, and rotational volumes in bitmap and AVI format.

Most systems currently available permit the use of a number of different rendering algorithms. For pelvic floor imaging, surface rendering seems most useful, although users may want to experiment with different degrees of transparency. The most convenient setting for pelvic floor imaging on Voluson systems seems to be a mix of 80% surface mode and 20% minimum mode which gives a very clear representation of the pubovisceral muscle. Other modes such as X-ray mode (used, e.g., to examine the fetal skeleton), pure minimum mode, and inversion mode, seem less useful. Modern systems also provide different color maps, overcoming a limitation of the human eye which is unable to distinguish the 256 shades of gray that are produced by the system.

4D Imaging

Four-dimensional imaging implies the real-time acquisition of volume ultrasound data, which can then be represented in orthogonal planes or rendered volumes. Recently, it has become possible to save cineloops of volumes, which is of major importance in pelvic floor imaging because it allows enhanced documentation of functional anatomy. Even on 2D single-plane imaging, a static assessment at rest gives little information compared with the evaluation of maneuvers such as a levator contraction and Valsalva. Their observation will allow assessment of levator function and delineate levator or fascial trauma more clearly. Avulsion of the pubovisceral muscle from the ATLA is often more evident on levator contraction and, if severe, on Valsalva. Most significant pelvic organ prolapse is not visible at rest in the supine position, unless severe. Fascial defects such as those defining a true rectocele (see Chapter 5) frequently only become visible on Valsalva.

The ability to perform a real-time 3D (or 4D) assessment of pelvic floor structures makes the technology potentially superior to MRI. Prolapse assessment by MRI requires ultrafast acquisition[19] which is of limited availability and will not allow optimal resolutions. Alternatively, some systems provide for imaging of the sitting or erect patient[16] but again accessibility will be limited for the foreseeable future. The sheer physical characteristics of MRI systems make it much harder for the operator to ensure efficient maneuvers because more than 50% of all women will not perform a proper pelvic floor contraction when asked,[20] and a Valsalva maneuver is often confounded by concomitant levator activation (see Chapter 4). Without real-time imaging, these confounders are impossible to control for. Therefore, ultrasound has major potential advantages when it comes to describing prolapse, especially when associated with fascial or muscular defects, and in terms of defining functional anatomy. Offline analysis packages such as GE Kretztechnik 4D View allow distance, area, and volume measurements in any user-defined plane (oblique or orthogonal) which is much superior to what is possible with DICOM viewer software on a standard set of single-plane MR images.

Volume Contrast Imaging

This recent technical development uses rendering algorithms as a means of improving resolutions in the coronal plane. As a result, speckle artifact is markedly reduced.[21] So far, measuring in the axial or C plane has been limited to raw data without significant postprocessing. Consequently, resolutions were much poorer than in the sagittal plane, reducing accuracy of measurements and our ability to identify structural changes. The latter were best detected on standard rendered volumes, which originally required a minimum thickness of 2 cm and did not allow quantification.

By using volume contrast imaging (VCI) on slices of a thickness of 1–3 mm, resolutions of about 1 mm can now be reached on axial or oblique axial slices (see Figure 3.4 for standard C plane imaging and VCI in the

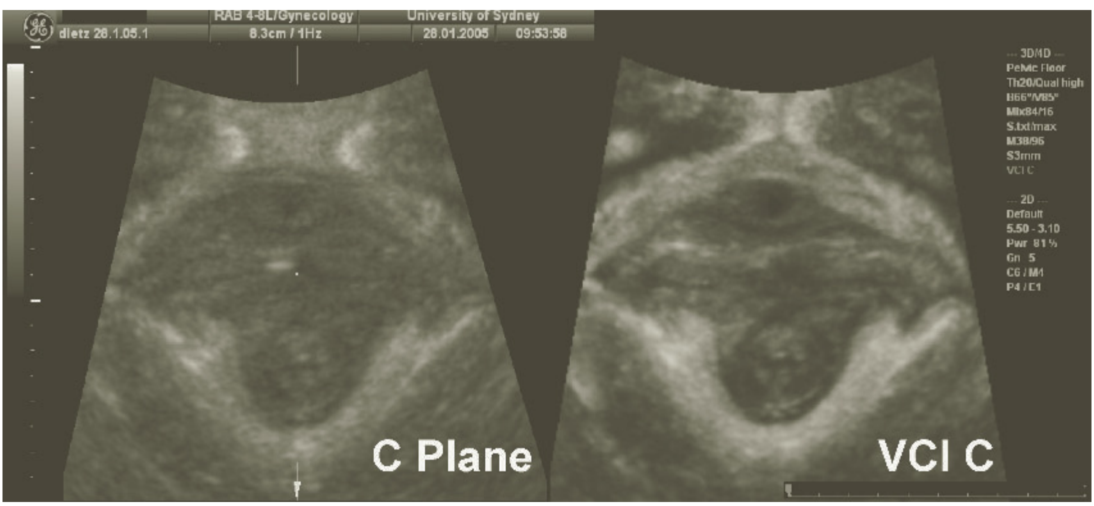

Figure 3.4. The effect of VCI algorithms on imaging quality in the axial plane. The images represent axial (C plane) slices tilted in a ventrocaudal to dorsocranial direction, oriented along the fiber direction of the pubovisceral muscle, with a standard C plane on the left. The right-hand image was obtained by applying VCI algorithms to the left-hand slice, using postprocessing with 4D View version 3.1. The slice thickness for the VCI image is set at 3 mm.

axial plane in a patient with major bilateral levator trauma after rotational forceps delivery) that allow distance and area measurements both on the system and offline.

Speckle Reduction Imaging

A further development in the use of rendering techniques for the improvement of spatial resolution is "speckle reduction imaging" (SRI) which can be used in the postprocessing of standard volume datasets analyzed by 4D View software, although volumes obtained with a system that has this option integrated seem to be superior. SRI can be applied in any of the three orthogonal planes and rendered volumes (see Figure 3.5). In general, six different steps of speckle reduction may be used, although there seems to be some loss of clarity and an increase in rendering artifacts with SRI 5 and 6. The likelihood of such artifacts seems to depend on the system with which the original volumes were obtained and may be less noticeable in volumes obtained on systems that have SRI as a hardware option.

Figure 3.5 shows an axial plane view of a right-sided levator injury in a rendered volume, the left image without processing, the right after SRI postprocessing using 4D View 5.0. One major advantage of those recent software developments is that they have been implemented both on the ultrasound system and on the software used for postprocessing, allowing significantly enhanced analysis of previously acquired volume data.

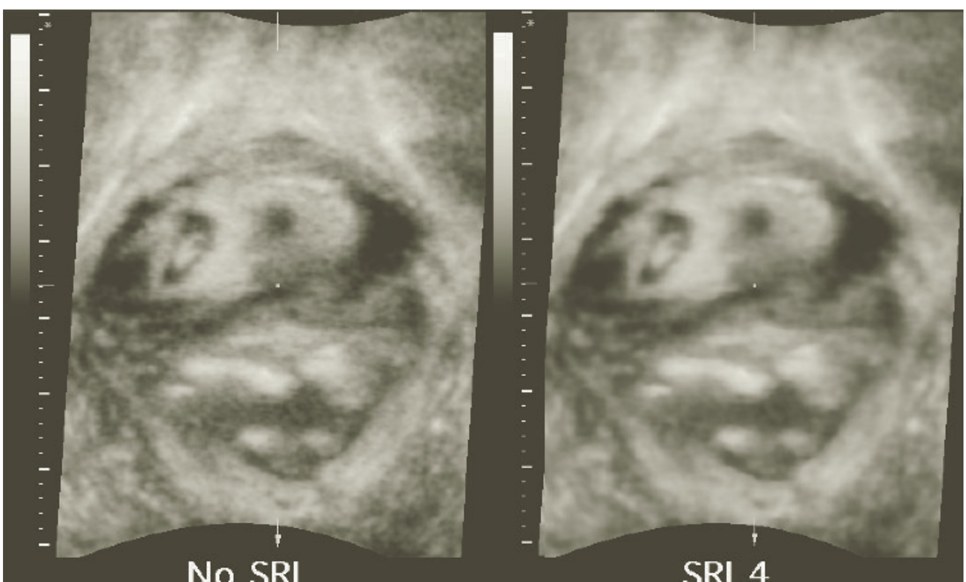

Figure 3.5. The effect of speckle reduction algorithms on axial plane rendered volumes in a patient with right-sided avulsion injury.

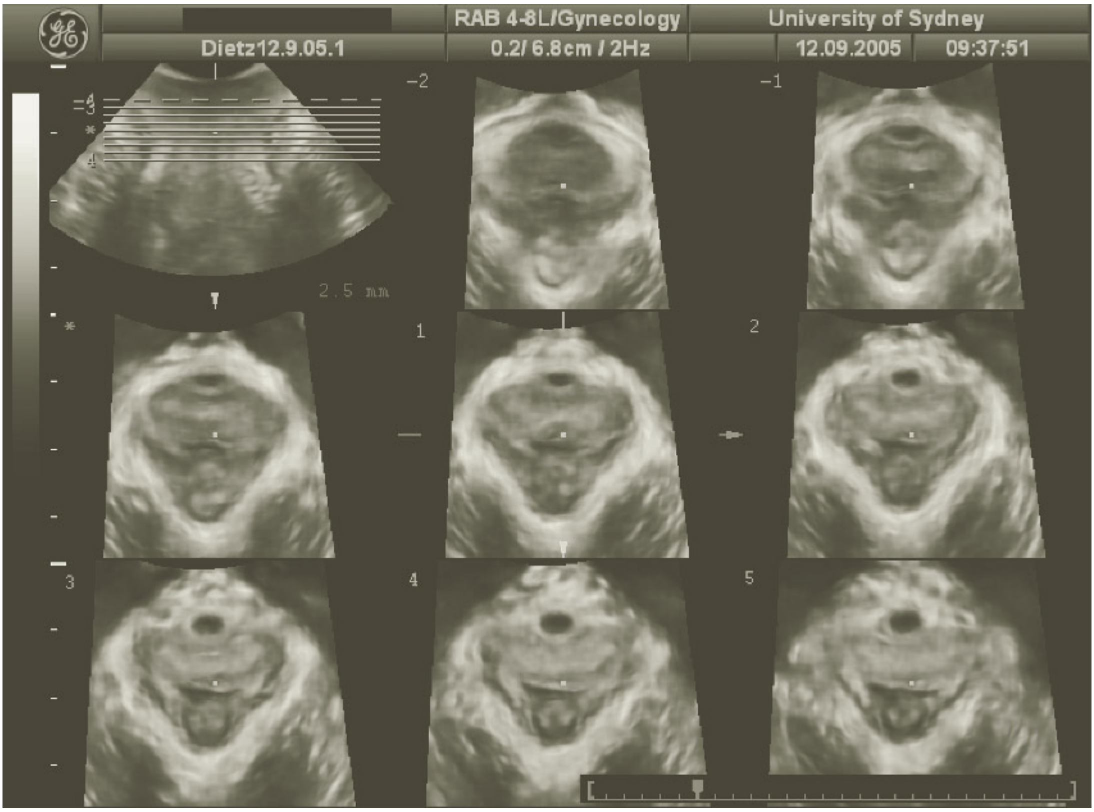

Figure 3.6. Normal pelvic floor. TUI provides cross-sectional imaging at user-definable depths, intervals, and at arbitrarily definable angles or tilts within the acquired volume. A cineloop of volumes will allow observation of the effect of maneuvers in multiple cross-sections at any given time.

Tomographic Ultrasound Imaging

During or after acquisition of volumes, it is now possible to process imaging information into slices of predetermined number and spacing, reminiscent of computed tomography or nuclear magnetic resonance imaging. This technique has been termed "multislice imaging" or tomographic ultrasound imaging (TUI) by manufacturers. As opposed to computed tomography or MRI, the location, number, depth, and tilt of slices can be adjusted at will after volume acquisition. The combination of true 4D (volume cineloop) capability and TUI or multislice imaging allows simultaneous observation of the effect of maneuvers at multiple different levels.

The pelvic floor easily lends itself to such techniques, and the author suggests using the plane of minimal dimensions (see Chapter 6) as plane of reference, with 2.5-mm steps recorded from 5 mm below this plane to 12.5 mm above, when using 4D View for analysis. There is one drawback of the current format of the reference screen which, for purposes of pelvic floor imaging, should be the midsagittal or A plane rather than the B or coronal plane. Hopefully, future versions of 4D View will allow a choice of reference planes.

Figure 3.6 shows the standard TUI format currently most appropriate to pelvic floor imaging, with the coronal plane for reference, and eight axial

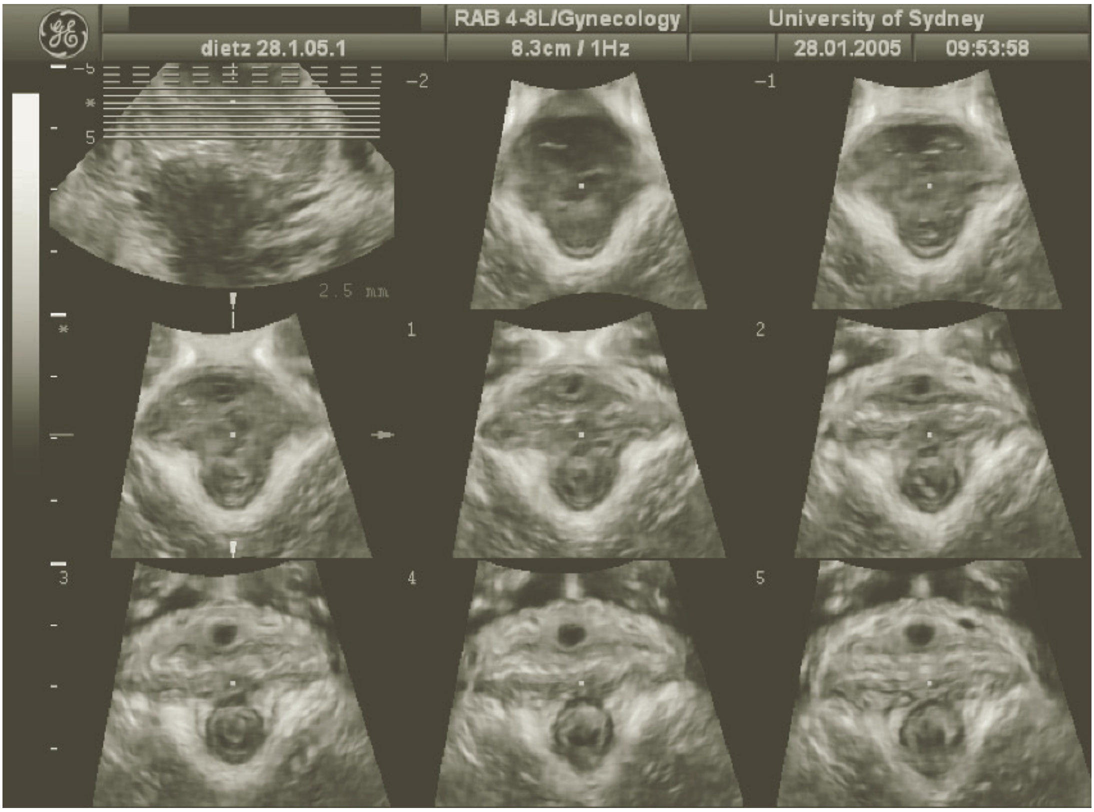

Figure 3.7. Bilateral levator avulsion (same patient as in 3.4) as demonstrated by TUI.

plane slices at a distance of 2.5 mm each, in a nulliparous patient with normal pelvic floor function and anatomy. Figure 3.7 demonstrates TUI findings in a patient with major bilateral avulsion injury of the pubovisceral muscle after rotational forceps delivery. The presence and extent of injuries is evident at a glance from one printout or film, without requiring any further manipulation of data, just as it is familiar to all of us from radiologic cross-sectional techniques. It is likely that such techniques will help with the standardization of assessment methods and allow more accurate classification and quantification of morphologic abnormalities.

As is the case for SRI and VCI, these software-based developments are available both in real time on systems of the Voluson series and offline as part of the latest versions of 4D View, allowing reanalysis of existing older volume data.

Practical Considerations

Pelvic floor ultrasound is highly operator dependent, as is true for all real-time imaging. Three-dimensional systems have the potential to reduce this operator dependence because volume acquisition is easily taught and should be within the capabilities of every sonographer or sonologist after a day's training. Although the method does require postprocessing (and the skills involved in this are more significant), static volume data typically of 1–6 MB in size can be de-identified and transmitted electronically so that evaluation may be obtained by e-mail, and this opens up entirely new possibilities for local and international cooperation. Unfortunately, the de facto software standard of 3D image files provided by licensing of the original technology has been lost. Currently, there are numerous proprietary standards developed by the different manufacturers. The DICOM committee is working on a unified standard for 3D storage and display, but users will have to exert significant pressure on manufacturers to cooperate in developing a DICOM standard for 3D ultrasound imaging data.

An initially underestimated advantage of 3D/4D ultrasound is the fact that all data can be stored electronically and may at any time be retrieved for postprocessing, reanalysis, or comparison with later findings. Although this requires fairly advanced storage capacities, the benefits will soon be apparent to any practitioner, especially the pelvic reconstructive surgeon. The method is particularly useful in the context of surgical audit. Cases 10 and 13 of the Appendix will hopefully give some indication as to how much 3D/4D pelvic floor ultrasound will simplify and enhance the assessment of new surgical techniques.

As of now, most publications on 3D ultrasound in obstetrics and gynecology deal with obstetric applications.[22] The visualization of fetal structures such as extremities and face has, to a large extent, driven research and development as well as the marketing of these systems. Although well-selected 3D data may enhance the understanding of certain conditions or abnormalities for both patients and caregivers,[22] some critics contend that 3D ultrasound has been a technology searching for an application. Pelvic floor imaging is a minor niche within the field of ultrasound in obstetrics and gynecology, but it may provide one of the first true indications for 3D and 4D volume ultrasound imaging.

References

1. Dietz HP, Steensma AB, Hastings R. Three-dimensional ultrasound imaging of the pelvic floor: the effect of parturition on paravaginal support structures. Ultrasound Obstet Gynecol 2003;21(6):589–595.
2. Gritzky A, Brandl H. The Voluson (Kretz) technique. In: Merz E, ed. 3-D Ultrasound in Obstetrics and Gynecology. Philadelphia: Lippincott Williams & Wilkins Healthcare; 1998:9–15.
3. Salehian O, Chan KL. Impact of three-dimensional echocardiography in valvular heart disease. Curr Opin Cardiol 2005;20(2):122–126.
4. Koelbl H, Hanzal E. Imaging of the lower urinary tract. Curr Opin Obstet Gynecol 1995;7(5):382–385.
5. Schaer GN. Ultrasonography of the lower urinary tract. Curr Opin Obstet Gynecol 1997;9:313–316.
6. Tunn R, Petri E. Introital and transvaginal ultrasound as the main tool in the assessment of urogenital and pelvic floor dysfunction: an imaging panel and practical approach. Ultrasound Obstet Gynecol 2003;22:205–213.
7. Plattner V, Leborgne J, Heloury Y, et al. MRI evaluation of the levator ani muscle: anatomic correlations and practical applications. Surg Radiol Anat 1991;13(2):129–131.

8. Strohbehn K, Ellis JH, Strohbehn JA, DeLancey JO. Magnetic resonance imaging of the levator ani with anatomic correlation. Obstet Gynecol 1996;87(2):277–285.
9. DeLancey JO, Speights SE, Tunn R, Howard D, Ashton Miller JA. Localized levator ani muscle abnormalities seen in MR images: site, size and side of occurrence. Int Urogynecol J 1999;10(S1):S20–S21.
10. Khullar V, Cardozo L. Three-dimensional ultrasound in urogynecology. In: Merz E, ed. 3-D Ultrasound in Obstetrics and Gynecology. Philadelphia: Lippincott Williams & Wilkins Healthcare; 1998:65–71.
11. Debus-Thiede G. Magnetic resonance imaging (MRI) of the pelvic floor. In: Schuessler B, Laycock J, Norton P, Stanton SL, eds. Pelvic Floor Reeducation – Principles and Practice. London: Springer; 1994:78–82.
12. Christensen LL, Djurhuus JC, Constantinou CE. Imaging of pelvic floor contractions using MRI. Neurourol Urodyn 1995;14(3):209–216.
13. Hjartardottir S, Nilsson J, Petersen C, Lingman G. The female pelvic floor: a dome – not a basin. Acta Obstet Gynecol Scand 1997;76(6):567–571.
14. Tunn R, Paris S, Fischer W, Hamm B, Kuchinke J. Static magnetic resonance imaging of the pelvic floor muscle morphology in women with stress urinary incontinence and pelvic prolapse. Neurourol Urodyn 1998;17(6):579–589.
15. Tunn R, DeLancey JO, Howard D, Thorp JM, Ashton-Miller JA, Quint LE. MR imaging of levator ani muscle recovery following vaginal delivery. Int Urogynecol J 1999;10(5):300–307.
16. Law PA, Danin JC, Lamb GM, Regan L, Darzi A, Gedroyc WM. Dynamic imaging of the pelvic floor using an open-configuration magnetic resonance scanner. J Magn Reson Imaging 2001;13(6):923–929.
17. Stoker J, Halligan S, Bartram C. Pelvic floor imaging. Radiology 2001;218:621–641.
18. DeLancey JO, Kearney R, Chou Q, Speights S, Binno S. The appearance of levator ani muscle abnormalities in magnetic resonance images after vaginal delivery. Obstet Gynecol 2003;101(1):46–53.
19. Dohke M, Mitchell DG, Vasavada SP. Fast magnetic resonance imaging of pelvic organ prolapse. Tech Urol 2001;7(2):133–138.
20. Bo K, Larson S, Oseid S, Kvarstein B, Hagen R, Jorgensen J. Knowledge about and ability to do correct pelvic floor muscle exercises in women with urinary stress incontinence. Neurourol Urodyn 1988;7:261–262.
21. Ruano R, Benachi A, Aubry M, Dumez Y, Dommergues M. Volume contrast imaging: a new approach to identify fetal thoracic structures. J Ultrasound Med 2004;23:403–408.
22. Timor-Tritsch IE, Platt LD. Three-dimensional ultrasound experience in obstetrics. Curr Opin Obstet Gynecol 2002;14(6):569–575.

4

The Anterior Compartment

Hans Peter Dietz

Bladder Neck Position and Mobility

One of the earliest parameters to be examined by translabial ultrasound was bladder neck mobility. This is because of the perception that a hypermobile bladder neck is an important factor in the etiology of female stress urinary incontinence. Although this is undoubtedly true to a degree, there are several other factors influencing continence, and the importance of this particular parameter should not be overestimated.

Bladder neck position and mobility can be assessed with a high degree of reliability. Points of reference are the central axis of the symphysis pubis,[1] or its inferoposterior margin[2] (see Figure 4.1). The former may potentially be more accurate because measurements are independent of transducer position or movement; however, because of calcification of the interpubic disc, the central axis is often difficult to obtain in older women, reducing reliability. This method, in widespread use in Central Europe, is also considerably more time consuming than use of the inferoposterior symphyseal margin as a point of reference because it requires not just one distance measurement but the construction of a 90° angle plus two distance measurements. Furthermore, imaging of the whole symphysis pubis precludes inclusion of the posterior (and often the central) compartment and therefore does not allow quantification of prolapse or assessment of the entire levator hiatus.

Imaging can be undertaken supine or erect, with the bladder full or empty. The full bladder is less mobile[3] and may prevent complete development of pelvic organ prolapse. In the standing position, the bladder is situated lower at rest but descends about as far as in the supine patient on Valsalva.[4] Either way, it is essential not to exert undue pressure on the perineum so as to allow full development of pelvic organ descent, although this may be difficult in women with severe prolapse such as vaginal eversion or procidentia. In such cases, there will be loss of contact with the perineum at some stage, making a full assessment impossible.

Measurements of bladder neck position relative to the symphysis pubis are generally performed at rest and on maximal Valsalva maneuver. The difference yields a numerical value for bladder neck descent (BND). On

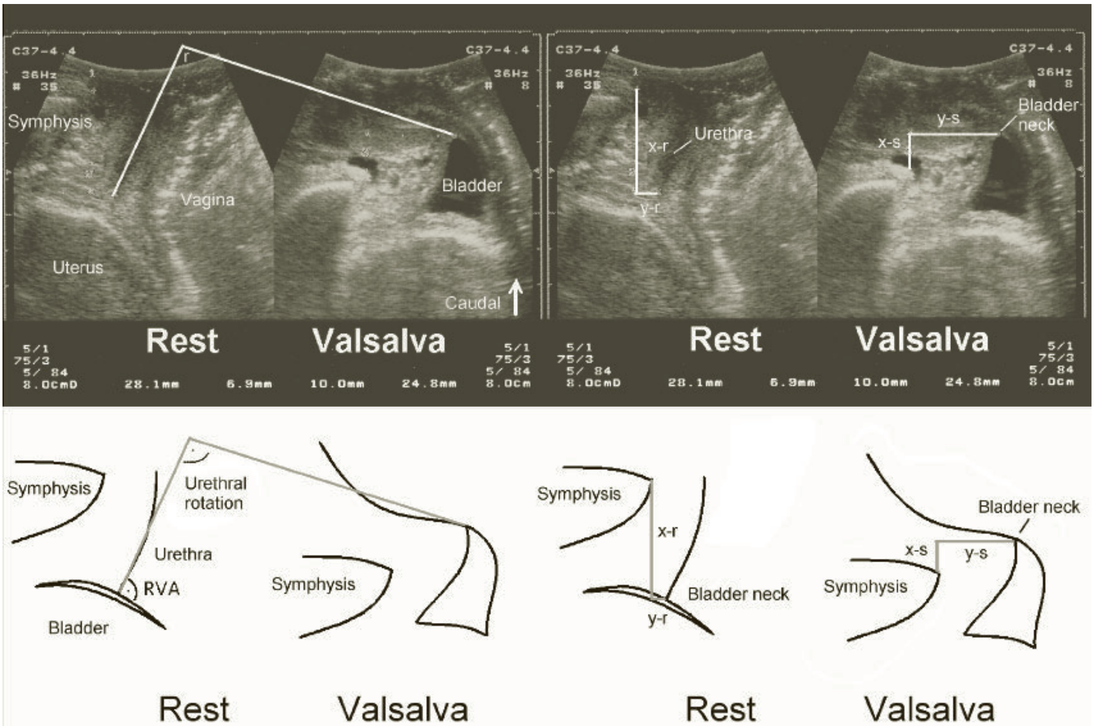

Figure 4.1. Some of the parameters used to evaluate a translabial scan for anterior compartment assessment. The upper row of images represents ultrasound images obtained at rest (left of each pair) and on maximal Valsalva (right of each pair), with drawings under each image illustrating the parameter's urethral rotation and retrovesical angle (RVA) (left pair) and bladder neck descent (BND) relative to the inferoposterior margin of the symphysis pubis (right pair). (Modified from Dietz HP et al. Bladder neck mobility is a heritable trait. Br J Obstet Gynaecol 2005;112:334–339, Blackwell Publishers, with permission.)

Valsalva, the proximal urethra may be seen to rotate in a posteroinferior direction. The extent of rotation can be measured by comparing the angle of inclination between the proximal urethra and any other fixed axis (see Figure 4.1). Some investigators measure the retrovesical (RVA) or posterior urethrovesical (PUV) angle between proximal urethra and trigone[5] (see Figure 4.1); others determine the angle γ between the central axis of the symphysis pubis and a line from the inferior symphyseal margin to the bladder neck.[6] Of all those ultrasound parameters of hypermobility, BND may have the strongest association with urodynamic stress incontinence (USI).[7] The reproducibility of this dynamic measurement has recently been assessed,[8] with a coefficient of variation (CV) of 0.16 between multiple effective Valsalva maneuvers, a % CV of 0.21 for interobserver variability, and a CV of 0.219 for a test-retest series at an average interval of 46 days. Intraclass correlations were between 0.75 and 0.98, indicating excellent agreement.[8]

There is no definition of "normal" for BND although cutoffs of 15, 20, and 25 mm have been proposed to define hypermobility. Mean values in women with stress incontinence are consistently around 30 mm (own unpublished data). Figure 4.2 shows a relatively immobile bladder neck before a first delivery (left), and a marked increase in bladder neck mobility after childbirth (right).

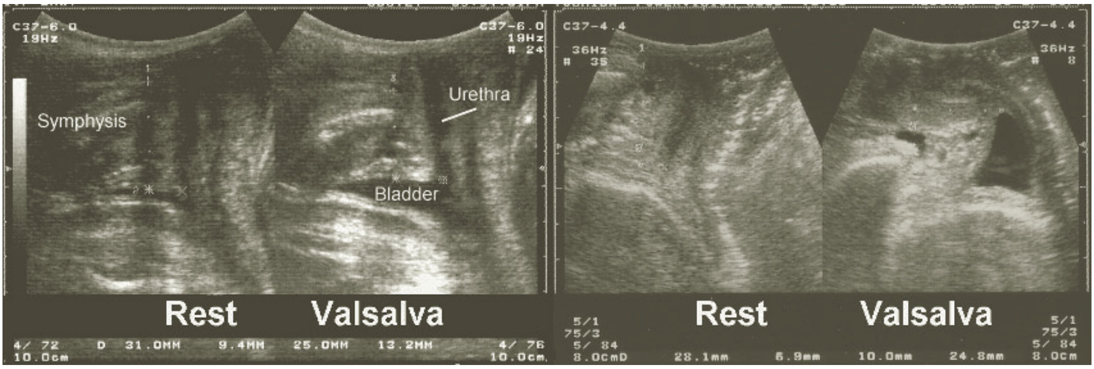

Figure 4.2. Marked increase in bladder neck mobility after vaginal delivery. The left pair of images demonstrates a virtually immobile bladder neck (BND = 31–25 = 6 mm), and the equivalent of a second-degree cystourethrocele 3 months postpartum BND = 28.1–(−10) = 38.1 mm). (From Dietz HP, Bennett MJ. The effect of childbirth on pelvic organ mobility. Obstet Gynecol 2003; 102:223–228, Lippincott Williams & Wilkins, with permission.)

Figure 4.3 demonstrates typical ultrasound findings in a patient with stress incontinence and a first-degree cystourethrocele, 25.5 mm of BND, and funneling. This image was taken with a very basic real-time B mode scanner (Toshiba Capasee), showing that rather inexpensive and/or outdated equipment will be sufficient for two-dimensional (2D) pelvic floor ultrasound as discussed in this chapter. For appearances on 3D/4D imaging, see Case 4 of the Appendix.

Bladder filling, patient position, and catheterization all have been shown to influence measurements,[1,3,4] and it can occasionally be quite difficult to obtain an effective Valsalva maneuver, especially in nulliparous women.

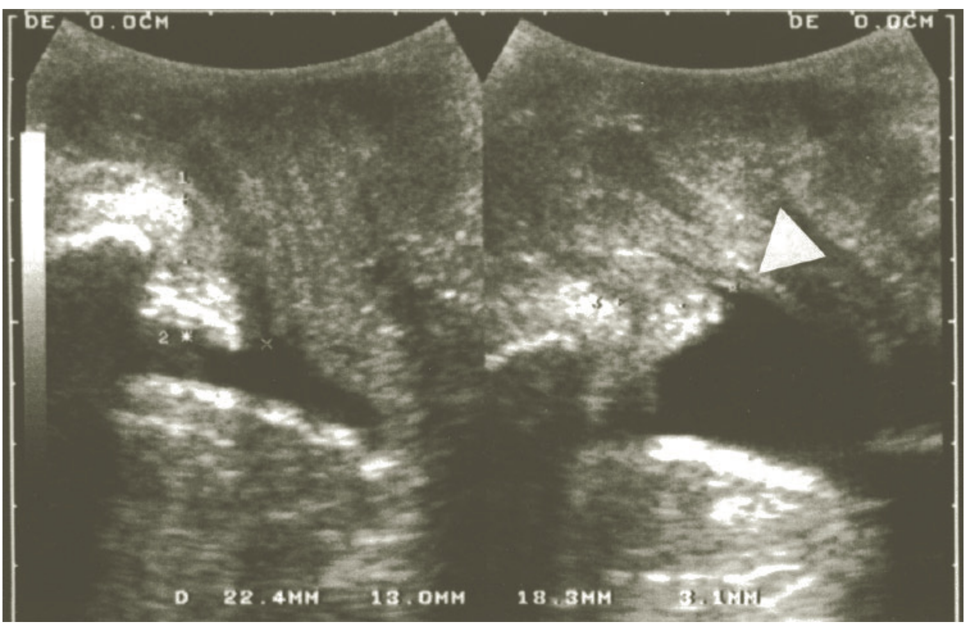

Figure 4.3. Typical ultrasound findings in a stress incontinent patient with a first-degree cystourethrocele, 25.5 mm of BND, 60° of urethral rotation, opening of the retrovesical angle to 180°, and funneling (arrow). (From Dietz HP, Ultrasound Imaging of the pelvic floor: 2D aspects. Ultrasound Obstet Gynaecol 2004; 23: 80–92, with permission.)

Perhaps not surprisingly, publications to date have presented widely differing reference measurements in nulliparous women. Whereas two recent series documented mean or median BND of only 5.1 mm[9] and 5.3 mm[10] in continent nulliparous women, another study on 39 continent nulliparous volunteers measured an average of 15 mm of BND.[11] The author has obtained BND measurements of 1.2–40.2 mm (mean 17.3 mm) in a group of 106 stress continent nulligravid young women of 18–23 years of age.[12]

It is likely that methodologic differences such as patient position, bladder filling, and quality of Valsalva maneuver (i.e., controlling for confounders such as concomitant levator activation) account for the above discrepancies, with all known confounders tending to reduce descent. Levator coactivation often affects the efficacy of a Valsalva maneuver, especially in nulliparous women, and is evident as a reduction of hiatal diameters in the midsagittal plane (see Figure 4.4). It seems that almost half of nulliparous women will contract the levator when asked to "push" or "bear down."[13] In fact, it has recently been shown that levator activation occurs with a whole range of stressors and probably is part of a generalized defensive reflex.[14]

Biofeedback, i.e., proper instruction, is necessary to reduce the impact of this confounder; otherwise false-negative findings are likely. This may explain the wide range of values reported for BND in nulliparous, asymptomatic women, and in women symptomatic for stress urinary incontinence and/or pelvic organ prolapse, it also has implications for situations in which prolapse assessment is attempted without the opportunity for either digital (at the time of a clinical assessment) or visual (on ultrasound imaging) biofeedback, e.g., on magnetic resonance imaging.[13]

Attempts at standardizing Valsalva maneuvers[15,16] have not found widespread application because this requires intraabdominal pressure measurement, i.e., a rectal balloon catheter. Other methods such as the use of a spirometer are likely to lead to suboptimal Valsalva maneuvers; the pressures used in the one study describing the use of such a device[15] were clearly insufficient to achieve maximal or even near-maximal descent.[16]

BND seems to be of some importance in the clinical management of patients with stress incontinence. It is likely to be a predictor of success

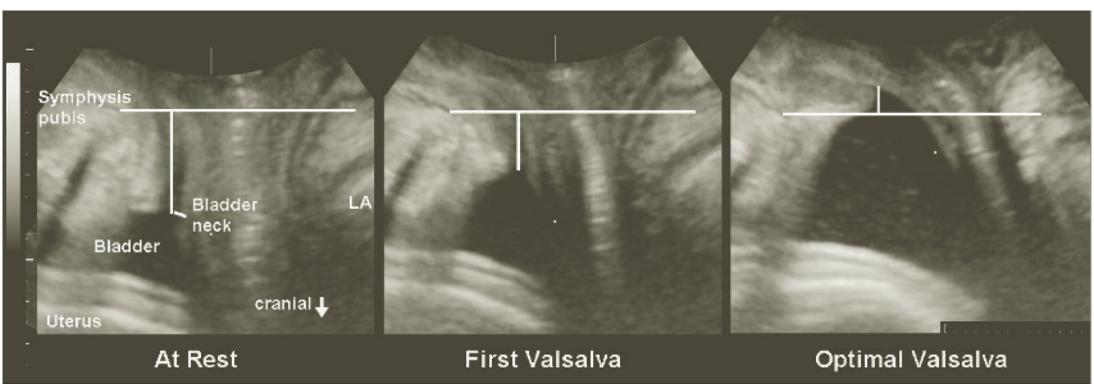

Figure 4.4. The effect of levator coactivation on BND. Midsagittal views at rest (left), on first Valsalva, confounded by levator coactivation (central image) and optimal Valsalva, after biofeedback teaching (right image). The horizontal line signifies the inferior margin of the symphysis pubis.

after suburethral slings. An association between preoperative bladder neck mobility and cure has been shown by X-ray,[17] Q-tip assessment,[18,19] and ultrasound[20] in that patients with a fixed urethra are less likely to be stress-dry postoperatively. This association between mobility and cure is explained by the need for dynamic compression of the urethra between tape and symphysis pubis (see also Chapter 7). The less mobility, the more difficult it may be to achieve just the right degree of tension to avoid either excessive obstruction, resulting in voiding dysfunction, or insufficient compression, resulting in recurrent stress leakage.[21]

The etiology of increased BND is likely to be multifactorial. The wide range of values obtained in young nulliparous women suggests a congenital component, and a recently published twin study has confirmed a high degree of heritability for anterior vaginal wall mobility.[22] Vaginal childbirth[23–26] is probably the most significant environmental factor (see Figure 4.2 for an example), with a long second stage of labor and vaginal operative delivery being associated with increased postpartum descent.[23] This association between increased bladder descent and vaginal parity is also evident in older women with symptoms of pelvic floor dysfunction.[26] It is not clear as to why bladder neck mobility should increase with childbirth. Hormonal effects have been postulated, and primigravid women seem to show more descent than nulliparae.[27] However, most of the effect seems to be attributable to vaginal childbirth,[23,24,28] and it has recently been shown that trauma to the levator ani muscle sustained during a vaginal delivery is associated with markedly increased bladder neck mobility.[29] Although levator trauma alone may be sufficient to explain some increase in bladder neck mobility after childbirth, it is likely that there may also be direct trauma to structures tethering the urethra to the pubic rami. Unfortunately, to date, resolutions have not been sufficient to further investigate this issue.

The pelvic floor is undoubtedly affected by labor and delivery, but the converse also seems to be true. It has been speculated that progress in labor may not be independent of pelvic floor biomechanics,[30] a hypothesis that was confirmed recently: anterior vaginal wall mobility on Valsalva was found to be a potential predictor of progress in labor.[31–33]

Funneling

In patients with stress incontinence, but also in asymptomatic women,[34] funneling of the internal urethral meatus may be observed on Valsalva (see Figure 4.3 and Cases 4, 5, and 14 of the Appendix) and sometimes even at rest. Funneling is often associated with leakage. Other indirect signs of urine leakage on B mode real-time imaging are weak grayscale echoes ("streaming") and the appearance of two linear ("specular") echoes defining the lumen of a fluid-filled urethra. However, funneling may also be observed in urge incontinence and must not be regarded as proof of USI. Its anatomic basis is unclear. Marked funneling has been shown to be associated with poor urethral closure pressures.[35,36]

Classifications developed for the evaluation of radiologic imaging[37] can be modified for ultrasound; however, this approach has not come into general use. The most frequent finding in cases of bladder neck hypermobility is the so-called rotational descent of the internal meatus, i.e., proximal urethra and trigone rotate around the symphysis pubis, that is, in a dorsocaudal direction. In such cases, the retrovesical angle opens to up to 160–180° from a normal value of 90–120°, and such change in the retrovesical angle is generally associated with funneling. A cystocele with intact retrovesical angle (90–120°) is frequently seen in continent prolapse patients (see Figure 4.5).

It has been surmised that this latter configuration distinguishes a central from a lateral defect of the endopelvic fascia[38] although proof for this hypothesis is lacking at present. Quite to the contrary, the cystocele with intact retrovesical angle seems to be particularly common (>50%) in women with levator defects, implying that it may well be attributable to damage to paravaginal supports (own unpublished observations).

Marked urethral kinking in patients with cystoceles can lead to voiding dysfunction (potentially worsened by straining) and urinary retention. Occult stress incontinence may be unmasked once a successful prolapse repair prevents urethral kinking, an effect that is entirely unsurprising if one considers appearances such as those in Figure 4.5.

Descent of the bladder to ≥10 mm below the symphysis pubis is strongly associated with symptoms of prolapse and has been proposed as constituting "significant" anterior compartment prolapse on the basis of receiver operator curve characteristics[39] (see Figure 4.6).

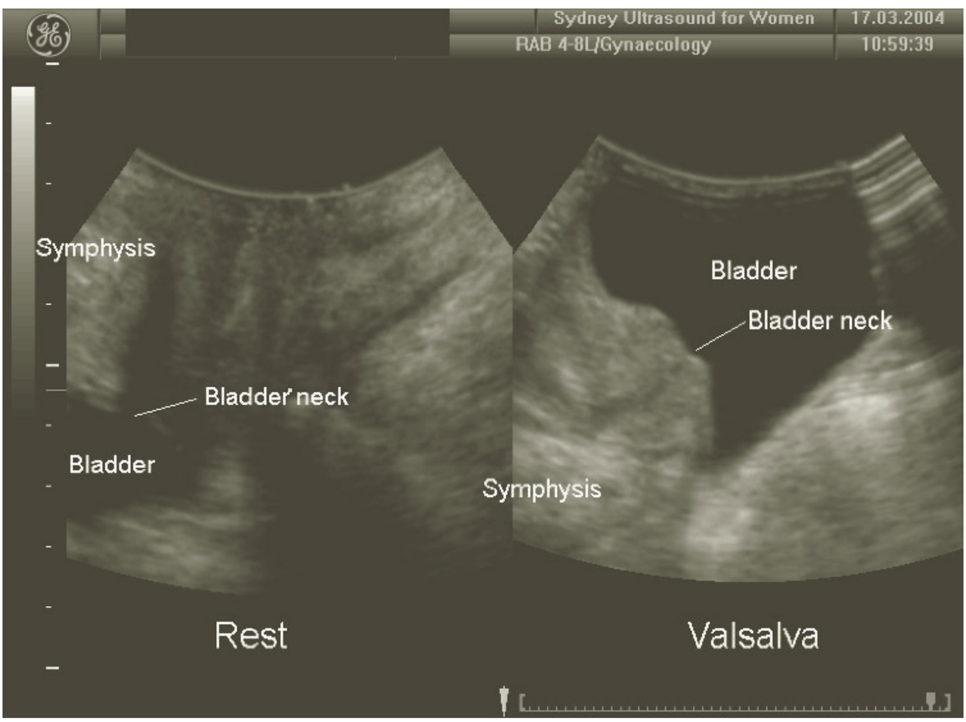

Figure 4.5. Marked cystocele with 4 cm of BND but intact retrovesical angle and no funneling, as seen in a continent patient with third-degree cystocele. The cystocele reaches to more than 4 cm below the symphysis pubis. The proximal urethra has rotated by more than 120°. (From: Dietz HP. Pelvic Floor Ultrasound. Current Medical Imaging Reviews 2006; 2: in print, Bentham Publishers.)

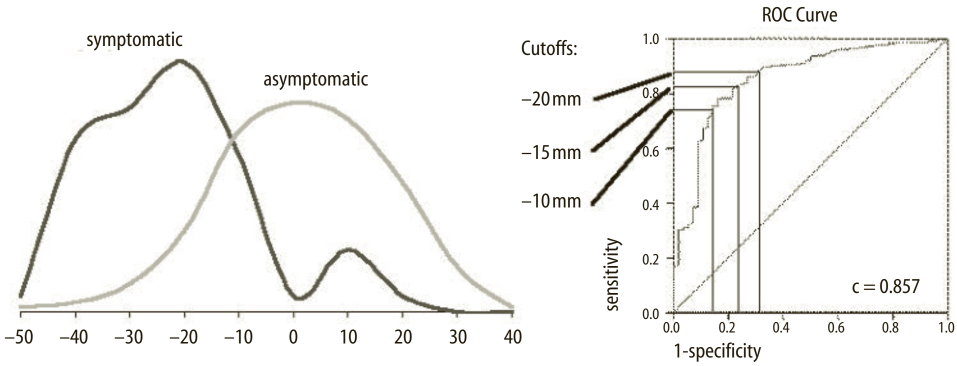

Figure 4.6. Histograms for bladder descent in millimeters (left) in asymptomatic (gray) and symptomatic women (black) and receiver operator curve (ROC) for bladder descent as a test for symptomatic prolapse (right). Lines define proposed cutoffs. (From Dietz.[39])

Color Doppler

Color Doppler ultrasound has been used to demonstrate urine leakage through the urethra on Valsalva maneuver or coughing.[40–42] Settings may vary considerably between systems, which implies that no general recommendations can be given. As a rule, it makes sense to set Doppler gain and scale to values that just permit the pickup of venous flow signals, e.g., from vessels posterior to the symphyseal margin, avoiding marked flash artifact[43] as tissues move with a Valsalva maneuver. Flash artifact is also responsible for the fact that observation of leakage on coughing is considerably more difficult than on Valsalva.

There are several proprietary Doppler methods,[43] and their suitability will vary from one system to the next. As a rule, CDV or velocity Doppler, will easily pick up urine flow in the urethra provided the urethral axis (and therefore flow) is at an acute angle (<45°) to the incident beam. If the urethra rotates markedly on Valsalva, the flow angle may veer so far as to reach 90° relative to the incident beam. In such a situation, CDV is unlikely to provide good signal intensity, and users may want to switch to Power or "Energy" Doppler.

Agreement between color Doppler and fluoroscopy was high in a controlled group with indwelling catheters and identical bladder volumes.[41] Both velocity (CDV, Figure 4.7) and energy mapping (CDE or "Power Doppler," Figure 4.8) were able to document leakage. CDV was slightly more likely to show a positive result, probably because of its better motion discrimination. This results in less flash artifact and better orientation, particularly on coughing, although imaging quality will depend on the systems used and selected color Doppler settings.

Routine sonographic documentation of stress incontinence during urodynamic testing clearly is feasible, and color Doppler imaging may also facilitate the documentation of leak point pressures.[42] Whether this is in fact desired will depend on the clinician and his/her preferences, and one may well argue that urine leakage and leak point pressures can be determined without access to expensive imaging equipment.

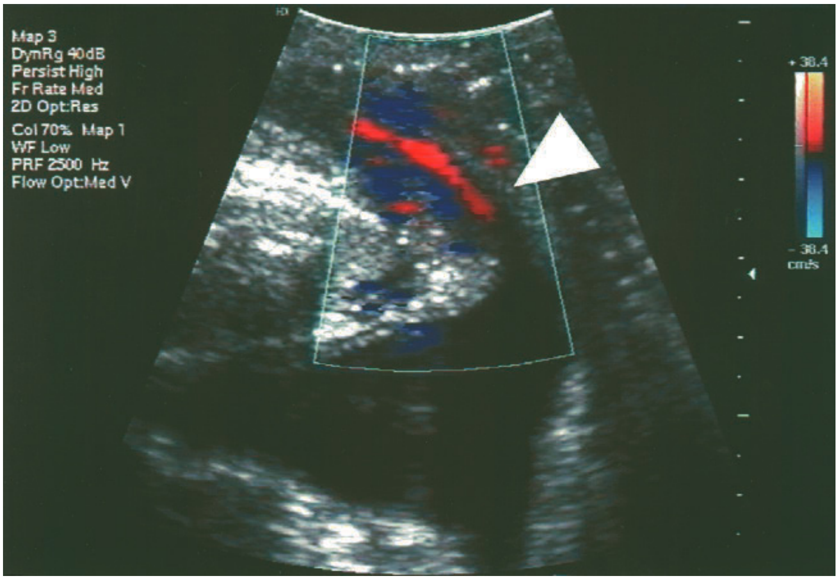

Figure 4.7. Loss of urine per urethram on Valsalva maneuver as documented on translabial color Doppler (velocity, CDV). This patient had a first-degree cystourethrocele and urodynamically proven stress incontinence. (From Dietz HP, Ultrasound Imaging of the pelvic floor: 2D aspects. Ultrasound Obstet Gynaecol 2004; 23: 80–92, with permission.)

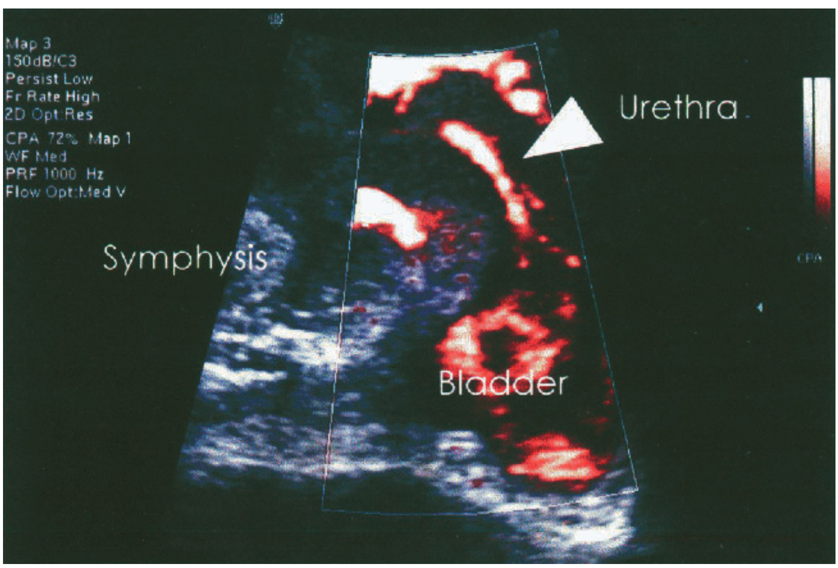

Figure 4.8. Loss of urine per urethram on Valsalva maneuver as documented on translabial color Doppler (Energy Doppler, CDE, or "Power Doppler"). This patient had a first-degree cystourethrocele and urodynamically proven stress incontinence. (From Dietz HP, Ultrasound Imaging of the pelvic floor: 2D aspects. Ultrasound Obstet Gynaecol 2004; 23: 80–92, with permission.)

Urethra

On translabial imaging, the urethra is evident as a vertical hypoechoic area (see Figures 4.1–4.4). This area is thought to include mucosa, vascular plexus, and the urethral smooth musculature. Its hypoechoic appearance is largely attributable to the fact that mucosal layers and smooth musculature run parallel to the incident beam (see Chapter 2). This is evident whenever there is significant urethral rotation, because a more perpendicular orientation of the urethra relative to the incident beam makes the structure more isoechoic and therefore less evident. The urethral rhabdosphincter surrounds this hypoechoic structure and appears as a double hyperechoic stripe on translabial ultrasound at rest, ventral and dorsal of the urethra proper. Its appearance seems to vary markedly depending on the approach used, i.e., whether intraurethral,[44] transrectal,[45] or translabial/perineal. Recent improvements in tissue discrimination have made identification much easier (see Figure 4.9).

In general, the rhabdosphincter seems more obvious in the axial compared with the midsagittal plane, as evident from Figures 6.2 and 6.5–6.9 in Chapter 6. This is at least partly attributable to the relative ease with which the human eye recognizes ring structures, a legacy of hundreds of millions of years of predator–prey relationships. Clearly, a number of authors, including this one, have misinterpreted findings in the past.[35] On principle, intraurethral ultrasound with transducers developed for intravascular imaging should help in identifying urethral morphology and help us determine what exactly we are imaging. Several authors used such techniques in the 1990s,[44,46,47] as well as more recently,[48] confirming that the rhabdosphincter often shows sonographic evidence of impairment in stress incontinent women, both in the sense of reduced contractility as well as changes in echogenicity and integrity.[48] However, the very limited availability of such transducers means that these techniques are unlikely to enter clinical practice in the near future.

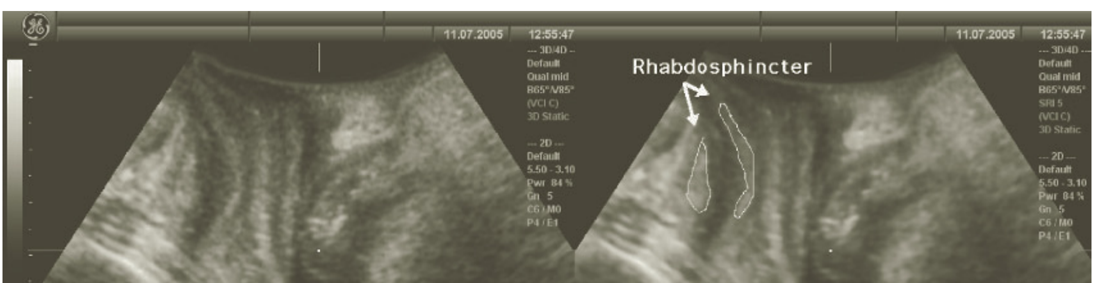

Figure 4.9. The urethral rhabdosphincter as imaged in the midsagittal plane (native imaging, left image) and on speckle reduction imaging (right image). Improved tissue discrimination allows recognition of a structure that is otherwise difficult to identify.

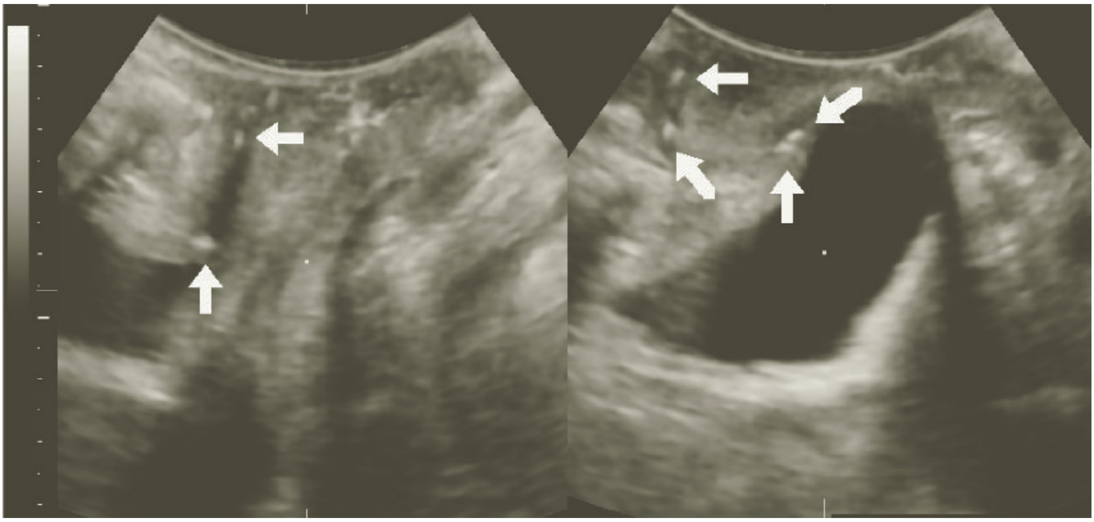

Figure 4.10. Hyperechoic urethral foci (arrows) in a patient with mixed urinary incontinence, a second-degree cystocele, and USI. Office cystourethroscopy was normal. The foci are more evident on Valsalva (right image).

On translabial scanning at rest, the rhabdosphincter appears hyperechoic as the incident beam is perpendicular to those fibers. On transvaginal ultrasound, parts of this circular or near-circular structure are vertical to the incident beam, others are parallel, and this has resulted in spurious findings, leading some authors to conclude that the rhabdosphincter is hypoechoic and noncircular.[48]

The resolution of currently used transducers for translabial imaging is insufficient to allow more than a global assessment of the dimensions of the urethra, but occasionally abnormalities such as stenosis or diverticula may be seen.[49] Although there have been attempts at quantitative assessment on transvaginal 3D ultrasound,[50,51] the above-mentioned artifacts make the data obtained by this methodology somewhat suspect. To date, no quantitative assessment of the urethral rhabdosphincter as seen on translabial ultrasound seems to have been undertaken, probably because of resolution issues.

Hyperechoic foci within the urethra (see Figure 4.10) are common, may be isolated or multiple, and probably are attributable to calcified urethral glands. There seems to be no association between symptoms or lower urinary tract conditions and the presence of such foci.[52]

Bladder Wall Thickness

There has recently been renewed interest in the quantification of bladder wall or detrusor wall thickness (BWT or DWT) by transvaginal and/or translabial ultrasound.[53,54] Measurements are obtained after bladder emptying and perpendicular to the mucosa, leading edge to leading edge (see Figure 4.11), close to the midline as identified by the urethra and bladder neck. Originally, three sites were assessed by transvaginal ultrasound: anterior wall, trigone, and dome of the bladder, and the mean of all three was calculated. The author believes that the trigone (because it is of different embryologic origin) is difficult to justify as a measurement location compared with the dome. In addition, there often is marked variation in trigonal thickness between the bladder neck and the interureteric ridge.

Another approach, currently used by the author, is to measure three sites on the dome, which can be performed either by translabial/introital or by transvaginal ultrasound. Above a bladder filling of 50 mL, DWT starts to decrease,[53] which is why in urogynecology measurements are usually undertaken after bladder emptying. DWT measurement by translabial ultrasound seems to be highly reproducible, with an intraclass correlation of 0.82 (CI 0.63–0.91) found in a series of 67 patients.[55]

A DWT of more than 5 mm seems to be associated with detrusor overactivity,[53,54,56] although this has recently been disputed.[57] In our own data, DWT is clearly higher in women with symptoms of urge incontinence and urodynamically proven detrusor overactivity, but the strength of the association seems insufficient to be of much use in clinical practice.[58] Increased DWT is likely the result of hypertrophy of the detrusor muscle, which is most evident at the dome; this may be the cause of symptoms or simply the effect of an underlying abnormality. Although DWT on its own seems only moderately predictive of detrusor overactivity, the method may be clinically useful when combined with symptoms of the overactive bladder.[59] In young women, DWT is almost universally below the threshold of 5 mm at the dome.[55]

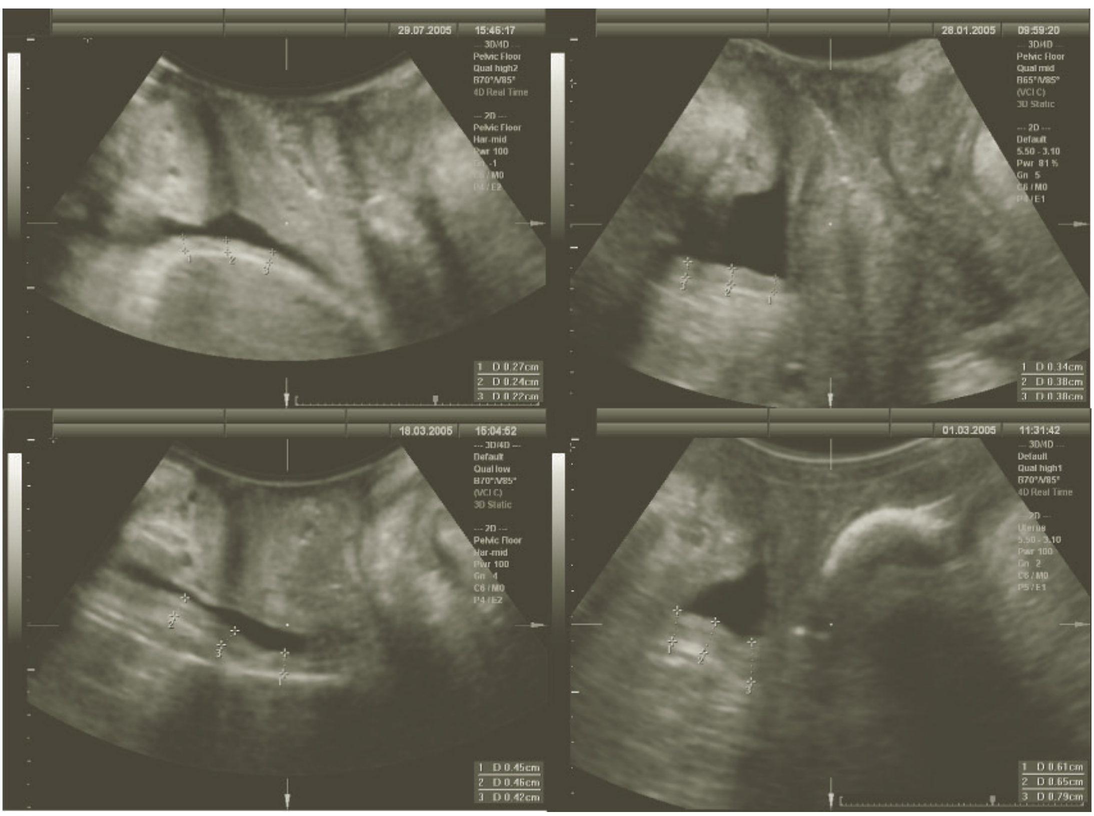

Figure 4.11. DWT as measured at the dome after bladder emptying: mean DWT is 2.5 (top left), 3.7 (top right), 4.4 (bottom left), and 6.8 (bottom right). Measurements of 5 mm and above are associated with symptoms and signs of detrusor overactivity.

There may to be an association between age and DWT,[60] which supports the hypothesis that increased DWT is indicative of acquired detrusor hypertrophy, and probably the result of years or decades of isometric contractions against a closed outlet. This is also supported by the finding that a history of nocturnal enuresis in childhood is associated with increased DWT in women seen for bladder dysfunction in later life,[61] which implies that, at least in some women, increased DWT is attributable to an underlying disorder that is either congenital or acquired in early childhood. Recently, DWT was shown to be a predictor of de novo detrusor overactivity after Burch colposuspension.[62] It is likely but remains to be proven that determination of this parameter can contribute to the workup of a patient with pelvic floor and bladder dysfunction, e.g., as a predictor of postoperative voiding function or de novo/worsened symptoms of the irritable bladder. See also Appendix Case 3 for increased DWT in a young patient with symptoms of urgency, frequency, and urge incontinence.

Levator Activity

Perineal ultrasound has been used for the quantification of pelvic floor muscle function, both in women with stress incontinence and continent controls,[63] as well as before and after childbirth.[64,65] A cranioventral shift of pelvic organs imaged in the midsagittal plane is taken as evidence of a levator contraction. The resulting displacement of the internal urethral

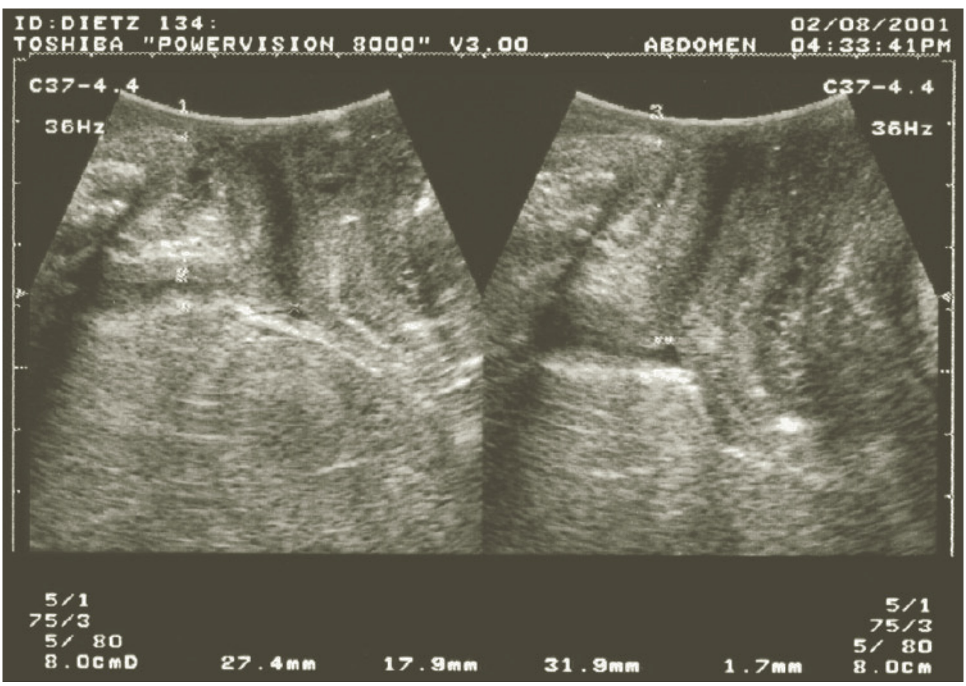

Figure 4.12. A pelvic floor muscle contraction as documented by translabial ultrasound in the midsagittal plane. The left image shows findings at rest; the right demonstrates cranioventral displacement of the bladder neck at maximal pelvic floor muscle contraction. (From Dietz HP, Ultrasound Imaging of the pelvic floor: 2D aspects. Ultrasound Obstet Gynaecol 2004; 23: 80–92, with permission.)

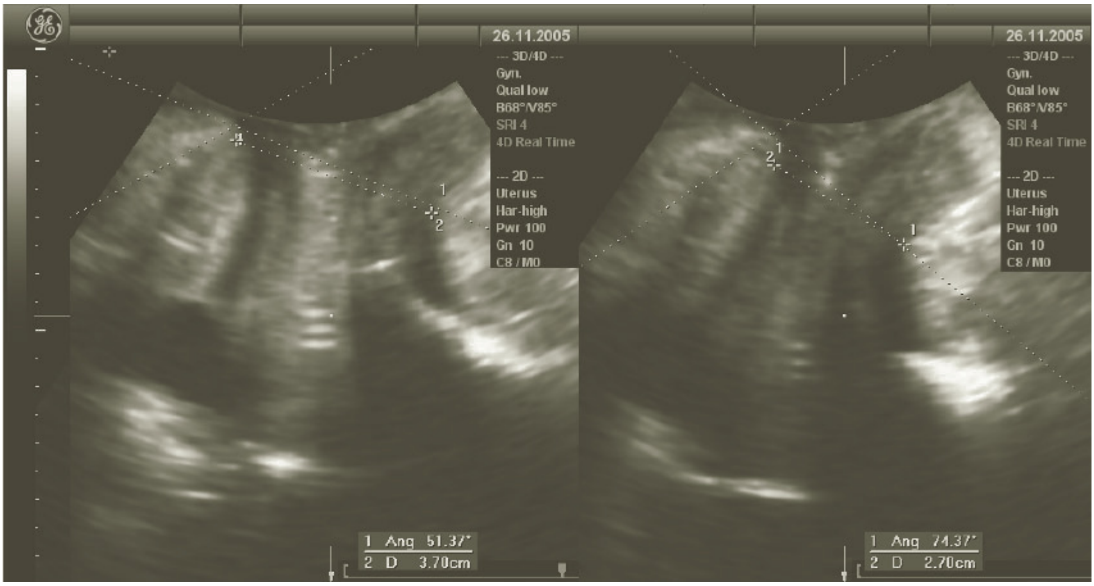

Figure 4.13. Quantification of pelvic floor muscle contraction by measuring the reduction in hiatal dimensions (from 37 to 27 mm, i.e., by 10 mm) or the increase in levator plate angle (from 51.37 to 74.37°, i.e., by 23°) on maximal pelvic floor muscle contraction.

meatus is measured relative to the inferoposterior symphyseal margin (see Figure 4.12). Case 2b of the Appendix demonstrates a pelvic floor contraction in a healthy nulliparous volunteer.

Another means of quantifying levator activity is to measure reduction of the levator hiatus in the midsagittal plane, or to determine the changing angle of the hiatal plane (the "levator plate angle") relative to the central symphyseal axis (see Figure 4.13). Narrowing of the hiatus without cranioventral displacement of the bladder neck implies that the patient has increased intraabdominal pressure while contracting the levator ani. This is a common problem and should be corrected by teaching proper technique,[66] e.g., by visual ultrasound biofeedback.[67]

Translabial ultrasound observation of pelvic floor activity has helped validate the concept of "the knack," i.e., of a reflex levator contraction immediately before increases in intraabdominal pressure such as those resulting from coughing.[68] Correlations between cranioventral shift of the bladder neck on the one hand and palpation/perineometry on the other hand have been shown to be good.[69] More recently, physiotherapists have begun to use transabdominal and translabial ultrasound to document pelvic floor muscle activity, with one author concluding that the translabial technique[70] is probably more accurate for this indication.

Prolapse Quantification

Translabial ultrasound may be used to quantify uterovaginal prolapse.[71,72] The inferior margin of the symphysis pubis serves as a convenient (if imperfect) line of reference against which the maximal descent of bladder, uterus, cul-de-sac, and rectal ampulla on Valsalva maneuver can be measured

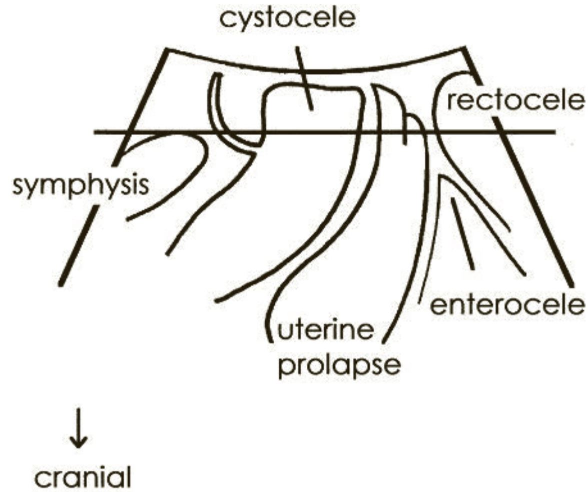

Figure 4.14. Prolapse quantification as demonstrated in a schematic drawing of ultrasound findings in the midsagittal plane. The inferior margin of the symphysis pubis is used as reference line. (From Dietz HP, Ultrasound Imaging of the pelvic floor: 2D aspects. Ultrasound Obstet Gynaecol 2004; 23: 80–92, with permission.)

(Figure 4.14) (see also Chapter 5 for uterine and posterior compartment prolapse). Because the hiatus on Valsalva is generally too large – especially in women with prolapse – to allow for simultaneous imaging of the entire symphysis pubis and the posterior compartment, it is often not possible to use a line perpendicular to the central axis of the symphysis pubis[73] as reference for descent of a rectocele or enterocele. Needless to say, procidentia or complete vaginal eversion generally preclude translabial imaging.

The main use of imaging for prolapse quantification may prove to be in outcome assessment after pelvic reconstructive surgery, both clinically and for research. The elevation (and frequently distortion) of the bladder neck arising from a colposuspension is easily documented[74,75] (see Figure 4.15 and Cases 7, 8, and 14 of the Appendix). Fascial and synthetic slings are visible posterior to the trigone or the urethra (see Chapter 7 and Cases 11 and 14 of the Appendix). Bulking agents such as Macroplastique show up anterior, lateral, and posterior to the proximal urethra (see Chapter 7). It has been demonstrated that overelevation of the bladder neck on colposuspension is unnecessary for cure of USI, and elevation may also have a bearing on postoperative symptoms of voiding dysfunction and de novo detrusor overactivity.[74,75]

Other Findings

Residual urine can conveniently be determined at the time of a routine translabial pelvic floor assessment, although the formula used for this purpose was developed for transvaginal ultrasound and has not yet been formally validated for translabial use. It may be necessary to let the patient perform a mild Valsalva maneuver to allow the most ventral part of the dome to rotate downward. The two largest diameters are measured perpendicular to each other (see Figure 4.16), and the result in centimeters is multiplied by 5.9. Deducting 14.9 gives the residual volume,[76,77] according to the formula $X * Y * 5.9 - 14.9$ = residual volume in milliliters.

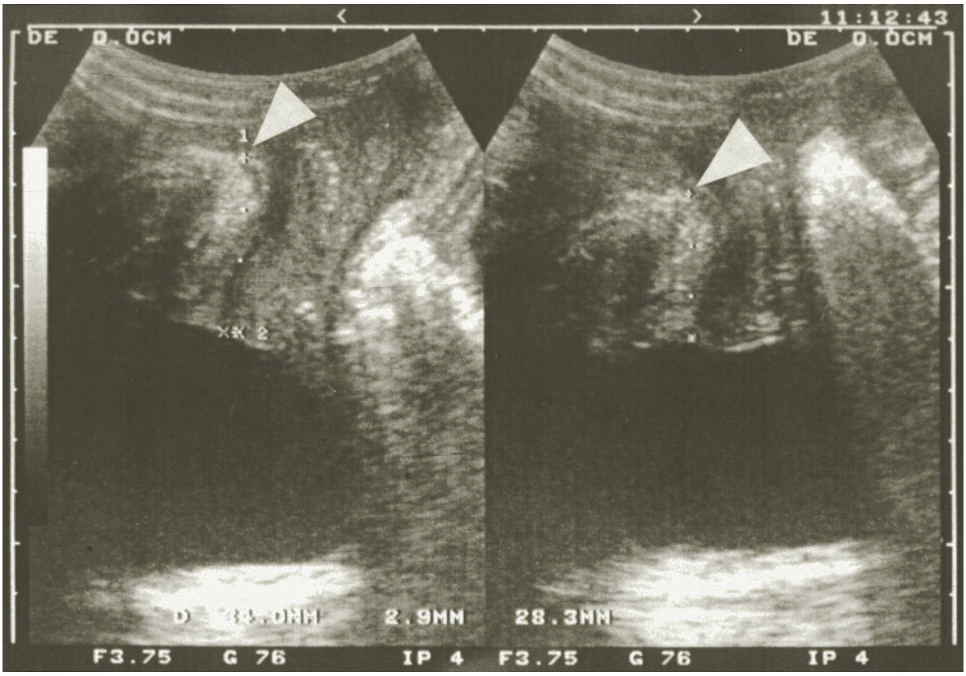

Figure 4.15. Immobilization of the bladder neck after successful Burch colposuspension, resulting in less than 6 mm of BND on Valsalva. The arrows indicate the point of reference, i.e., the inferoposterior margin of the symphysis pubis. (From Dietz HP, Ultrasound Imaging of the pelvic floor: 2D aspects. Ultrasound Obstet Gynaecol 2004; 23: 80–92, with permission.)

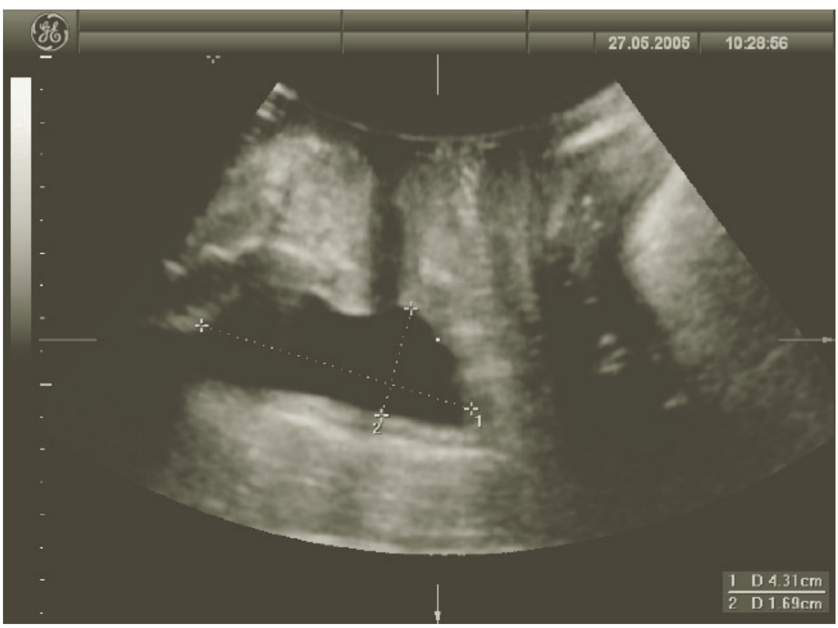

Figure 4.16. Determination of residual urine volume on translabial ultrasound. The two largest bladder diameters are measured perpendicular to each other and multiplied by 5.9. Deducting 14.9 gives residual urine volume in millimeters, in this case resulting in 4.31 * 1.69 * 5.9 − 14.9 = 28 mL.

A range of other abnormalities, incidental or expected, may at times be imaged on translabial ultrasound, although a full pelvic ultrasound assessment does of course require a transvaginal approach. Urethral diverticula[78,79] (see Figure 4.17) are unlikely to be missed, especially if the examination is performed after the patient voids, and if care is taken to inspect the paraurethral areas. Most are located dorsal to the urethra as in Figure 4.17, but occasionally one may be found ventral or anterior to the urethra, i.e., developing into the space of Retzius, as in Case 15 of the Appendix. The main differential diagnosis is Gartner cysts, i.e., a cystic remnant of the Wolffian duct located in the vaginal wall (see Figure 4.18 and Case 9 of the Appendix), but it is generally possible to differentiate the two because of their location relative to the urethra. In addition, urethral diverticula are more likely to be symptomatic and tender on examination, and often appear rather complex showing a convoluted or multicystic structure, often with internal echogenicity. Both urethral diverticula and Gartner cysts may occasionally be confused with a nabothian follicle, but correct identification of the cervix will make such a mistake highly unlikely. A Valsalva maneuver will lead to differential movement of the tissues and help in correctly attributing cystic structures to the vaginal wall, cervix, bladder, or urethra.

Finally, labial cysts may be detected close to the transducer surface in parasagittal planes, and the odd vaginal fibroma may cause circumscribed isoechoic findings within the vaginal wall. Occasionally, a bladder tumor may be found (Figure 4.19), and intravesical stents and bladder diverticula

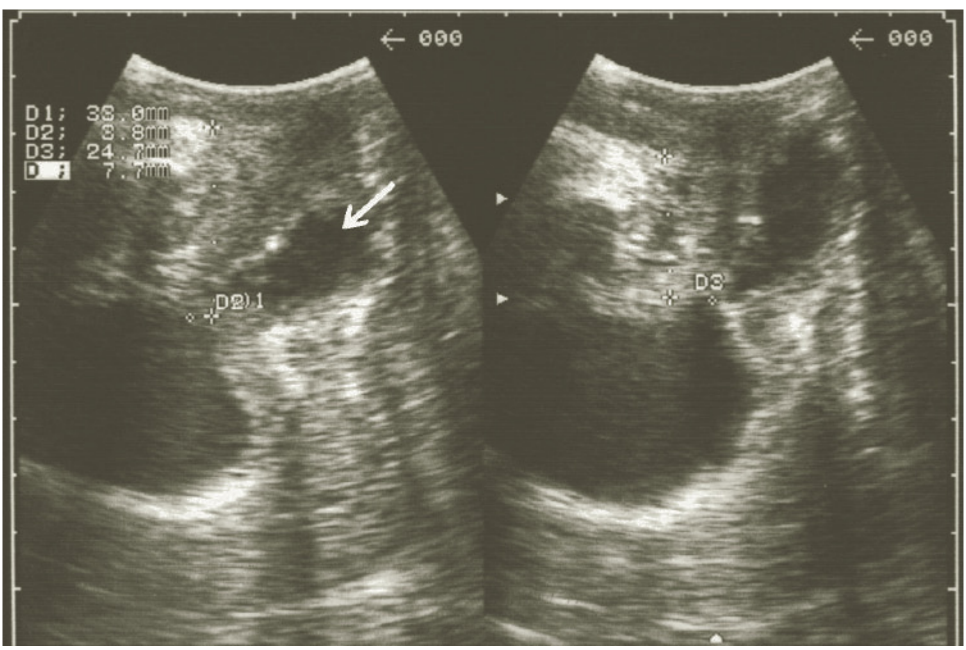

Figure 4.17. Urethral diverticulum mimicking a cystourethrocele as seen on the right image taken on maximal Valsalva. The neck of the diverticulum was situated close to the bladder neck, and this was confirmed on surgical exploration. (From Dietz HP, Ultrasound Imaging of the pelvic floor: 2D aspects. Ultrasound Obstet Gynaecol 2004; 23: 80–92, with permission.)

Figure 4.18. Gartner duct cyst (arrow) close to the bladder neck and cervix. (From Dietz HP, Ultrasound Imaging of the pelvic floor: 2D aspects. Ultrasound Obstet Gynaecol 2004; 23: 80–92, with permission.)

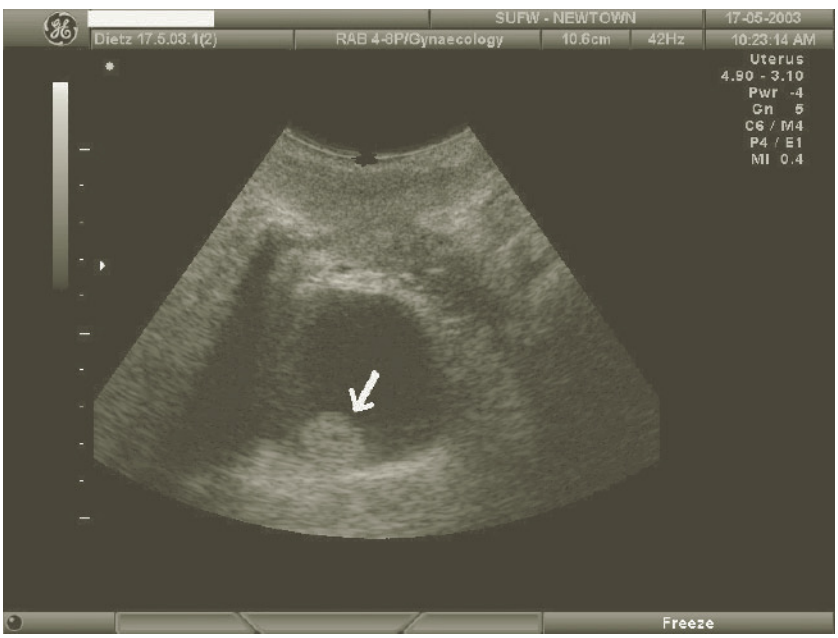

Figure 4.19. Transitional cell carcinoma (arrow) of the bladder, an incidental finding on translabial ultrasound performed for symptoms of stress incontinence. (From Dietz HP, Ultrasound Imaging of the pelvic floor: 2D aspects. Ultrasound Obstet Gynaecol 2004; 23: 80–92, with permission.)

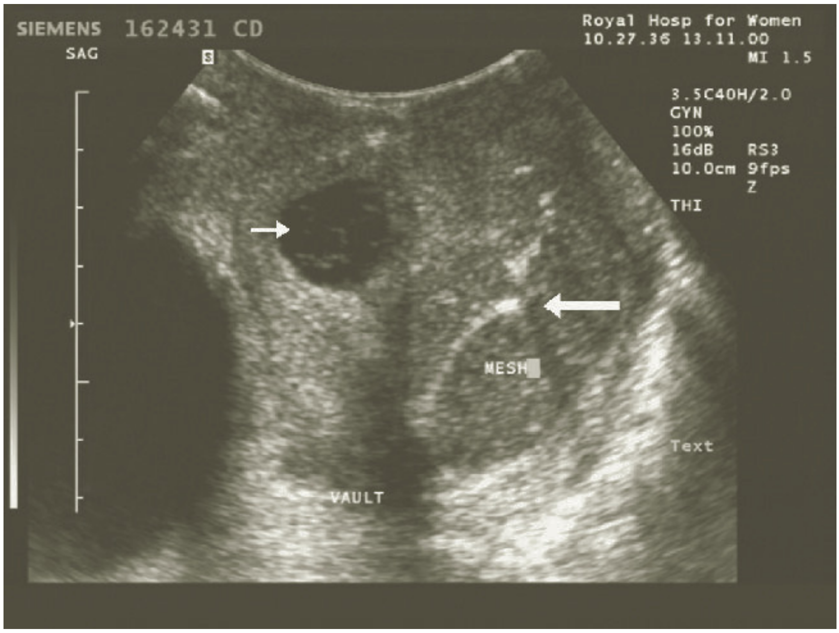

Figure 4.20. Hematoma surrounding mesh after laparoscopic sacrocolpopexy (large arrow). There is a second, smaller hematoma under a posterior colporrhaphy (small arrow). The patient was examined because of persistent postoperative voiding difficulty and pain. (From Dietz HP, Ultrasound Imaging of the pelvic floor: 2D aspects. Ultrasound Obstet Gynaecol 2004; 23: 80–92, with permission.)

can also be visualized.[38] Postoperative hematomata may be visible after vaginal surgery or suburethral slings and at times explain clinical symptoms such as voiding dysfunction or persistent pain (see Figure 4.20).

References

1. Schaer GN, Koechli OR, Schuessler B, Haller U. Perineal ultrasound: determination of reliable examination procedures. Ultrasound Obstet Gynecol 1996; 7(5):347–352.
2. Dietz HP, Wilson PD. Anatomical assessment of the bladder outlet and proximal urethra using ultrasound and videocystourethrography. Int Urogynecol J 1998;9(6):365–369.
3. Dietz HP, Wilson PD. The influence of bladder volume on the position and mobility of the urethrovesical junction. Int Urogynecol J 1999;10(1):3–6.
4. Dietz HP, Clarke B. The influence of posture on perineal ultrasound imaging parameters. Int Urogynecol J 2001;12(2):104–106.
5. Alper T, Cetinkaya M, Okutgen S, Kokcu A, Lu E. Evaluation of urethrovesical angle by ultrasound in women with and without urinary stress incontinence. Int Urogynecol J 2001;12(5):308–311.
6. Martan A, Masata J, Halaska M, Voigt R. Ultrasound imaging of the lower urinary system in women after Burch colposuspension. Ultrasound Obstet Gynecol 2001;17(1):58–64.
7. Dietz HP, Clarke B, Herbison P. Bladder neck mobility and urethral closure pressure as predictors of genuine stress incontinence. Int Urogynecol J 2002; 13(5):289–293.

8. Dietz HP, Eldridge A, Grace M, Clarke B. Test-retest reliability of the ultrasound assessment of bladder neck mobility. Int Urogynecol J 2003;14(S1):S57–S58.
9. Reed H, Waterfield A, Freeman RM, Adekanmi OA. Bladder neck mobility in continent nulliparous women: normal references. Int Urogynecol J 2002;13(suppl 1):S4.
10. Brandt FT, Albuquerque CD, Lorenzato FR, Amaral FJ. Perineal assessment of urethrovesical junction mobility in young continent females. Int Urogynecol J 2000;11(1):18–22.
11. Peschers UM, Fanger G, Schaer GN, Vodusek DB, DeLancey JO, Schuessler B. Bladder neck mobility in continent nulliparous women. Br J Obstet Gynaecol 2001;108(3):320–324.
12. Dietz HP, Eldridge A, Grace M, Clarke B. Pelvic organ descent in young nulligravid women. Am J Obstet Gynecol 2004;191:95–99.
13. Oerno A, Dietz HP. Levator co-activation is an important confounder of pelvic organ descent on Valsalva. ICS Annual Scientific Meeting 2006, Christchurch, New Zealand. Abstract.
14. van der Velde J, Laan E, Everaerd W. Vaginismus, a component of a general defensive reaction. An investigation of pelvic floor muscle activity during exposure to emotion-inducing film excerpts in women with and without vaginismus. Int Urogynecol J 2001;12(5):328–331.
15. King JK, Freeman RM. Is antenatal bladder neck mobility a risk factor for postpartum stress incontinence? Br J Obstet Gynaecol 1998;105(12):1300–1307.
16. Martan A, Masata J, Halaska M, Kasikova E, Otcenasek M, Voigt R. The effect of increasing of intraabdominal pressure on the position of the bladder neck in ultrasound imaging. Annual Meeting, International Continence Society 2001, Seoul, South Korea. Abstract.
17. Fritel X, Zabak K, Pigne A, Demaria F, Benifla JL. Predictive value of urethral mobility before suburethral tape procedure for urinary stress incontinence in women. J Urol 2002;168(6):2472–2475.
18. Liapis A, Bakas P, Lazaris D, Creatsas G. Tension-free vaginal tape in the management of recurrent stress incontinence. Arch Gynecol Obstet 2004;269(3):205–207.
19. Bakas P, Liapis A, Creatsas G. Q-tip test and tension-free vaginal tape in the management of female patients with genuine stress incontinence. Gynecol Obstet Invest 2002;53(3):170–173.
20. Masata J, Martan A, Svabik K, Drahoradova P, Pavlikova M, Hlasenska J. Changes in urethra mobility after TVT operation [article in Czech]. Ceska Gynekol 2005;70(3):220–225.
21. Dietz HP, Wilson PD. The 'iris effect': how two-dimensional and three-dimensional ultrasound can help us understand anti-incontinence procedures. Ultrasound Obstet Gynecol 2004;23(3):267–271.
22. Dietz HP, Hansell NK, Grace ME, Eldridge AM, Clarke B, Martin NG. Bladder neck mobility is a heritable trait. Br J Obstet Gynaecol 2005;112(3):334–339.
23. Dietz HP, Bennett MJ. The effect of childbirth on pelvic organ mobility. Obstet Gynecol 2003;102(2):223–228.
24. Peschers U, Schaer G, Anthuber C, DeLancey JO, Schuessler B. Changes in vesical neck mobility following vaginal delivery. Obstet Gynecol 1996;88(6):1001–1006.
25. Meyer S, De Grandi P, Hohlfeld P, Megalo A. The birth trauma: short and long term effects of forceps delivery compared to spontaneous delivery on different pelvic floor parameters. Int Urogynecol J 1999;10(S1):S1.
26. Dietz HP, Clarke B, Vancaillie TG. Vaginal childbirth and bladder neck mobility. Aust N Z J Obstet Gynaecol 2002;42(5):522–525.

27. Dietz HP, Eldridge AM, Grace ME, Clarke B. Does pregnancy affect pelvic organ mobility? Aust NZ J Obstet Gynaecol 2004;44:517–520.
28. Meyer S, De Grandi P, Schreyer A, Caccia G. The assessment of bladder neck position and mobility in continent nullipara, multipara, forceps-delivered and incontinent women using perineal ultrasound: a future office procedure? Int Urogynecol J 1996;7(3):138–146.
29. Dietz HP, Lanzarone V. Levator trauma after vaginal delivery. Obstet Gynecol 2005;106:707–712.
30. Digesu GA, Toosz-Hobson P, Bidmead J, Cardozo LD, Robinson D. Pregnancy, childbirth and urinary incontinence: Caesarean for all? Neurourol Urodyn 2000;19(4):508–509.
31. Balmforth J, Toosz-Hobson P, Cardozo L. Ask not what childbirth can do to your pelvic floor but what your pelvic floor can do in childbirth. Neurourol Urodyn 2003;22(5):540–542.
32. Dietz HP, Moore KH, Steensma AB. Antenatal pelvic organ mobility is associated with delivery mode. Aust N Z J Obstet Gynaecol 2003;43:70–74.
33. Dietz HP, Lanzarone V, Simpson JM. Predicting operative delivery. Ultrasound Obstet Gynecol 2006;27(4):409–415.
34. Schaer GN, Perucchini D, Munz E, Peschers U, Koechli OR, DeLancey JO. Sonographic evaluation of the bladder neck in continent and stress-incontinent women. Obstet Gynecol 1999;93(3):412–416.
35. Dietz HP, Clarke B. The urethral pressure profile and ultrasound imaging of the lower urinary tract. Int Urogynecol J 2001;12(1):38–41.
36. Huang WC, Yang JM. Bladder neck funneling on ultrasound cystourethrography in primary stress urinary incontinence: a sign associated with urethral hypermobility and intrinsic sphincter deficiency. Urology 2003;61(5):936–941.
37. Green TH. Urinary stress incontinence: differential diagnosis, pathophysiology, and management. Am J Obstet Gynecol 1975;122(3):378–400.
38. Tunn R, Petri E. Introital and transvaginal ultrasound as the main tool in the assessment of urogenital and pelvic floor dysfunction: an imaging panel and practical approach. Ultrasound Obstet Gynecol 2003;22:205–213.
39. Dietz HP. What's "normal" pelvic organ descent, and what's prolapse? ICS Annual Scientific Meeting 2006, Christchurch, New Zealand. Abstract.
40. Dietz HP, McKnoulty L, Clarke B. Translabial color Doppler for imaging in urogynecology: a preliminary report. Ultrasound Obstet Gynecol 1999;14:144–147.
41. Dietz HP, Clarke B. Translabial color Doppler urodynamics. Int Urogynecol J 2001;12(5):304–307.
42. Masata J, Martan A, Halaska M, Kasikova E, Otcenasek M, Voigt R. Detection of Valsalva leak point pressure with colour Doppler: new method for routine use. Neurourol Urodyn 2001;20(4):494–496.
43. Kremkau FW. Diagnostic Ultrasound: Principles and Instruments. St. Louis: WB Saunders; 2005.
44. Schaer GN, Schmid T, Peschers U, DeLancey JO. Intraurethral ultrasound correlated with urethral histology. Obstet Gynecol 1998;91(1):60–64.
45. Kuo HC. Transrectal sonographic investigation of urethral and paraurethral structures in women with stress urinary incontinence. J Ultrasound Med 1998;17(5):311–320.
46. Klein HM, Kirschner Hermanns R, Lagunilla J, Gunther RW. Assessment of incontinence with intraurethral US: preliminary results. Radiology 1993;187(1):141–143.
47. Kirschner Hermanns R, Klein HM, Mueller U, Schaefer W, Jakse G. Intraurethral ultrasound in women with stress incontinence. Br J Urol 1994;74(3):315–318.

48. Mitterberger M, Pinggera GM, Mueller T, et al. Dynamic transurethral sonography and 3D reconstruction of the rhabdosphincter and urethra. J Ultrasound Med 2006;25:315–320.
49. Huang WC, Yang JM. Transvaginal sonography in the treatment of a rare case of total urethral stenosis with a vesicovaginal fistula. J Ultrasound Med 2002; 21(4):463–467.
50. Toozs-Hobson P, Khullar V, Cardozo L. Three-dimensional ultrasound: a novel technique for investigating the urethral sphincter in the third trimester of pregnancy. Ultrasound Obstet Gynecol 2001;17(5):421–424.
51. Robinson D, Toozs Hobson P, Cardozo L, Digesu GA. Correlating structure and function: three-dimensional ultrasound of the urethral sphincter. Ultrasound Obstet Gynecol 2004;23:272–276.
52. Yang JM, Huang WC. The significance of urethral hyperechogenicity in female lower urinary tract symptoms. Ultrasound Obstet Gynecol 2004;24(1): 67–71.
53. Khullar V, Salvatore M, Cardozo L, Bourne T, Abbott D, Kelleher C. A novel technique for measuring bladder wall thickness in women using transvaginal ultrasound. Ultrasound Obstet Gynecol 1994;4:220–223.
54. Khullar V, Cardozo LD, Salvatore S, Hill S. Ultrasound: a noninvasive screening test for detrusor instability. Br J Obstet Gynaecol 1996;103(9):904–908.
55. Lekskulchai O, Dietz HP. Normal values for detrusor wall thickness in young Caucasian women. International Continence Society Annual Scientific Meeting 2005, Montreal. Abstract.
56. Robinson D, Anders K, Cardozo L, Bidmead J, Toozs-Hobson P, Khullar V. Can ultrasound replace ambulatory urodynamics when investigating women with irritative urinary symptoms? Br J Obstet Gynaecol 2002;109(2):145–148.
57. Yang JM, Huang WC. Bladder wall thickness on ultrasound cystourethrography. J Ultrasound Med 2003;22:777–782.
58. Lekskulchai O, Dietz HP. Detrusor wall thickness as a test for detrusor overactivity in women. ICS Annual Scientific Meeting 2006, Christchurch, New Zealand.
59. Soligo M, Khullar V, Salvatore S, Luppino G, Arcari V, Milani R. Overactive bladder definition and ultrasound measurement of bladder wall thickness: the right way without urodynamics. Neurourol Urodyn 2002;21(4):284–285.
60. Vella M, Parsons M, Cardozo L. Does bladder wall thickness increase with age? Int Urogynecol J 2005;16(S2):S100.
61. Lekskulchai O, Dietz HP. Detrusor wall thickness in women with a history of childhood nocturnal enuresis. ICS Annual General Meeting 2006, Christchurch, New Zealand. Abstract.
62. Robinson D, Khullar V, Cardozo L. Can bladder wall thickness predict postoperative detrusor overactivity? Int Urogynecol J 2005;16(S2):S106.
63. Wijma J, Tinga DJ, Visser GH. Perineal ultrasonography in women with stress incontinence and controls: the role of the pelvic floor muscles. Gynecol Obstet Invest 1991;32(3):176–179.
64. Peschers UM, Schaer GN, DeLancey JO, Schuessler B. Levator ani function before and after childbirth. Br J Obstet Gynaecol 1997;104(9):1004–1008.
65. Dietz HP. Levator function before and after childbirth. Aust N Z J Obstet Gynaecol 2004;44(1):19–23.
66. Bo K, Larson S, Oseid S, Kvarstein B, Hagen R, Jorgensen J. Knowledge about and ability to do correct pelvic floor muscle exercises in women with urinary stress incontinence. Neurourol Urodyn 1988;7:261–262.
67. Dietz HP, Wilson PD, Clarke B. The use of perineal ultrasound to quantify levator activity and teach pelvic floor muscle exercises. Int Urogynecol J Pelvic Floor Dysfunct 2001;12(3):166–168.

68. Miller JM, Perucchini D, Carchidi LT, DeLancey JO, Ashton-Miller J. Pelvic floor muscle contraction during a cough and decreased vesical neck mobility. Obstet Gynecol 2001;97(2):255–260.
69. Dietz HP, Jarvis SK, Vancaillie TG. The assessment of levator muscle strength: a validation of three ultrasound techniques. Int Urogynecol J 2002;13(3): 156–159.
70. Thompson J, O'Sullivan PB, Briffa K, Neumann P, Court S. Assessment of pelvic floor movement using transabdominal and transperineal ultrasound. Int Urogynecol J Pelvic Floor Dysfunct 2005;16(4):285–292.
71. Creighton SM, Pearce JM, Stanton SL. Perineal video-ultrasonography in the assessment of vaginal prolapse: early observations. Br J Obstet Gynaecol 1992;99(4):310–313.
72. Dietz HP, Haylen BT, Broome J. Ultrasound in the quantification of female pelvic organ prolapse. Ultrasound Obstet Gynecol 2001;18(5):511–514.
73. Schaer GN, Koelbl H, Voigt R, et al. Recommendations of the German Association of Urogynecology on functional sonography of the lower female urinary tract. Int Urogynecol J 1996;7(2):105–108.
74. Bombieri L, Freeman RM. Do bladder neck position and amount of elevation influence the outcome of colposuspension? Br J Obstet Gynaecol 2003;110(2): 197–200.
75. Viereck V, Pauer HU, Bader W, et al. Introital ultrasound of the lower genital tract before and after colposuspension: a 4-year objective follow-up. Ultrasound Obstet Gynecol 2004;23(3):277–283.
76. Haylen BT, Frazer MI, Sutherst JR, West CR. Transvaginal ultrasound in the assessment of bladder volumes in women. Preliminary report. Br J Urol 1989; 63(2):149–151.
77. Haylen BT. Verification of the accuracy and range of transvaginal ultrasound in measuring bladder volumes in women. Br J Urol 1989;64(4):350–352.
78. Mouritsen L, Bernstein I. Vaginal ultrasonography: a diagnostic tool for urethral diverticulum. Acta Obstet Gynecol Scand 1996;75(2):188–190.
79. Tunn R, Bergmann-Hensel U, Beyersdorff D, Heinrich G, Fischer W, Hamm B. Diagnosis of urethral diverticula and periurethral masses [article in German]. Rofo 2001;173(2):109–114.

5

The Central and Posterior Compartments

Anneke B. Steensma

Prolapse Assessment

Translabial ultrasound has been utilized for prolapse quantification, not just for the anterior compartment, but in the assessment of central and posterior compartment as well.[1,2] The uterus itself may be difficult to identify because it is iso- to hypoechoic, similar to vaginal tissues. A specular (line-like) echo often indicates the leading edge of the cervix. At times, nabothian follicles help with identification of the cervix, but in postmenopausal women the uterus may be so small as to be virtually invisible on translabial imaging, even if there is significant descent. The same holds true for a retroverted uterus, especially if significant rectal contents or a rectocele shadow the area of interest, and a well-supported uterus may be outside the field of view, in particular if higher-frequency transducers are used. Needless to say, a full sonographic assessment of the uterus requires transvaginal scanning. Despite all those limitations, however, the cervix can often be located translabially (see Figure 5.1 for a second-degree uterine prolapse), and the same holds true for the apex of the vault after hysterectomy (see Figure 5.2).

The bladder neck or the leading edge of a cystocele is used for the quantification of anterior vaginal wall descent, the cervix or Pouch of Douglas for the central compartment, and the most caudal aspect of the rectal ampulla – or the leading edge of rectocele contents – for quantification of posterior compartment descent. The inferior margin of the symphysis pubis anchors a horizontal line of reference against which descent can be measured (see Figures 5.1 and 5.5). Ultrasound quantification of central and anterior compartments seems to agree well with clinical prolapse assessment by the prolapse quantification system of the international continence society (ICS POP-Q)[3], with correlations of $r = 0.77$ for uterine prolapse, $r = 0.72$ for anterior vaginal wall, and $r = 0.53$ for posterior vaginal wall prolapse described in a comparative study.[2] The vault after hysterectomy may also be visualized in the midsagittal plane (see Figure 5.2), but can be difficult to identify, especially if there is a rectocele or if the ampulla is unusually full.

Descent of the posterior compartment is associated with symptoms of prolapse, although the correlation is not as strong as for the anterior com-

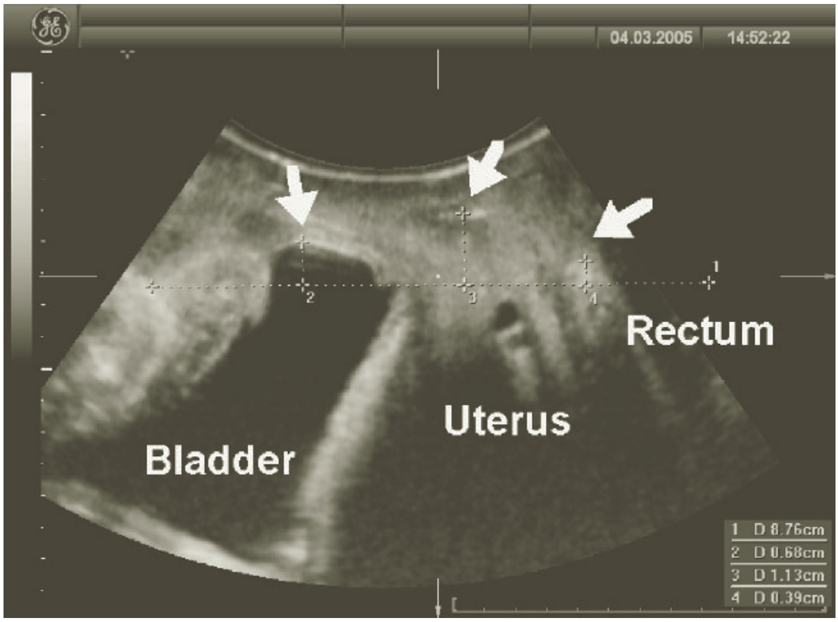

Figure 5.1. Prolapse quantification by transperineal ultrasound. Measurements are against a horizontal line through the inferior margin of the symphysis pubis. Clinically there is a second-degree cystocele and second-degree uterine prolapse.

partment. In women with isolated posterior compartment prolapse, descent of the rectal ampulla or of rectocele contents to 15 mm below the symphysis or below seems to be associated with symptoms of prolapse and has been proposed as a cutoff for "significant descent" on the basis of receiver operator curve characteristics (see Figure 5.3).[4]

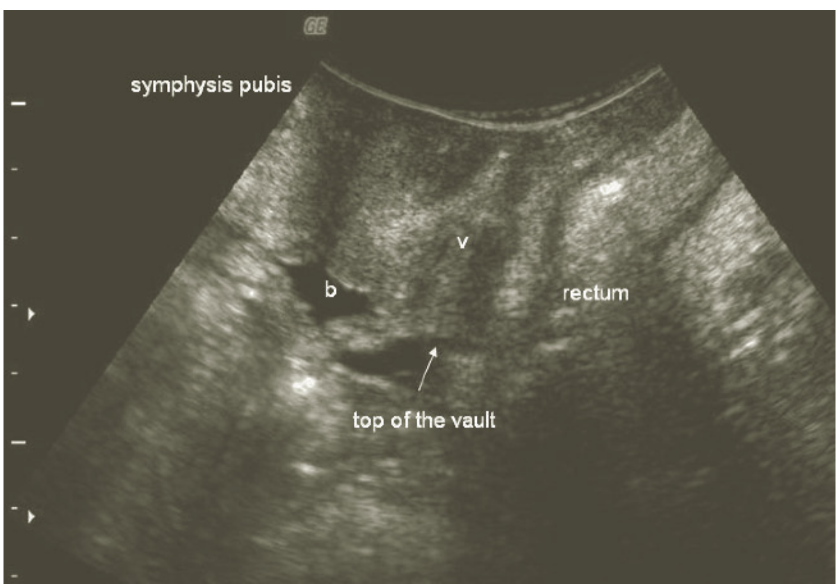

Figure 5.2. The midsagittal plane at rest in a patient after abdominal hysterectomy (v = vagina, b = bladder). The pouch of Douglas is outlined by intraperitoneal fluid.

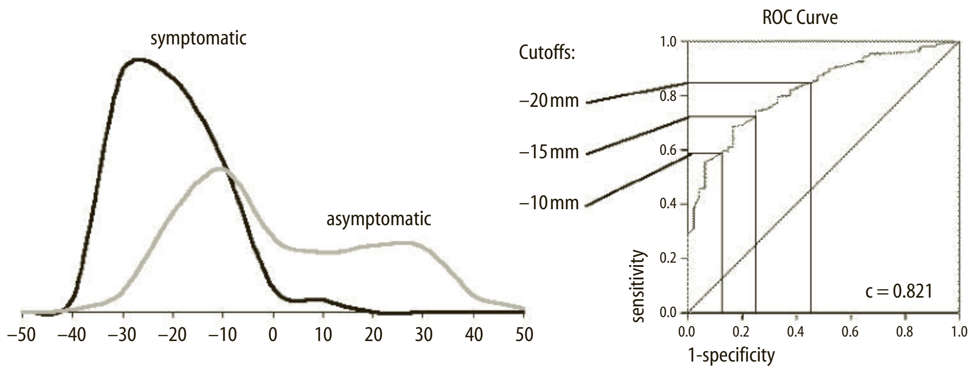

Figure 5.3. Histograms for maximum rectal descent relative to the inferoposterior margin of the symphysis pubis, in millimeters (left) in asymptomatic (gray) and symptomatic women (black) and receiver operator curve (ROC) for rectal descent as a test for symptomatic prolapse (right). Lines define proposed cutoffs.

Anterior Rectocele

Correlations between clinical prolapse grading and ultrasound may not be quite as good for the posterior compartment as they are for cystocele or uterine descent, but it is possible to distinguish between "true" and "false" rectocele, i.e., a defect of the rectovaginal septum (see Figure 5.4) and increased distensibility of the septum and/or perineal hypermobility without fascial defects[5] (see Figure 5.5). This distinction matters, because both entities may produce symptoms of prolapse, but only "true" rectoceles are associated with symptoms of straining at stool, incomplete bowel emptying, and vaginal digitation, i.e., symptoms of obstructed defecation.[6]

The traditional distinction among low, midlevel, and high rectocele[7] is not supported by ultrasound data. From experience to date, "true

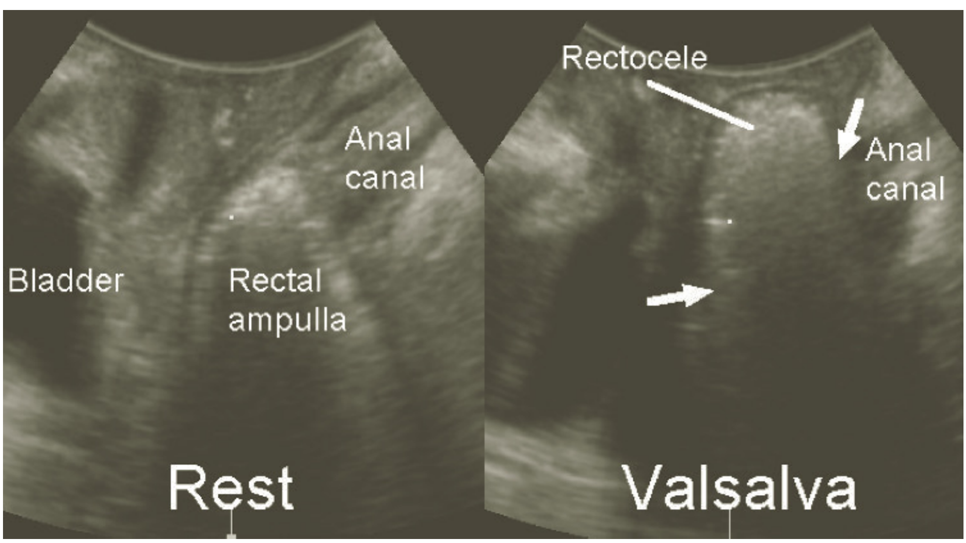

Figure 5.4. "True" rectocele with an obvious rectovaginal septal defect apparent on Valsalva, measuring about 25 mm in depth. The presumptive margins of the defect are indicated by arrows.

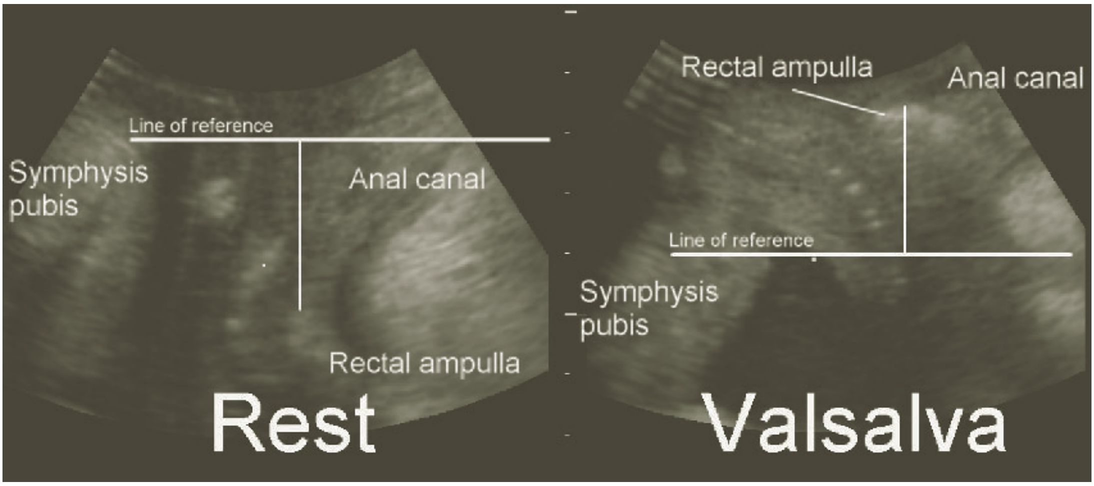

Figure 5.5. Descent of the rectal ampulla without actual herniation of rectal contents into the vagina, termed "perineal hypermobility." (From Dietz HP, Steensma AB. Posterior compartment prolapse on two-dimensional and three-dimensional pelvic floor ultrasound: the distinction between true rectocele, perineal hypermobility and enterocele. Ultrasound Obstet Gynaecol 2005; 26: 73–77, with permission.)

rectoceles" or fascial defects seem to almost always be found in the same area, i.e., very close to the anorectal junction, and they are usually transverse. Quantification involves measurement of rectocele depth, using a line extending the cranioventral aspect of the internal anal sphincter as a baseline from which to measure the maximal depth of the herniation,[5] as shown in Figures 5.6 and 5.10. Rendered volumes at the level of the hiatus in the

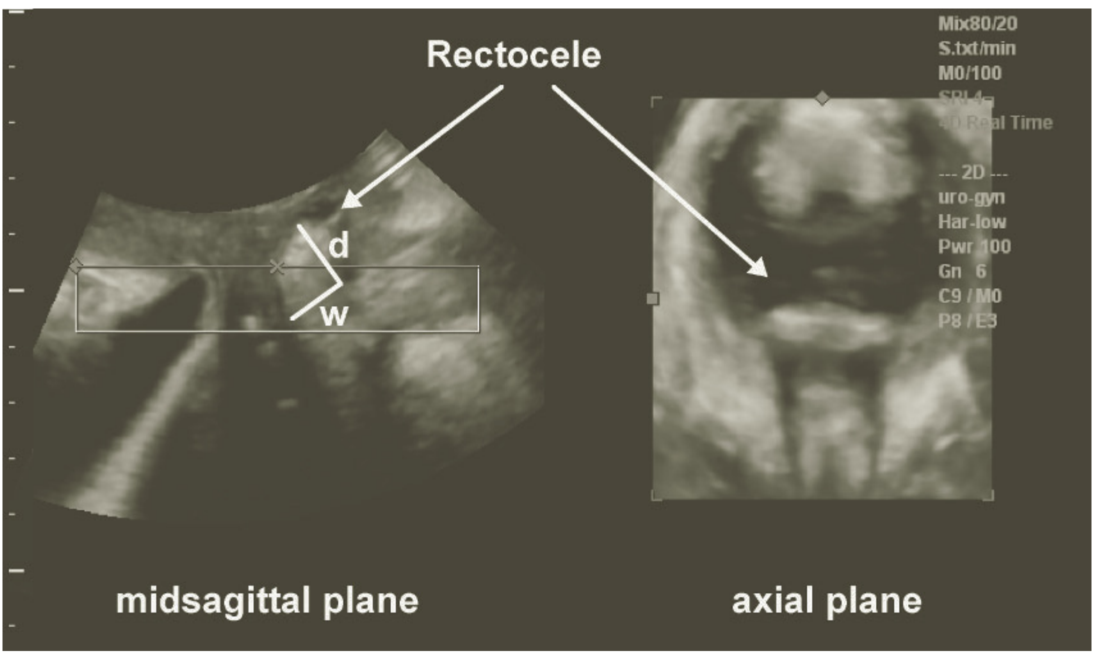

Figure 5.6. Small but typical defect of the rectovaginal septum at the level of the anorectal junction, imaged in the midsagittal plane (left) and as seen on a rendered volume in the axial plane (right); d = depth, w = width.

axial plane, or C plane imaging in general, can show the total extent of the defect and demonstrate asymmetries (see Figure 5.6).

True rectoceles may be present in young nulliparous women,[8] but they are more common in the parous.[5] In some women, they clearly arise in childbirth, and if they are present before the delivery, defects tend to enlarge.[9] Many are asymptomatic, but there is a significant association between bowel symptoms such as incomplete bowel emptying and manual evacuation on the one hand, and the presence and depth of defects on the other hand.[6] Routine posterior repair often results in reduction or distortion of such defects, without achieving actual closure. Defect-specific repair tends to be more effective in closing defects but may not affect concomitant perineal hypermobility. Major levatorplasty, as frequently performed in the past, often creates a hyperechogenic scar plate in front of the defect.

Posterior Rectocele

Posterior rectocele is said to be a common finding in children with constipation and evacuatory dysfunction but is rarely seen in adults. As in anterior rectocele, the area of defect is very close to the anorectal junction, but seems to develop posteriorly or dorsally (see Figure 5.7). At times, appearances are suggestive of an intussusception of the anal canal into the rectum.

Enterocele

One of the main advantages of translabial ultrasound is the ease with which rectocele can be distinguished from enterocele.[5] The latter is diagnosed if there is a herniation of fluid-containing peritoneum, small bowel, sigmoid,

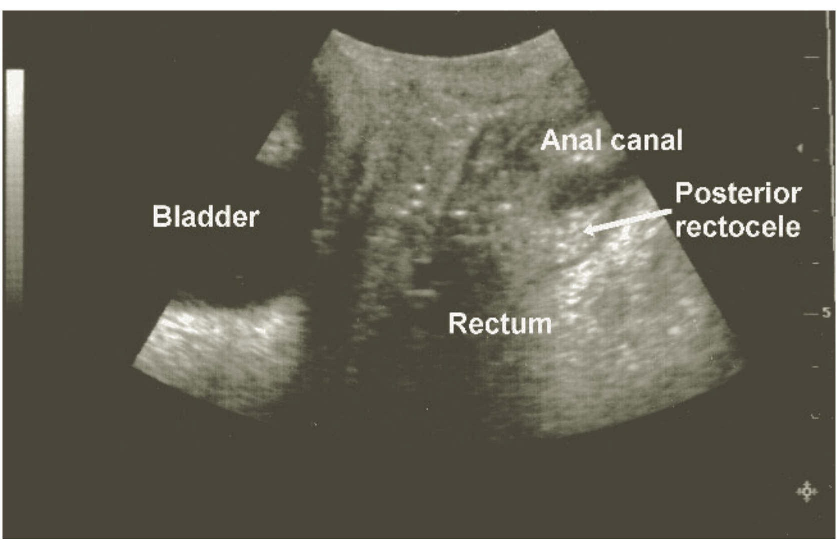

Figure 5.7. Posterior rectocele at the level of the anorectal junction.

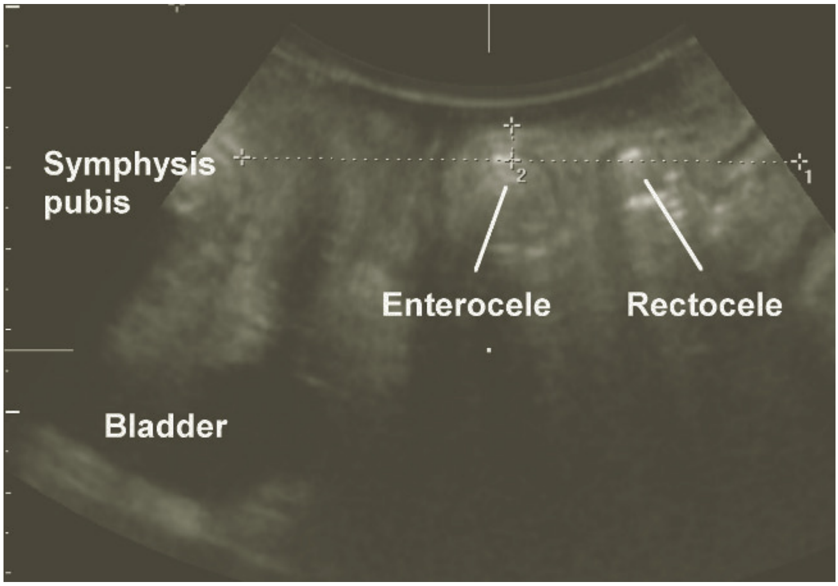

Figure 5.8. Enterocele as demonstrated in the midsagittal plane on maximal Valsalva. The herniation is filled by a loop of small bowel, giving a bull's eye–like appearance. Peristalsis often puts the diagnosis beyond doubt. In this patient, there also is a small rectocele.

or omentum anterior to the anorectal junction, separating the vagina from the rectal ampulla (see Figure 5.8). Hysterectomy is considered to be the main risk factor for enterocele, and the majority of patients will have other concomitant pelvic floor abnormalities.

Enterocele is frequently overlooked on clinical examination, and its relation to pelvic floor symptoms remains unclear. At defecogram, multiorgan opacification is necessary for the diagnosis of enterocele, and this exposes the patient to a relatively high dose of radiation. Magnetic resonance imaging (MRI) has the advantage of demonstrating all compartments as well as the capability to perform a limited dynamic investigation, but MRI is expensive and not widely available.

With transperineal imaging it is relatively easy to detect enterocele. In the midsagittal plane, a maximal Valsalva will demonstrate downward movement of iso- to hyperechoic abdominal contents anterior to the anorectal junction, with or without vault prolapse. Small bowel peristalsis may help with the identification of structures filling the hernia (see Figure 5.8).

Functional Imaging

Most recently, colorectal surgeons have started to use translabial ultrasound to complement or replace defecography, although it seems that first attempts have involved the use of contrast medium.[10,11] It is very likely that ultrasound will become useful in the clinical assessment of women with symptoms of obstructed defecation. Not just rectocele (anterior or poste-

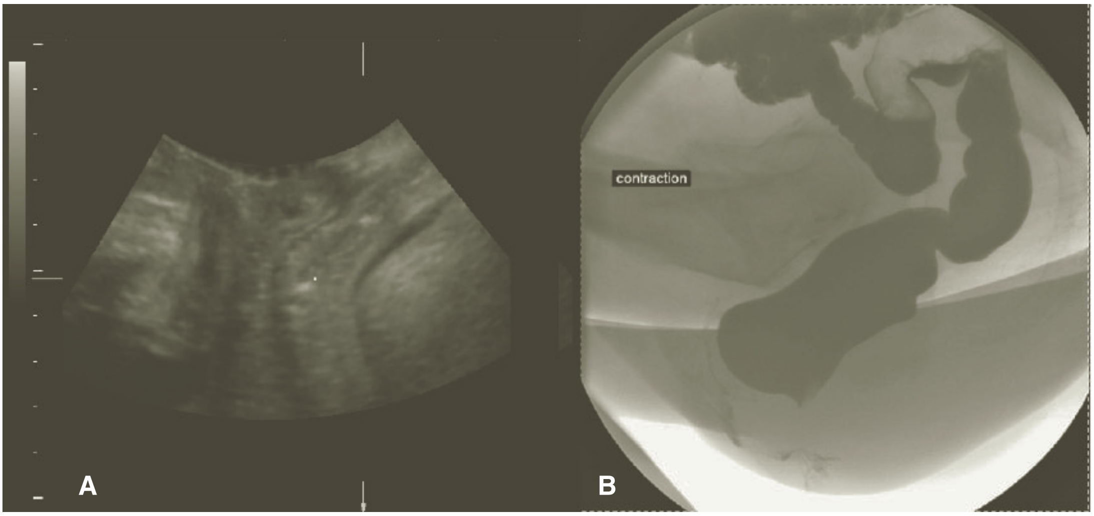

Figure 5.9. Comparison of 3D translabial ultrasound **(A)** and defecogram **(B)** at maximum levator contraction in a 57-year-old patient.

rior) and enterocele can be demonstrated using dynamic 2D or 3D ultrasound, anismus may be evident as a spastic levator that does not allow descent of pelvic structures during Valsalva. As in conventional proctography, it is possible to measure the anorectal angle to assess the levator ani complex during contraction and relaxation of the pelvic floor and at straining. Figures 5.9 and 5.10 show comparisons of translabial ultrasound and defecation proctography, on levator contraction (Figure 5.9) and on maximal Valsalva (Figure 5.10), in a patient with symptoms of obstructed defecation and a large rectocele.

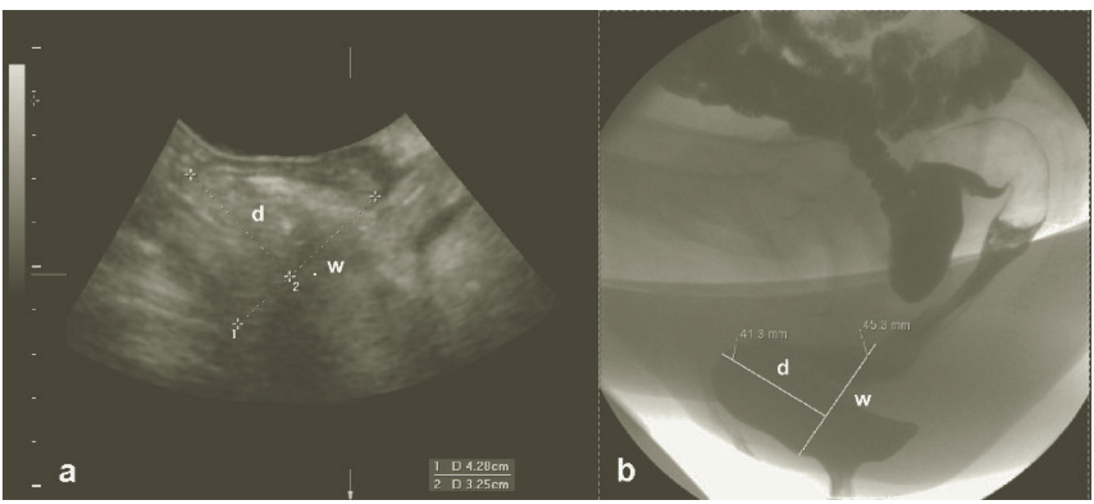

Figure 5.10. Large rectocele as seen on maximal Valsalva, in the same patient as in Figure 5.9. Both methods demonstrate a rectocele of more than 3 cm in depth.

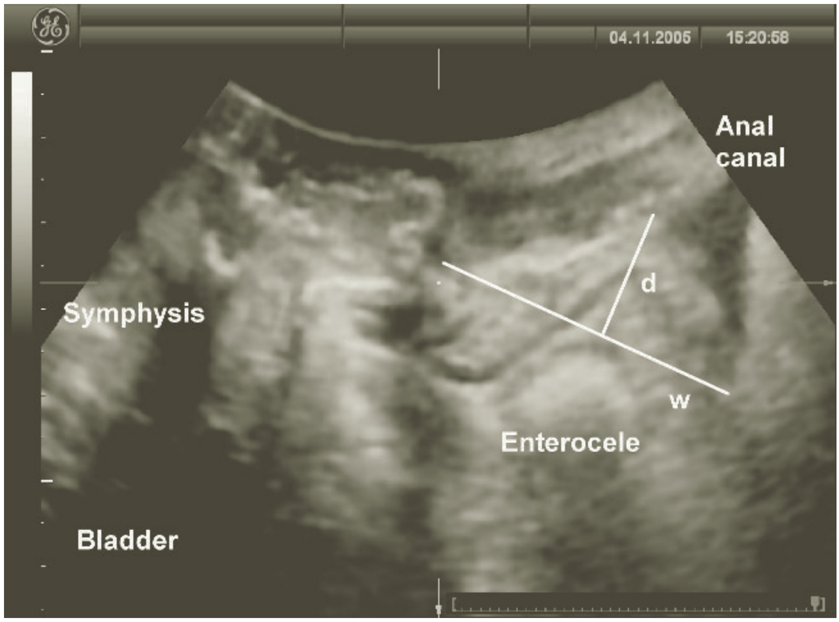

Figure 5.11. Incipient rectal prolapse in a patient after vaginal vault suspension and enterocele repair.

Rectal Intussusception and Rectal Prolapse

On functional pelvic floor ultrasound imaging, rectal intussusception or occult rectal prolapse is occasionally demonstrated in women without any symptoms of evacuatory dysfunction. However, the method is also capable of demonstrating symptomatic rectal prolapse. Normally, the anal canal is tubular, with little difference between luminal diameters along most of its length (see, e.g., Figures 5.9 and 5.10). In less marked cases of rectal intussusception or "occult" prolapse, rectal wall and small bowel enter the proximal anal canal, forcing it open and producing an arrow-shaped distension on Valsalva (see Figures 5.11 and 5.12). This appearance is pathognomonic

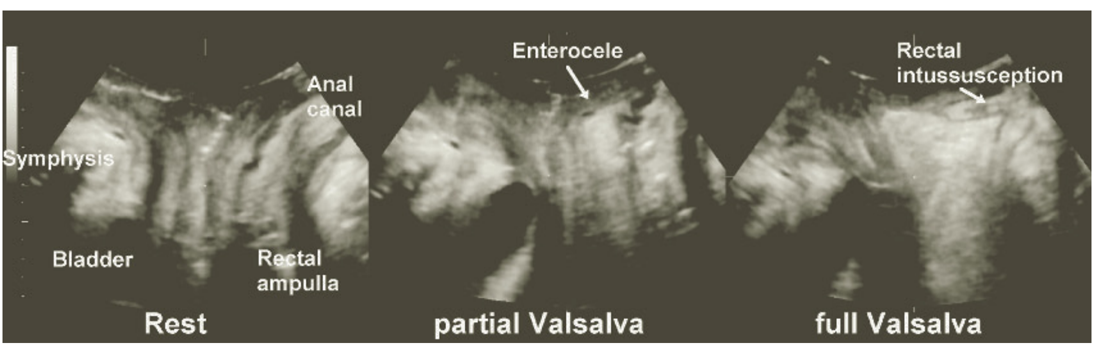

Figure 5.12. Development of a rectal intussusception on Valsalva: There is an enterocele which initially compresses the rectal ampulla (central image) and then invaginates the rectal mucosa and muscularis (right image) into the anal canal which opens up in a typical conical configuration.

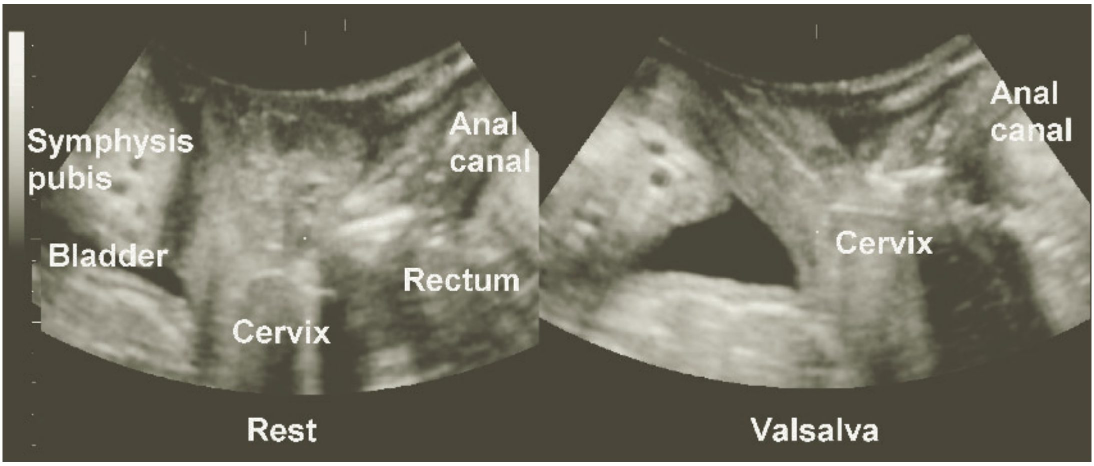

Figure 5.13. First-degree uterine descent, with the cervix "plugging" the anal canal in a patient with obstructed defecation.

and very similar to images obtained on defecation proctography.[12] If there is overt rectal prolapse, the enterocele will be seen to "flow" through the anal canal, inverting rectal mucosa, until the prolapse exits through the external anal sphincter. The maximal depth of an intussusception may be measured by connecting the most proximal aspects of the internal anal sphincter and measuring to the apex of the intussusception (see Figure 5.11).

Apart from rectocele and rectal intussusception or prolapse, pelvic floor ultrasound may identify other, less common causes of obstructed defecation. It appears that an abnormally mobile anteverted uterus may impinge on the rectal ampulla and virtually "plug" it on Valsalva, a situation that is termed a "colpocele" by colorectal surgeons (see Figure 5.13). This may cause the sensation of incomplete emptying and prompt the patient to strain at stool – which only makes matters worse, similar to the situation in rectal intussusception. There may be no other finding that more graphically illustrates how much we still have to learn about pelvic floor function – and how much pelvic floor ultrasound can teach us as well as our patients. Once the situation is demonstrated to the patient on imaging, attempts at behavior modification may well be much more likely to succeed.

Clearly, much work will have to be done in defining the role of the new method in the evaluation of women with obstructed defecation, in particular in comparison with defecation proctography.

Anal Sphincter Imaging

The anal sphincter is generally imaged by endoanal ultrasound, using high-resolution probes with a field of vision of 360°. This method is firmly established as one of the cornerstones of a colorectal diagnostic workup for anal incontinence and covered extensively in the colorectal and radiologic literature.[13–18] Because of the limited availability of such probes in gynecology, obstetricians and gynecologists have taken to using high-frequency curved array probes placed exoanally, i.e., transperineally,[19–21] in the coronal rather than the midsagittal plane as described for all other applications in this text.

There are advantages to this approach – not just from the point of view of the patient. Exoanal imaging reduces distortion of the anal canal and allows dynamic evaluation of the anal sphincter and mucosa at rest and on sphincter contraction, which seems to enhance the definition of muscular defects. However, resolutions may be inferior,[22] and good comparative studies are still lacking.

Figure 5.14 demonstrates normal appearances on translabial imaging of the anal sphincter complex in the coronal plane. The mucosa is visualized as a hyperechoic area, often star-shaped, representing the folds of the empty anal canal.[20] The internal anal sphincter (IAS) is seen as a hypoechoic ring, the external anal sphincter (EAS) as an echogenic structure surrounding the internal sphincter.[19–21] There may be some variation of appearances depending on age and hormonal status.[13] On contraction, the anal canal narrows slightly, the mucosal star may be less pronounced, and defects of the sphincter will become more obvious.

Anal sphincter injuries seem to occur much more frequently than previously reported, although this may well be attributable to ineffective intrapartum detection rather than covered, truly "occult" defects.[23] On ultrasound, sphincter defects appear as a discontinuity of the ring structures of the EAS and/or IAS. In the coronal plane, defects are conveniently described using a clock face notation. In the longitudinal plane, sphincter defects can be described by measuring the length of the defect relative to total sphincter length.

After repair of third- and fourth-degree tears, ultrasound frequently demonstrates residual defects (see Figures 5.15–5.17), and the extent of

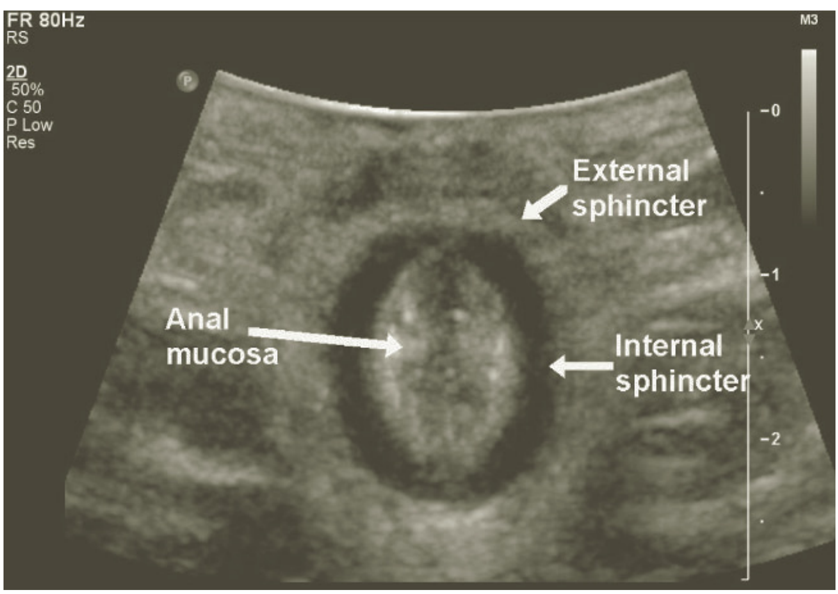

Figure 5.14. Translabial imaging of a normal anal sphincter at rest.

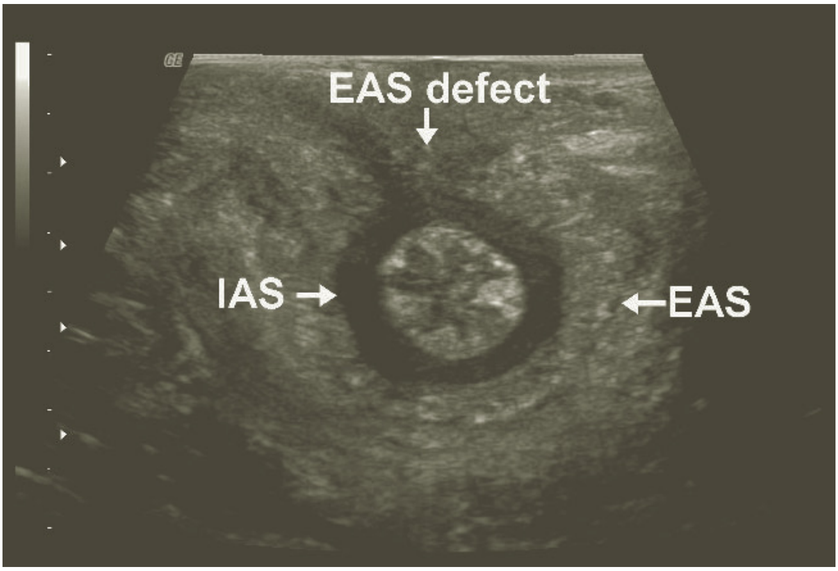

Figure 5.15. Full-thickness defect in the external anal sphincter (EAS) complex from 11 to 12 o'clock, as visualized with translabial ultrasound in the transverse or coronal plane. IAS = internal anal sphincter.

such incompletely or inadequately repaired defects seems associated with decreased sphincter pressures and an increased risk of anal incontinence.[24]

Childbirth and obstetric trauma is by far the dominant cause of anal sphincter defects. The main risk factor is considered to be instrumental vaginal delivery.[25] Anal incontinence is common after third- and fourth-degree tears, even if they are recognized and repaired at the time of injury, and can have a devastating effect on a woman's quality of life. The condition may have been underreported because of the social stigma involved. Early

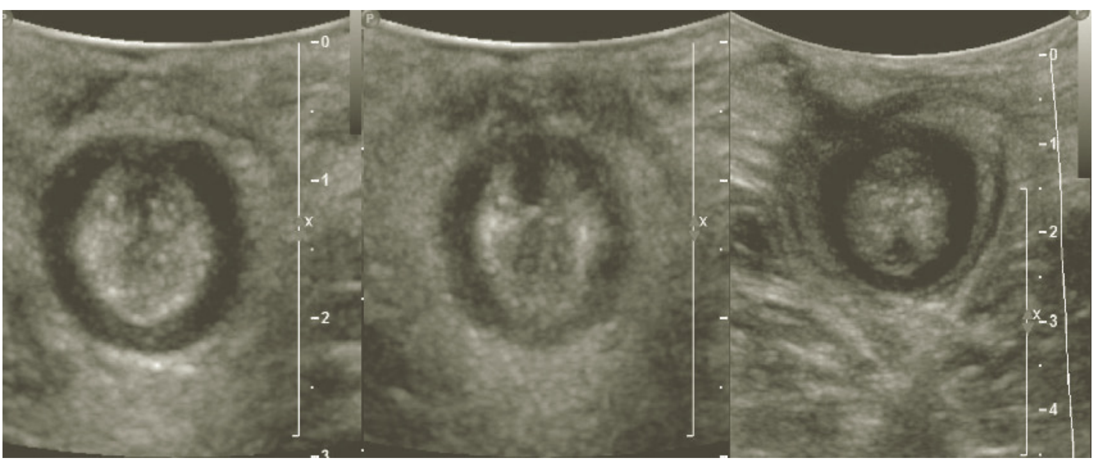

Figure 5.16. Varying appearances 6–8 weeks after repair of third-degree tears.

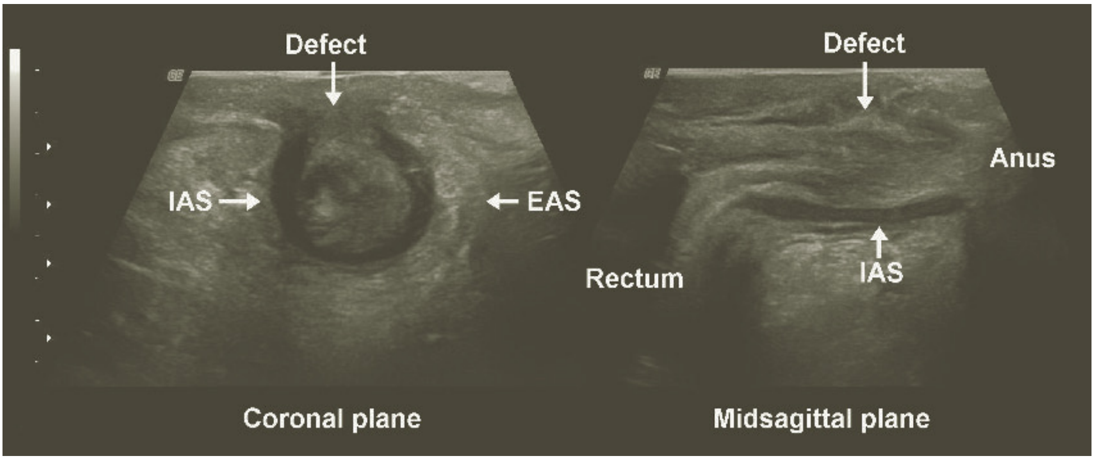

Figure 5.17. Defect of the internal and external sphincter complex as visualized in the transverse (coronal) (left) from 11 to 1 o'clock and in 50% of the IAS visualized in the longitudinal plane (midsagittal) (right) in a 60-year-old woman complaining of severe fecal incontinence.

recognition and repair of sphincter injuries are likely to be of benefit.[26] Pelvic floor ultrasound may well have a major role in the evaluation of patients after traumatic delivery, but further studies are needed to define the role of exoanal in comparison to endoanal ultrasound.

References

1. Creighton SM, Pearce JM, Stanton SL. Perineal video-ultrasonography in the assessment of vaginal prolapse: early observations. Br J Obstet Gynaecol 1992; 99(4):310–313.
2. Dietz HP, Haylen BT, Broome J. Ultrasound in the quantification of female pelvic organ prolapse. Ultrasound Obstet Gynecol 2001;18(5):511–514.
3. Bump RC, Mattiasson A, Bo K, et al. The standardization of terminology of female pelvic organ prolapse and pelvic floor dysfunction. Am J Obstet Gynecol 1996;175(1):10–17.
4. Dietz HP. What's "normal" pelvic organ descent, and what's prolapse? ICS Annual Scientific Meeting 2006, Christchurch, New Zealand.
5. Dietz HP, Steensma AB. Posterior compartment prolapse on two-dimensional and three-dimensional pelvic floor ultrasound: the distinction between true rectocele, perineal hypermobility and enterocele. Ultrasound Obstet Gynecol 2005;26:73–77.
6. Dietz HP, Korda A. Which bowel symptoms are most strongly associated with a true rectocele? Aust N Z J Obstet Gynaecol 2005;45:505–508.
7. Davis K, Kumar D. Posterior pelvic floor compartment disorders. Best Pract Res Clin Obstet Gynaecol 2006;19(6):941–958.
8. Dietz HP, Clarke B. Prevalence of rectocele in young nulliparous women. Aust N Z J Obstet Gynaecol 2005;45(5):391–394.
9. Dietz HP, Steensma AB. The role of childbirth in the actiology of rectocele. Br J Obstet Gynaecol 2006;13:264–267.
10. Beer-Gabel MMD. Dynamic transperineal ultrasound in the diagnosis of pelvic floor disorders: pilot study. Dis Colon Rectum 2002;45(2):239–248.
11. Beer-Gabel M, Teshler M, Schechtman E, Zbar AP. Dynamic transperineal ultrasound vs. defecography in patients with evacuatory difficulty: a pilot study. Int J Colorectal Dis 2004;19(1):60–67.

12. Mellgren A, Bremmer S, Johansson C, et al. Defecography. Results of investigations in 2816 patients. Dis Colon Rectum 1994;37(11):1133–1141.
13. Starck M, Bohe M, Fortling B, Valentin L. Endosonography of the anal sphincter in women of different ages and parity. Ultrasound Obstet Gynecol 2005; 25(2):169–176.
14. Damon H, Henry L, Bretones S, Mellier G, Minaire Y, Mion F. Postdelivery anal function in primiparous females: ultrasound and manometric study. Dis Colon Rectum 2000;43(4):472–477.
15. Williams AB, Bartram CI, Halligan S, et al. Alteration of anal sphincter morphology following vaginal delivery revealed by multiplanar anal endosonography. BJOG 2002;109(8):942–946.
16. Gold DM, Bartram CI, Halligan S, Humphries KN, Kamm MA, Kmiot WA. Three-dimensional endoanal sonography in assessing anal canal injury. Br J Surg 1999;86(3):365–370.
17. Frudinger A, Bartram CI, Halligan S, Kamm M. Examination techniques for endosonography of the anal canal. Abdom Imaging 1998;23(3):301–303.
18. Schaefer A, Enck P, Fuerst G, Kahn T, Frieling T, Luebke HJ. Anatomy of the anal sphincters. Comparison of anal endosonography to magnetic resonance imaging. Dis Colon Rectum 1994;37(8):777–781.
19. Peschers UM, DeLancey JO, Schaer GN, Schuessler B. Exoanal ultrasound of the anal sphincter: normal anatomy and sphincter defects. Br J Obstet Gynaecol 1997;104(9):999–1003.
20. Timor-Tritsch IE, Monteagudo A, Porges RF, Santos R. Simple ultrasound evaluation of the anal sphincter in female patients using a transvaginal transducer. Ultrasound Obstet Gynecol 2005;25(2):177–183.
21. Yagel S, Valsky DV. Three-dimensional transperineal sonography for evaluation of the anal sphincter complex: another dimension in understanding peripartum sphincter trauma. Ultrasound Obstet Gynecol 2006;27(2):119–123.
22. Cornelia L, Stephan B, Michel B, Antoine W, Felix K. Trans-perineal versus endo-anal ultrasound in the detection of anal sphincter tears. Eur J Obstet Gynecol Reprod Biol 2002;103(1):79–82.
23. Andrews A, Sultan A, Thakar R, Jones P. Occult anal sphincter injuries–myth or reality? BJOG 2006;113:195–200.
24. Starck M, Bohe M, Valentin L. The extent of endosonographic anal sphincter defects after primary repair of obstetric sphincter tears increases over time and is related to anal incontinence. Ultrasound Obstet Gynecol 2006;27(2): 188–197.
25. Sultan AH, Kamm MA, Hudson CN, Thomas JM, Bartram CI. Anal sphincter disruption during vaginal delivery. N Engl J Med 1993;329(26):1905–1911.
26. Faltin DL, Boulvain M, Floris LA, Irion O. Diagnosis of anal sphincter tears to prevent fecal incontinence: a randomized controlled trial. Obstet Gynecol 2005;106:6–13.

6

Axial Plane Imaging

Hans Peter Dietz

Levator Ani Complex

It is only very recently that imaging of the levator ani has become feasible using translabial ultrasound. The inferior aspects of the levator ani were identified in early studies using transvaginal techniques[1] and translabial freehand volume acquisition[2] as well as on translabial ultrasound using a Voluson system,[3] but the focus of these reports was on the urethra and paraurethral tissues. With translabial acquisition, the whole levator hiatus and surrounding muscle (pubococcygeus and puborectalis) can be visualized, provided acquisition angles are at or above 70°. As with magnetic resonance imaging (MRI), it is currently impossible to distinguish the different components of the pubovisceral or puborectalis/pubococcygeus complex. Several studies in nulliparous women have found no major asymmetries of the pubovisceral muscle, both on MRI[4] and on ultrasound,[5,6] supporting the hypothesis that significant morphologic abnormalities of the levator are likely to be evidence of delivery-related trauma. Contrary to MRI data,[7] no significant side differences were found on ultrasound biometry, neither for thickness nor for area.

Regarding biometric parameters of the puborectalis/pubococcygeus complex and the levator hiatus, there has been good agreement between three-dimensional ultrasound and MRI, both for dimensions of the levator hiatus[5,7] and levator thickness.[5,8] In general, it is to be expected that ultrasound measurements should be more reproducible because of the ease with which measurements in the axial plane can be obtained in the plane of minimal dimensions, whether at rest, on Valsalva, or on pelvic floor muscle contraction. Figure 6.1 demonstrates the process of obtaining the plane of minimal dimensions.

On MRI, the plane of minimal dimensions is virtually impossible to image reproducibly because of slow acquisition speeds, even of single predefined planes. The latest software developments available for 3D/4D ultrasound such as volume contrast imaging and speckle reduction imaging should result in a further improvement in resolution and therefore reproducibility of ultrasound measurements. Diameter and area measurements of the pubococcygeus–puborectalis complex may not be sufficiently repro-

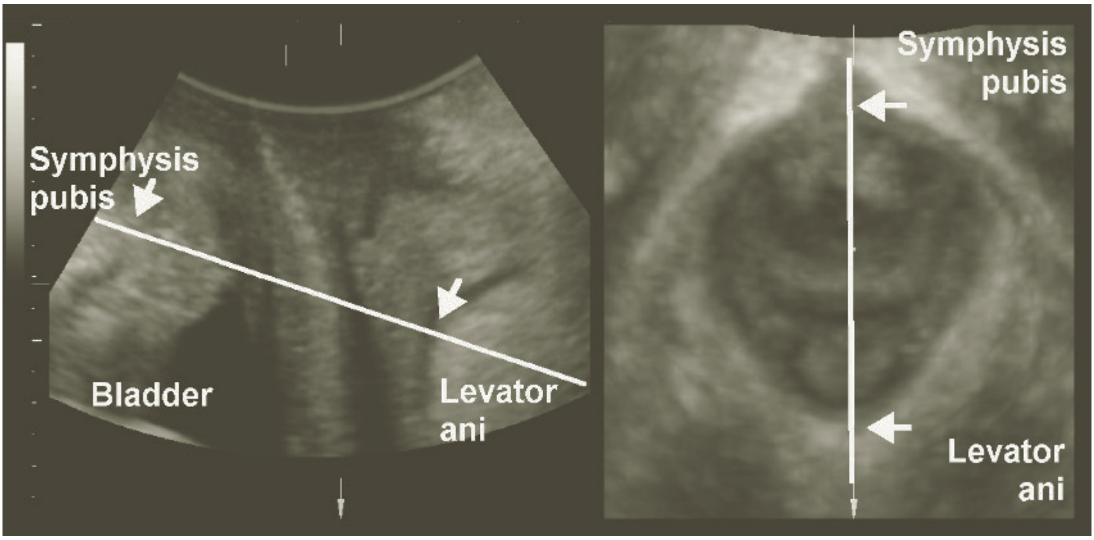

Figure 6.1. Determination of hiatal dimensions. The left-hand image shows the location of the plane of minimal dimensions as seen on the midsagittal view. This plane is tilted in a ventrocaudal to dorsocranial direction as evidenced by the line transecting the image running from the posterior surface of the symphysis to the anterior margin of the most central aspect of the puborectalis loop (white arrows). The right image represents the plane of minimal dimensions in the axial or C plane, with the vertical line showing the location of the midsagittal plane. Arrows identify the minimal sagittal diameter of the hiatus.

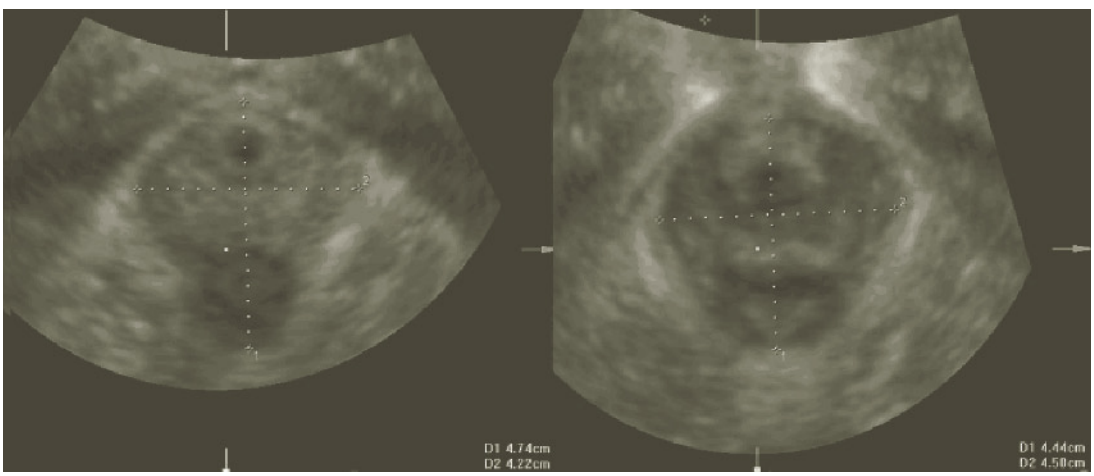

Figure 6.2. Area and diameter measurements of the levator hiatus [plane of minimal dimensions at rest (left) and on Valsalva (right)] in a nulliparous volunteer. (From Dietz HP, Shek C, Clarke B. Biometry of the pubovisceral muscle and levator hiatus by 3D pelvic floor ultrasound. Ultrasound Obstet Gynaecol 2005;25(6):580–585 , with permission.)

and descent (because downward displacement of organs may displace the levator laterally), it is much more interesting that hiatal area at rest is associated with pelvic organ descent on Valsalva. These data constitute the first real evidence for the hypothesis that the state of the levator ani is important for pelvic organ support,[9] even in the absence of levator trauma.

As a rule of thumb, a hiatal area of less than 25 cm^2 on Valsalva is unlikely to be associated with significant prolapse. We classify an area of 30–34.9 cm^2 as mild, 35–39.9 cm^2 as moderate, and 40+ cm^2 as severe ballooning, with extreme cases reaching 50 cm^2 and above. Interestingly, there are nulliparous women who show moderate to marked ballooning on Valsalva. Whereas the highest measurement in a series of 52 young women[5] was 35 cm^2 the author has recently documented ballooning to more than 50 cm^2 in a nulliparous professional athlete with an asymptomatic three-compartment prolapse and enterocele, without there being any evidence of an abnormal connective tissue phenotype. To put this in perspective, the area required by a term-sized fetal head is in the order of 70–90 cm^2.

Apart from static dimensions, relative enlargement of the hiatus on Valsalva may be a measure of compliance or elasticity which may influence the progress of labor, pelvic floor trauma, and future prolapse. However, childbirth obviously has an effect on width and distensibility of the hiatus (see Figure 6.3). And finally, hiatal dimensions are likely to affect treatment outcome if (or when) treatment for pelvic floor dysfunction becomes

Figure 6.3. Increase in hiatal dimensions on Valsalva after vaginal delivery (rendered volumes, axial plane).

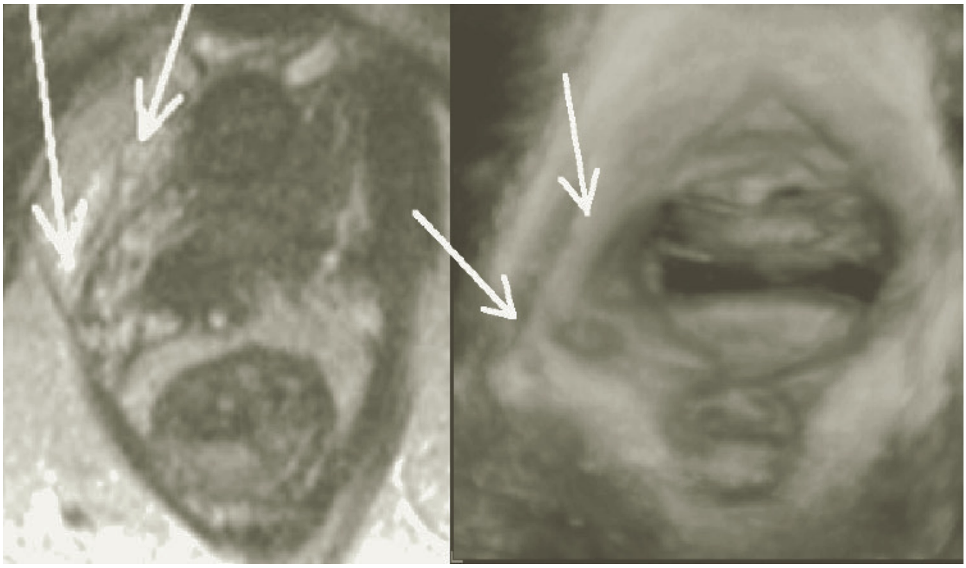

Figure 6.4. Avulsion injury of the right pubovisceral muscle, on MRI (left) and 3D ultrasound (right). Although the images were obtained in different patients, they illustrate the most common pattern of delivery-related levator trauma. The arrows indicate vaginal detachment (top arrows) and detachment of the levator ani (bottom arrows). (MRI courtesy of Dr. Ben Adekanmi, York, UK.)

necessary. The author believes that marked enlargement of the levator hiatus on Valsalva reduces the likelihood of successful pessary management and probably makes successful surgical prolapse correction less likely.[10] In women that show a hiatal area on Valsalva of more than 40 cm^2 one would expect a high likelihood of posterior compartment prolapse after a colposuspension procedure – or a large cystocele after sacrospinous colpopexy, because neither procedure would be expected to address the issue of excessive distensibility of the levator hiatus. Clearly, much work will have to be done in this field over the next decade, and pelvic floor imaging is likely to have a significant impact on the development of prolapse surgery.

The most common morphologic abnormality of the levator ani, an avulsion of the pubovisceral muscle off the pelvic sidewall, is clearly related to childbirth (see Figures 6.4–6.6 and Cases 5, 10, 12, and 13 of the Appendix) and is often palpable as an asymmetric loss of substance in the inferomedial or ventrocaudal portion of the muscle. The digital detection of morphologic abnormality seems to require significant training however, even if palpation of such trauma was described more than 60 years ago.[11] In a recently completed blinded study, the author found poor agreement between palpation by a trained physiotherapist and ultrasound imaging.[12] Technical issues also help explain the poor agreement found in this study. In women with poor resting tone and minimal or absent voluntary function, defects may be impossible to detect by digital examination. However, a recent study using MR detection of levator defects demonstrated much better agreement between imaging and vaginal palpation, provided the operators were trained specifically for this task.[13]

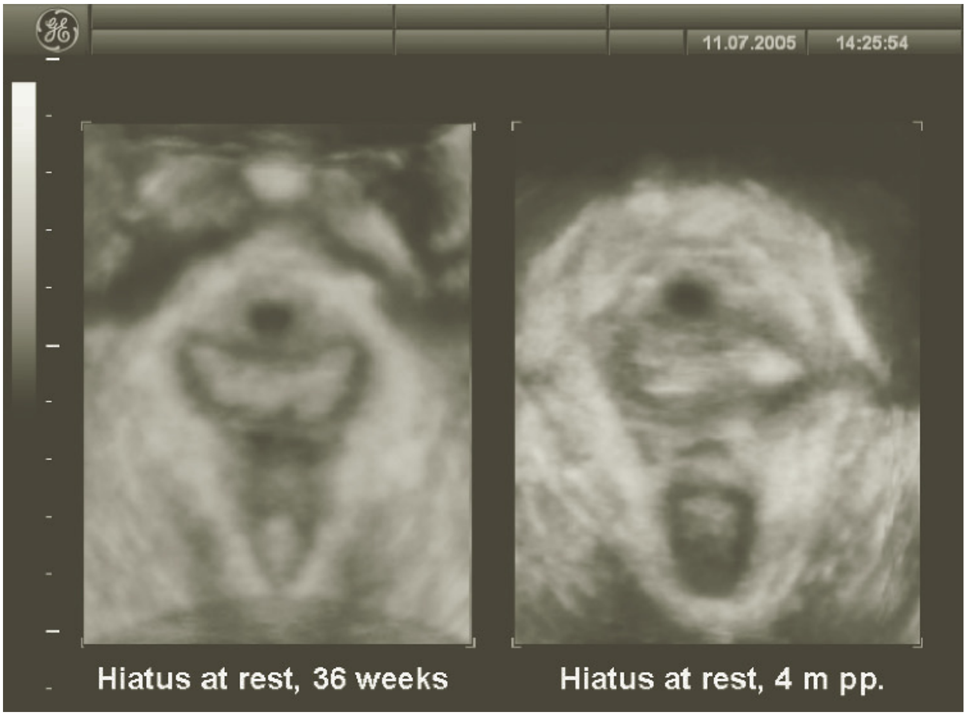

Figure 6.5. Axial plane rendered volumes. The right image shows a left-sided minor defect of the pubovisceral muscle 4 months after vaginal delivery.

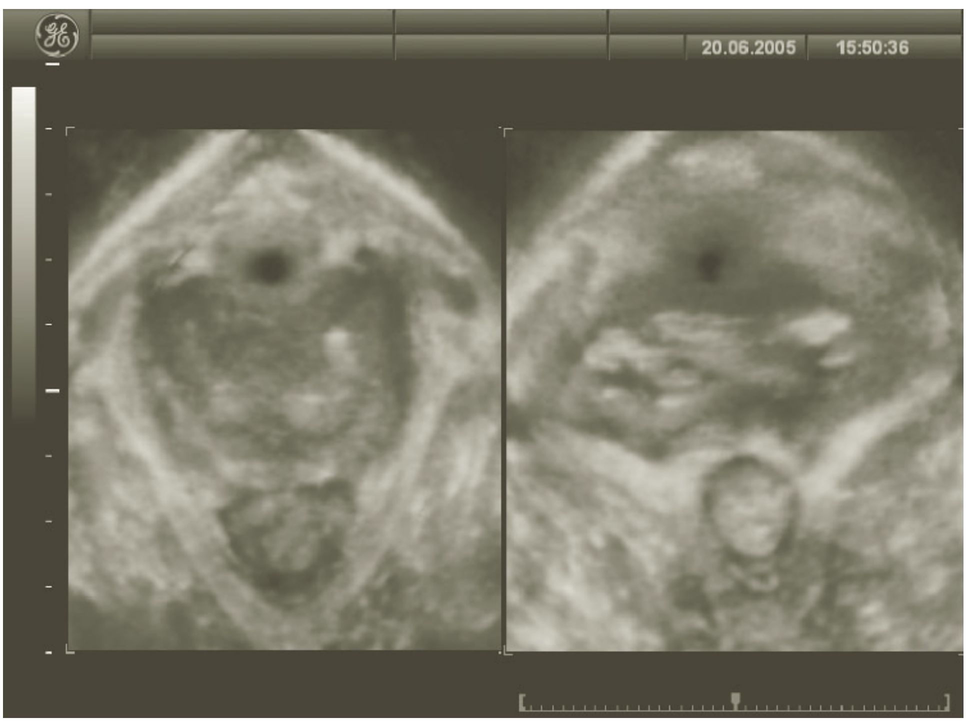

Figure 6.6. Bilateral avulsion injury. The left image was obtained at 37 weeks' gestation in a nulliparous patient. The right image shows a bilateral major defect of the pubovisceral muscle 4 months after vaginal delivery in the same patient.

Thinning of muscle, which may be obvious on imaging, is harder to palpate than gaps in the continuity of the muscle or complete absence as in avulsion injury. Having said that, bilateral defects (see Figure 6.6, also Figures 3.4 and 3.7, and Cases 10 and 13 of the Appendix) may be more difficult to palpate than unilateral avulsion because of the lack of asymmetry, and they are also much less common.

The detection of avulsion defects by translabial 3D/4D ultrasound seems highly reproducible.[14] Both rendered volumes (surface/transparency mode, rendered from caudally to cranially) and single slices in the C or axial plane may be used to help with the identification of defects. The recent development of tomographic ultrasound imaging (TUI) (see Figures 3.6, 3.7, 6.8, and 6.9) is particularly useful in this regard because it allows the screening of one 3D volume at a glance, especially once speckle reduction algorithms have been used to enhance resolutions in the axial plane. Generally, defects seem to be most clearly evident on levator contraction. On Valsalva, defects may open up further, but once full distension of the hiatus is reached the defect is often obscured by flattening of the area of interest against the pelvic sidewall, particularly in women with significant prolapse.

Difficulties may arise in elderly women with marked urogenital atrophy and/or scarring, especially if voluntary function is absent or with very thin or atrophic muscle. When in doubt, the author has found that measurement of the "levator sling muscle gap,"[15] i.e., the distance between the urethral lumen and the most medial aspect of the pubovisceral muscle insertion, is helpful, with a gap of <2.6 mm likely to indicate normal anatomy (unpublished data). Once one is more familiar with the identification of defects by vaginal palpation, an internal examination will further help with the interpretation of ultrasound findings, especially if they are equivocal.

Such defects of the pubovisceral muscle are surprisingly common for a form of childbirth-related trauma that has received virtually no attention to date. In a recently completed study, the author found that more than one third of women delivering vaginally at an average age of 31.6 years had such injuries,[6] an incidence that is unexpectedly high compared with observations in older symptomatic women[14] and previously published rates in women who had their first child at a younger age, both on clinical examination[11] and MRI.[4] This discrepancy may be explained by an association between maternal age at first delivery and the incidence of major levator trauma[14,16] which is worrying given the marked trend toward delayed childbearing in developed countries. It seems likely that women today run a higher risk of sustaining significant trauma to the levator ani muscle, compared with their mothers or grandmothers. This implies that urogynecology—and urogynecologic imaging—is likely to be a growth area for the foreseeable future.

Regarding causation, there seems to be an association with operative delivery,[6] but analogous to the situation with anal sphincter trauma, it seems that precipitate delivery may also cause major levator trauma. This implies that any association with length of second stage and other parameters indicating a difficult delivery may not be linear, making prediction more difficult.

The clinical significance of such defects is becoming clearer. The author's own data suggest that levator avulsion is associated with anterior and central compartment prolapse,[14] but not with urodynamic findings or symptoms of bladder dysfunction in a series of more than 300 primary urogynecologic assessments. Cross-sectional studies of levator anatomy in asymptomatic and symptomatic older women are needed to determine whether such abnormalities are associated with clinical symptoms or conditions in the general population. Another interesting question is whether major morphologic abnormalities of the levator ani affect surgical outcomes. From experience to date and MRI data,[17] it appears that major levator trauma, i.e., avulsion of the puborectalis/pubococcygeus from the pelvic sidewall, seems to be associated with early presentation and recurrent prolapse after surgical repair.

Clearly, there are different degrees of levator trauma. In the future we should be able to distinguish not just unilateral and bilateral trauma, but also isolated defects of the pubococcygeus or muscle, partial (Figure 6.5) and/or complete avulsions puborectalis (Figure 6.6), and global deficiencies of the whole levator (Figure 6.7) which are probably more likely to be caused by neuropathy rather than direct trauma. In the meantime, we may be able to quantify the extent of trauma by using TUI which allows both scoring according to the number of slices showing defects (see Figure 6.8), and quantification of cranioventral and ventrodorsal defect dimensions. Both defect score and maximal width seem associated with symptoms and signs of prolapse.[18]

Figure 6.7. Virtually complete absence of the pubovisceral muscle on the right side after Forceps delivery.

Figure 6.8. TUI of limited bilateral levator trauma, affecting the lowermost aspects of the right pubovisceral muscle and more cranial aspects on the left. The defect score is 6 (2 on right, 4 on left).

On a final note, it appears that the literature to date contains no reports of attempts at surgical correction. This is nothing short of amazing when one considers that such defects may in fact be visible in the delivery suite. Most avulsion injuries are occult, but some become visible due to vaginal tears, resulting in a typical appearance with the vagina detached from the pelvic sidewall, the inferior public ramus and obturator fascia denuded of muscle, and the muscle retracted pararectally. We may have to learn how to reattach the levator, a task that may require us to acquire some of the skills of orthopedic surgeons. Imaging will of course be instrumental in documenting the success of failure of such attempts.

Paravaginal Supports

It has long been speculated that anterior vaginal wall prolapse and stress urinary incontinence are at least partly attributable to disruption of paravaginal and/or paraurethral support structures, i.e., the endopelvic fascia and pubourethral ligaments, at the time of vaginal delivery.[19] In a pilot study using the now obsolete technology of freehand acquisition of 3D volumes, alterations in paravaginal supports were observed in 5 of 21 women seen both ante- and postpartum, and the interobserver variability of the qualitative assessment of paravaginal supports was shown to be good.[2] In light of current knowledge, however, the loss of tenting documented in this study was probably at least partly attributable to levator avulsion.

Structures supporting urethra and bladder can also be assessed by transrectal or transvaginal 3D ultrasound using probes designed for pelvic or prostatic imaging.[1,20] In a recent small series, researchers from Austria have claimed that the endopelvic fascia may be evaluated directly by transrectal 3D ultrasound, describing defects in an echogenic structure underlying the bladder neck and proximal urethra. Such defects almost exclusively occurred in vaginally parous women and were unexpectedly complex.[21]

It remains to be shown whether loss of paravaginal tenting or defects in suburethral/paraurethral echogenic structures are in fact equivalent to what is clinically described as a "paravaginal defect," a concept that is controversial in clinical urogynecology.[22–24] In a recent study on 62 women presenting with pelvic floor disorders, only weak correlations were found between a blinded clinical assessment for paravaginal defects and the presence or absence of tenting in single planes or rendered volumes obtained by 3D translabial ultrasound, and even this weak correlation was only seen on Valsalva.[25] This may be attributable to inadequate clinical assessment techniques or possibly an insufficiently sensitive imaging method. Recent evidence suggests that the clinical assessment for paravaginal defects has poor repeatability.[26,27] However, another (if less likely) explanation may be that true paravaginal defects are either not common and/or irrelevant for anterior vaginal wall support.

Urethra and Urethral Supports

The first use of 3D pelvic floor ultrasound, albeit with a transvaginal probe, was in investigating urethral structure.[28,29] Although there seems to be disagreement as to what has actually been measured in some of the studies of urethral sonoanatomy,[20,28,30] it seems that the volume of the hypoechoic structures surrounding the urethra (smooth muscle, vascular plexus, and mucosa) is associated with closure pressure.[28] On 3D ultrasound in the axial plane, one is generally able to detect a circular hyperechogenic structure surrounding the mid urethra (see Figure 6.9) which, judging from intraurethral ultrasound and axial plane MRI, corresponds to the striated urethral sphincter.

It is less clear, however, whether observation of static urethral anatomy is of any clinical relevance. We do, after all, have inexpensive and practical diagnostic tools to assess urethral function. In the author's opinion, resolutions at present are not sufficient for translabial ultrasound to contribute to the assessment of urethral function. This may change with the advent of small parts 4D and matrix probes which will likely allow much more detailed insights into urethral anatomy, without distortion and in a noninvasive manner. This probably also applies to urethral supports which are starting to be studied in more detail on MRI and ultrasound.[21]

Figure 6.9. TUI in a parous patient without bladder symptoms and normal pelvic floor anatomy. There is a hyperechogenic ring structure (arrows) surrounding the midportion of the urethra in slices 1–4, i.e., extending over at least 10 mm, which represents the urethral rhabdosphincter.

Other Findings

At times, imaging in the axial plane can help clarify anatomic relationships in more complex prolapse cases, especially if there is significant asymmetry. The extent of a cystocele may become more obvious (see Figure 6.10), and side differences, e.g., caused by major levator trauma or neuropathy, can be detected in the coronal plane (see Figure 6.11). Rectoceles are usually clearly apparent because of their hyperechoic nature (see Figure 6.12 and Case 6 of the Appendix).

Cystic structures in the vagina are more easily assessed on 3D ultrasound, especially regarding their relationship with the urethra (see Figure 6.13 and Case 9 of the Appendix for Gartner cysts, Case 15 for a urethral diverticulum). The exact location of a pessary can also be determined more easily on 3D imaging, although Figure 6.14 is mainly given to acquaint readers with the very distinct appearances of a ring pessary. These appear virtually completely anechoic because of total reflection of incoming acoustic waves. Implants and suburethral slings will be discussed in Chapter 7.

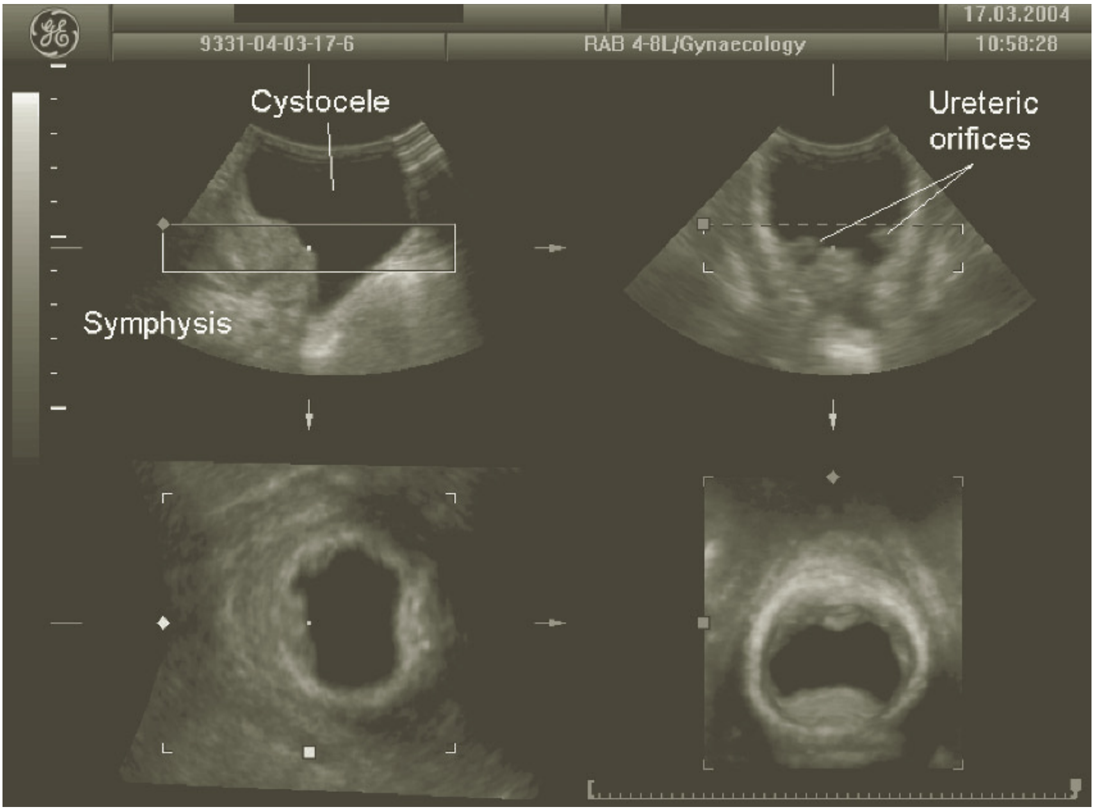

Figure 6.10. Large cystocele with intact retrovesical angle as seen on 3D ultrasound in the midsagittal plane (top left), coronal plane (top right), axial plane (bottom left), and in a rendered volume (axial plane) (bottom right). In the coronal plane, the ureteric orifices are clearly visible and well outside the pelvis. The axial plane and rendered volume do not show the levator ani because they are situated well below the hiatus. (Dietz HP. Pelvic Floor Ultrasound. Current Medical Imaging Reviews 2006; 2: in print, Bentham Publishers.)

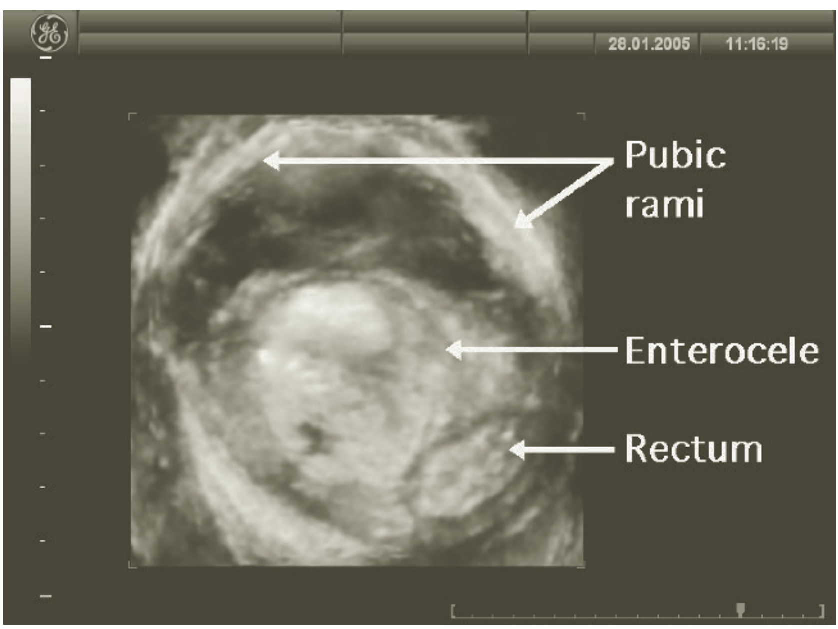

Figure 6.11. Marked asymmetry of prolapse as seen in the axial plane. The left pubovisceral muscle is globally impaired, likely because of neuropathy, with asymmetric development of recto- and enterocele on Valsalva.

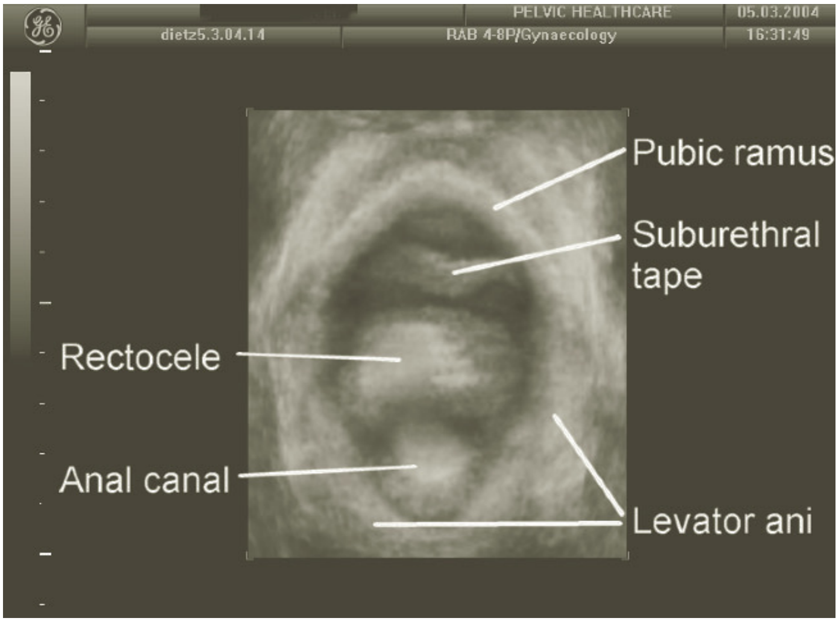

Figure 6.12. A rendered volume of a patient with a second-degree rectocele. The hyperechoic structure of the rectocele is seen to fill a large part of the hiatus. There also is a suburethral tape. (Dietz HP. Pelvic Floor Ultrasound. Current Medical Imaging Reviews 2006; 2: in print, Bentham Publishers, with permission.)

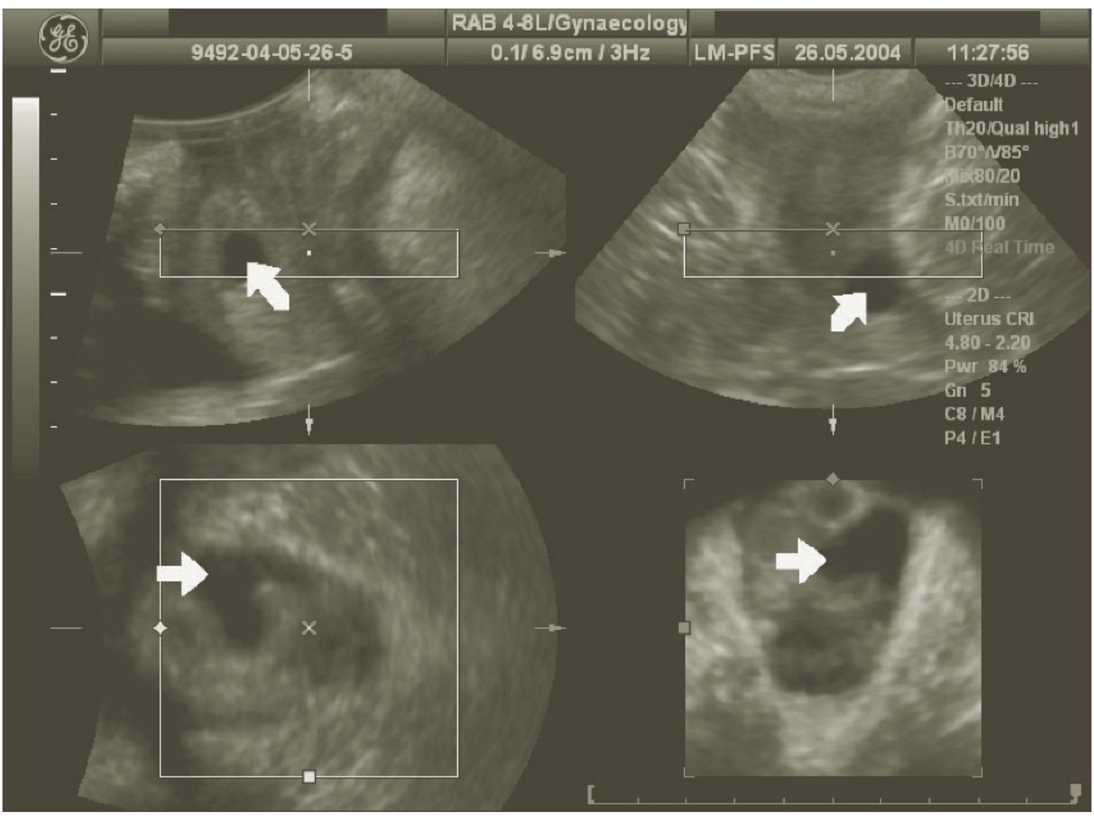

Figure 6.13. The complex appearance of a Gartner cyst on 3D ultrasound, mimicking a cystocele on clinical examination.

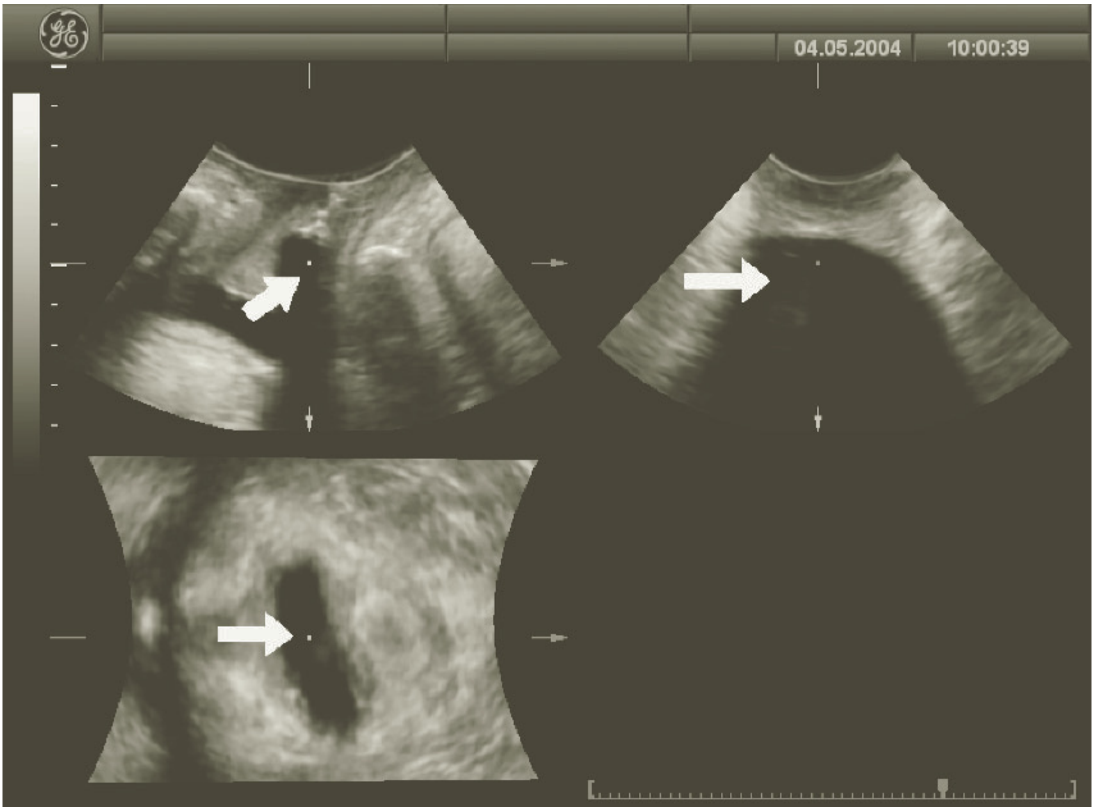

Figure 6.14. Prolapse pessaries may cause unusual and distinct sonographic patterns. In this case, a silicone ring pessary results in complete reflection (and refraction) of incoming soundwaves, resulting in anechoic areas encompassing the pessary and an acoustic shadow which is evident in the midsagittal and the coronal plane.

References

1. Wisser J, Schaer G, Kurmanavicius J, Huch R, Huch A. Use of 3D ultrasound as a new approach to assess obstetrical trauma to the pelvic floor. Ultraschall Med 1999;20(1):15–18.
2. Dietz HP, Steensma AB, Hastings R. Three-dimensional ultrasound imaging of the pelvic floor: the effect of parturition on paravaginal support structures. Ultrasound Obstet Gynecol 2003;21(6):589–595.
3. Khullar V, Cardozo L. Three-dimensional ultrasound in urogynecology. In: Merz E, ed. 3-D Ultrasound in Obstetrics and Gynecology. Philadelphia: Lippincott Williams & Wilkins Healthcare; 1998:65–71.
4. DeLancey JO, Kearney R, Chou Q, Speights S, Binno S. The appearance of levator ani muscle abnormalities in magnetic resonance images after vaginal delivery. Obstet Gynecol 2003;101(1):46–53.
5. Dietz HP, Shek C, Clarke B. Biometry of the pubovisceral muscle and levator hiatus by three-dimensional pelvic floor ultrasound. Ultrasound Obstet Gynecol 2005;25(6):580–585.
6. Dietz HP, Lanzarone V. Levator trauma after vaginal delivery. Obstet Gynecol 2005;106(4):707–712.

7. Fielding JR, Dumanli H, Schreyer AG, et al. MR-based three-dimensional modeling of the normal pelvic floor in women: quantification of muscle mass. AJR Am J Roentgenol 2000;174(3):657–660.
8. Tunn R, DeLancey JO, Howard D, Thorp JM, Ashton-Miller JA, Quint LE. MR imaging of levator ani muscle recovery following vaginal delivery. Int Urogynecol J 1999;10(5):300–307.
9. DeLancey JO. Anatomy. In: Cardozo L, Staskin D, eds. Textbook of Female Urology and Urogynaecology. London: Isis Medical Media; 2001:112–124.
10. Barry C, Dietz HP, Rane A. An independent audit of mesh repair for the treatment of rectocele. 34th Annual Scientific Meeting of the International Continence Society 2004, Paris, France. Abstract 435.
11. Gainey HL. Post-partum observation of pelvic tissue damage. Am J Obstet Gynecol 1943;46:457–466.
12. Dietz HP, Hay-Smith J, Hyland G. Vaginal palpation and 3D pelvic floor ultrasound in the diagnosis of avulsion defects of the levator ani. Neurourol Urodyn 2006;25(5):424–427.
13. Kearney R, Miller JM, Delancey JO. Interrater reliability and physical examination of the pubovisceral portion of the levator ani muscle, validity comparisons using MR imaging. Neurourol Urodyn 2006;25(1):50–54.
14. Dietz HP, Steensma AB. The prevalence of major abnormalities of the levator ani in urogynaecological patients. Br J Obstet Gynaecol 2005;113:1–5.
15. Hoyte L, Schierlitz L, Zou K, Flesh G, Fielding JR. Two- and 3-dimensional MRI comparison of levator ani structure, volume, and integrity in women with stress incontinence and prolapse. Am J Obstet Gynecol 2001;185(1):11–19.
16. Kearney R, Miller J, Ashton-Miller J, Delancey J. Obstetric factors associated with levator ani muscle injury after vaginal birth. Obstet Gynecol 2006;107(1):144–149.
17. Adekanmi OA, Freeman R, Puckett M, Jackson S. Cystocele: does anterior repair fail because we fail to correct the fascial defects? A clinical and radiological study. Int Urogynecol J 2005;16(S2):S73.
18. Dietz HP. The classification of major morphological abnormalities of the pubovisceral muscle. ICS 2006, Christchurch. Abstract.
19. DeLancey JO. The anatomy of the pelvic floor. Curr Opin Obstet Gynecol 1994;6(4):313–316.
20. Kuo H. The relationships of urethral and pelvic floor muscles and the urethral pressure measurements in women with stress urinary incontinence. Eur Urol 2000;37(2):149–155.
21. Reisinger E, Stummvoll W. Visualization of the endopelvic fascia by transrectal three-dimensional ultrasound. Int Urogynecol J 2006;17:165–169.
22. Ostrzenski A, Osborne NG. Ultrasonography as a screening tool for paravaginal defects in women with stress incontinence: a pilot study. Int Urogynecol J 1998;9(4):195–199.
23. Martan A, Masata J, Halaska M, Otcenasek M, Svabik K. Ultrasound imaging of paravaginal defects in women with stress incontinence before and after paravaginal defect repair. Ultrasound Obstet Gynecol 2002;19(5):496–500.
24. Nguyen JK, Hall CD, Taber E, Bhatia NN. Sonographic diagnosis of paravaginal defects: a standardization of technique. Int Urogynecol J 2000;11(6):341–345.
25. Dietz HP, Pang S, Korda A, Benness C. Paravaginal defects: a comparison of clinical examination and 2D/3D ultrasound imaging. Aust N Z J Obstet Gynaecol 2005;45:187–190.
26. Segal JL, Vassallo BJ, Kleeman SD, Silva WA, Karram MM. Paravaginal defects: prevalence and accuracy of preoperative detection. Int Urogynecol J 2004;15(6):378–383.

27. Whiteside JL, Barber MD, Paraiso MF, Hugney CM, Walters MD. Clinical evaluation of anterior vaginal wall support defects: interexaminer and intraexaminer reliability. Am J Obstet Gynecol 2004;191(1):100–104.
28. Khullar V, Salvatore S, Cardozo LD. Three dimensional ultrasound of the urethra and urethral pressure profiles. Int Urogynecol J 1994;5(S1):319.
29. Athanasiou S, Khullar V, Boos K, Salvatore S, Cardozo L. Imaging the urethral sphincter with three-dimensional ultrasound. Obstet Gynecol 1999;94(2): 295–301.
30. Schaer GN, Schmid T, Peschers U, Delancey JO. Intraurethral ultrasound correlated with urethral histology. Obstet Gynecol 1998;91(1):60–64.

7

Imaging of Implant Materials

Hans Peter Dietz

Suburethral Slings

The imaging of synthetic implants may yet prove to be a major factor in the uptake of pelvic floor ultrasound in clinical practice, in particular because currently used mesh implants seem to be much more difficult (if not impossible) to detect on magnetic resonance and X-ray imaging.[1–3] Synthetic suburethral slings such as the tensionless vaginal tape (TVT), suprapubic arc tape (Sparc), intravaginal slingplasty (IVS), Monarc, and transobturator TVT (TOT) have become very popular during the last 10 years[4–7] and are now the primary anti-incontinence procedures in many developed countries. These slings are not without their problems, even if biocompatibility is markedly better than for previously used synthetic slings, and they differ from each other in some important aspects.

Imaging may be indicated in research, in order to determine location and function of such slings, and possibly even for assessing in vivo biomechanical characteristics. Clinically, complications such as recurrence of stress incontinence, voiding dysfunction, erosion, and postoperative symptoms of the irritable bladder may benefit from imaging assessment. Often, patients will not remember the exact nature of previous incontinence or prolapse surgery, and implants may be identified in women who are not aware of their presence, let alone their type.

Allografts such as Pelvicol are impossible to visualize after as short a time as 2 months, and the echogenicity of fascial grafts seems to vary widely. In contrast, most of the modern synthetic implant materials are highly echogenic, with TVT, Sparc, TOT, and Monarc usually being more clearly visible than the IVS. Three-dimensional (3D) ultrasound can locate the implant over its entire intrapelvic course,[8] from the pubic rami to behind the urethra, and back up on the contralateral side (see Figure 7.1 and Case 14 of the Appendix).

Variations in placement such as asymmetry, varying width, the effect of tape division, and tape twisting can be visualized (see Figure 7.2). The difference between transobturator tapes and TVT-type implants, difficult to distinguish on 2D imaging (see Figure 7.3), is readily apparent on rendered volumes (see Figure 7.4 and Cases 11 and 14 of the Appendix). Another way

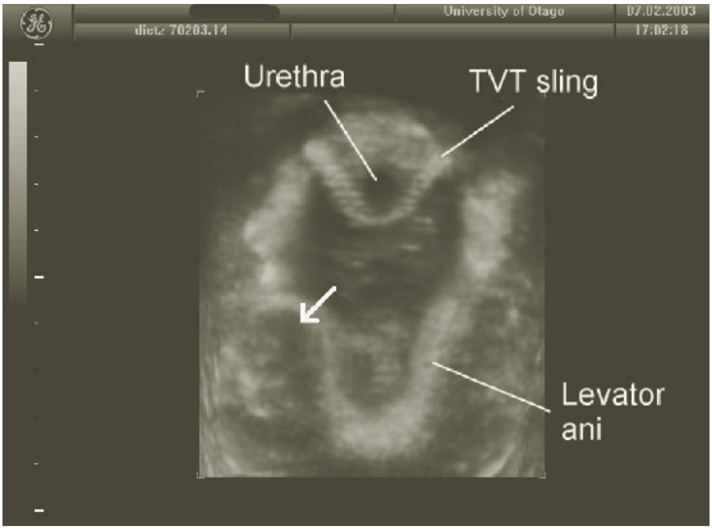

Figure 7.1. Rendered volume, axial plane, showing the levator hiatus and a TVT surrounding the urethra. There is a localized abnormality of the right levator ani that is of uncertain significance. (From Dietz HP Ultrasound Imaging of the Pelvic Floor: 3D aspects. Ultrasound Obstet Gynecol 2004;23(6):615–625, with permission.)

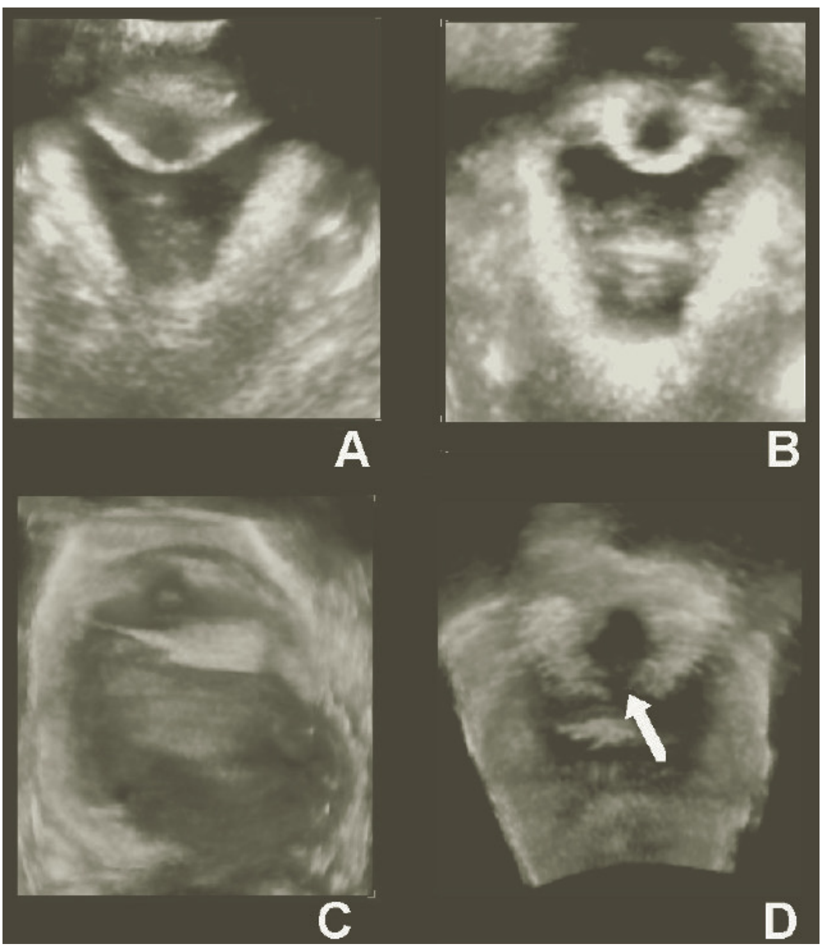

Figure 7.2. Pelvic floor ultrasound can document variations in tape placement, especially in the axial plane: usual appearances **(A)**, very tight placement **(B)**, tape twisting **(C)**, and findings after tape division (arrow) **(D)**. (Modified from: Dietz HP, Wilson PD. The Iris effect: How 2D and 3D volume ultrasound can help us understand anti-incontinence procedures. Ultrasound Obstet Gynecol 2004;23:267–271, with permission.)

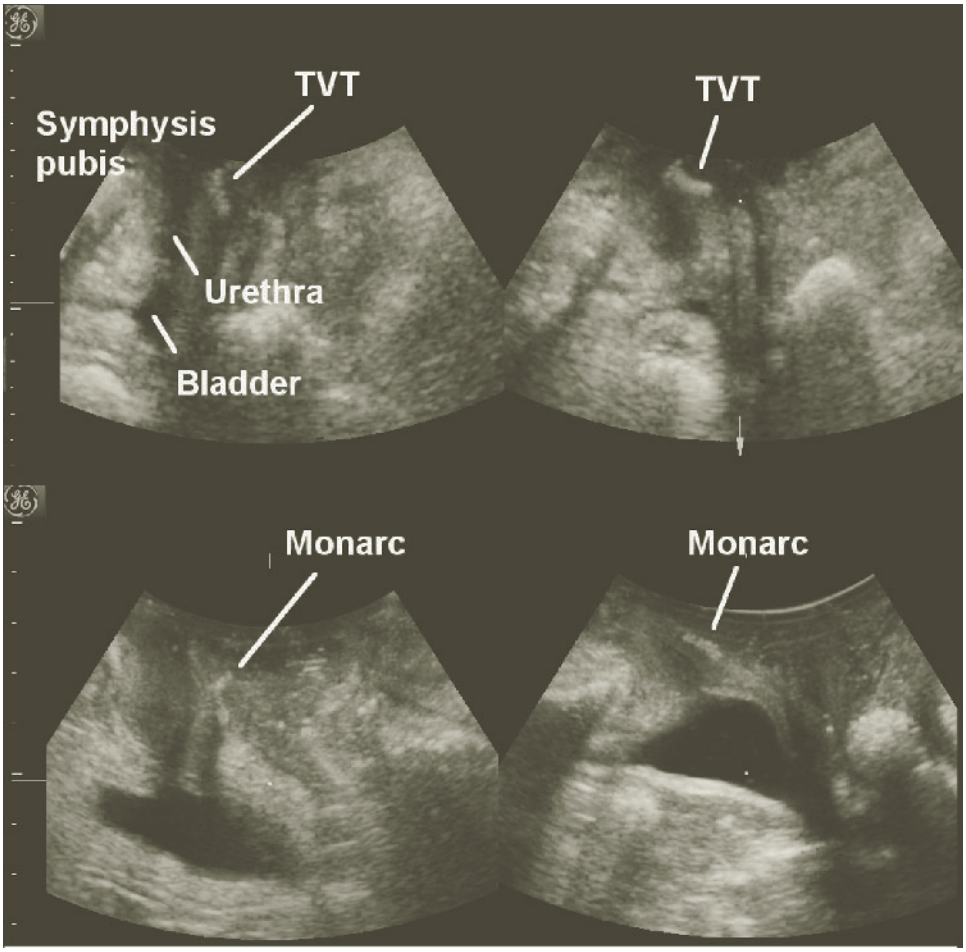

Figure 7.3. Transretzius tapes (TVT, IVS, Sparc, etc.) and transobturator tapes (Monarc, TOT) are impossible to distinguish in the midsagittal plane. The left-hand images are taken at rest, the right ones on maximal Valsalva. (From Dietz HP, Barry C, Lim Y, Rane A (2006) TVT vs Monarc: a comparative study. Int Urogynecol J Pelvic Dysfunct DOI 10.1007/s00192-006-0065-2.)

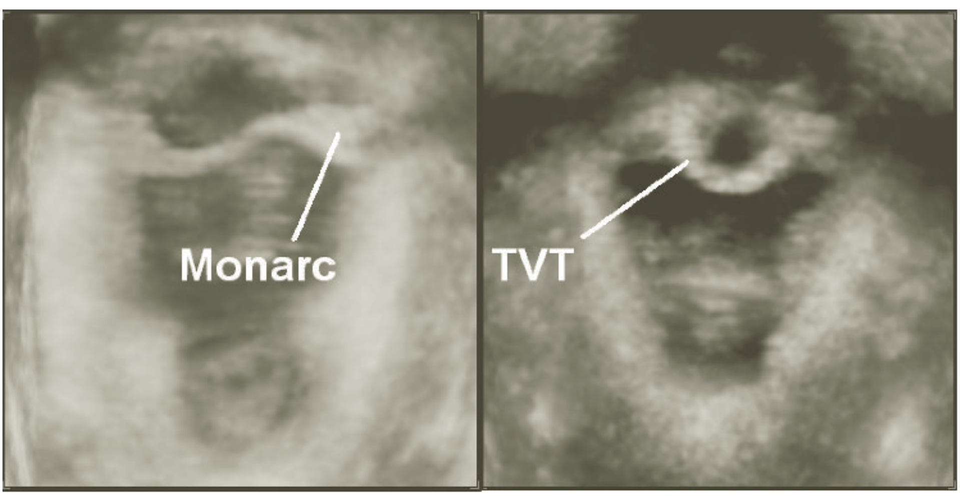

Figure 7.4. The distinction between transobturator tapes and transretzius tapes is obvious in the axial plane. (From Dietz HP, Barry C, Lim Y, Rane A (2006) TVT vs Monarc: a comparative study. Int Urogynecol J Pelvic Dysfunct DOI 10.1007/s00192-006-0065-2.)

of determining the nature of a suburethral sling is to follow the tape in oblique parasagittal views until the levator ani insertion is reached. Most transobturator tapes seem to traverse the muscle (see Figure 7.5), uni- or bilaterally,[9] or they at least get very close to its insertion (see Case 11 of the Appendix).

It is also possible, to a degree, to distinguish different types of materials, with the IVS being much less echogenic than the TVT or Sparc (see Figure 7.6). Again, this can be important in the assessment of postoperative sling complications. An IVS tape is more likely to erode than the TVT, and it seems to cause unusual foreign body reactions, leading to sequestration of the tape, chronic infection, sinus formation, etc.[10] It is very likely therefore that 3D imaging will turn out to be helpful in the assessment of patients with suburethral slings.

Because the Sparc carries a central suture that prevents pretensioning,[11] it generally seems flatter and wider than TVTs, and the IVS never assumes the strip-like appearance seen for TVT and Sparc in Figure 7.6. However, most suburethral tapes can assume a tight c-shape, in particular on Valsalva. The more pronounced this effect is at rest, the tighter one may assume the tape to be. The position of suburethral tapes does not seem to change much over time, although a gradual caudal displacement of the TVT together with surrounding tissues has been described,[12,13] in particular in women after concomitant anterior repair.

Regarding the location of slings relative to the urethra and/or the bladder neck, it has been claimed that mid urethral placement is preferable or even essential for success, but the author agrees with others who hold that variations in placement do not seem to have much of an impact on success.[2,14,15] From a theoretical point of view, if suburethral slings work by "dynamic compression,"[16] i.e., kinking or compression of the urethra against the posteroinferior contour of the symphysis pubis whenever intraabdominal pressure is raised, then it should not matter much for success as to whether the obstruction affects proximal or distal urethra.

If one accepts this hypothesis, then it also follows that any type of suburethral tape can be inserted too loosely or too tightly. The degree of obstruction (and therefore the likelihood of stress continence and postoperative voiding dysfunction) is likely to depend on at least three factors: the physical location of the sling (i.e., placement relative to the urethra), its biomechanical properties (i.e., stiffness or elasticity), and the stiffness or elasticity of surrounding tissues (i.e., the degree of urethral mobility or prolapse). Location or placement on its own does not seem to be the dominant predictor of success, as seen above. Biomechanical properties vary greatly among different types of implants,[17] but on its own this factor does not seem to affect outcomes greatly.[18] The degree of urethral mobility may well be at least as important a predictor of outcome, as shown on X-ray imaging.[19] One final predictor of postoperative stress continence, urethral closure pressure, may further confound relationships.

Despite the complexity of the issue, it is the opinion of the author that preoperative ultrasound is likely to help in predicting the likelihood of operative success. Patients with a mild degree of urethral hypermobility – i.e., between 2.5 and 3.5 cm of bladder neck descent – and a thick urethral sphincter complex on B mode ultrasound, seem to do better than those with

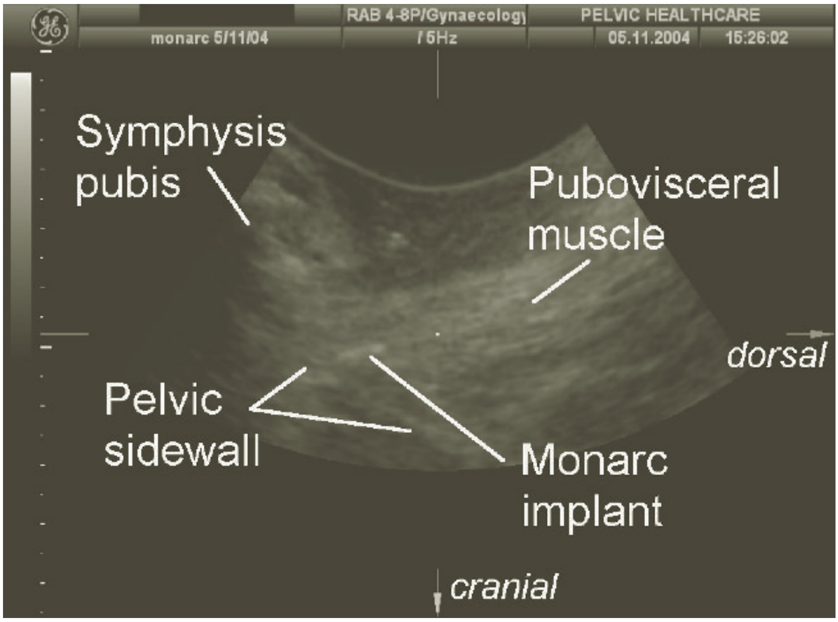

Figure 7.5. Oblique parasagittal view (A plane) showing a Monarc implant traversing the most ventrocaudal aspects of the levator ani muscle.

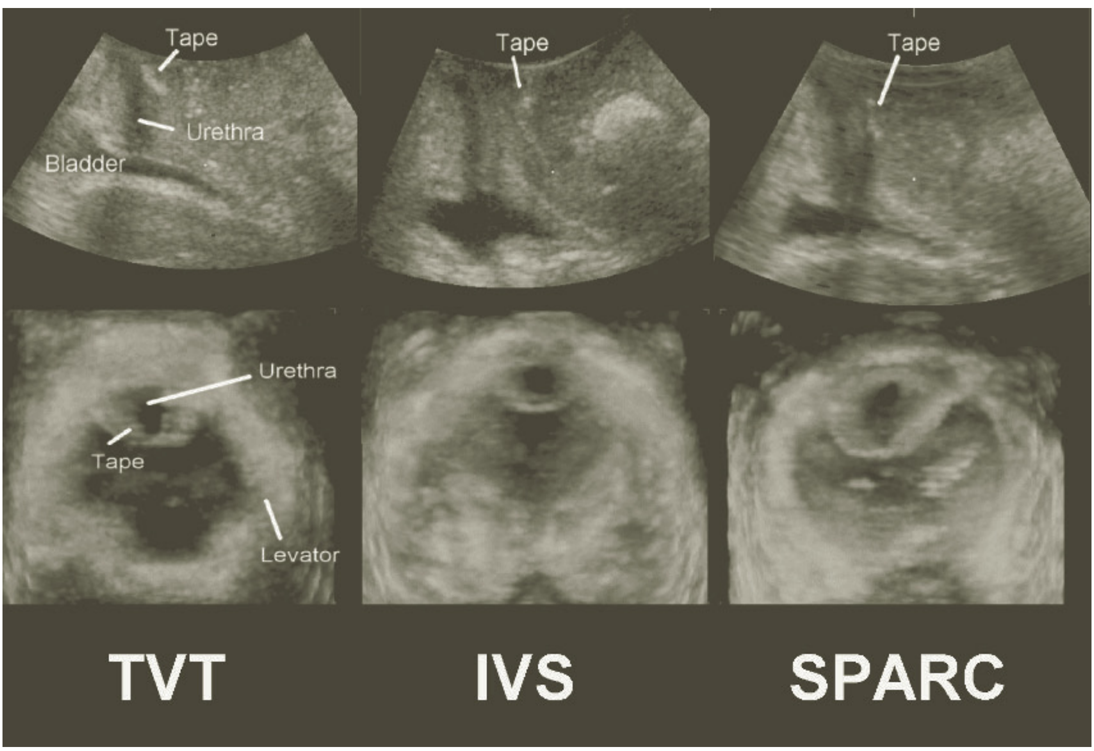

Figure 7.6. A comparison of TVT, IVS, and Sparc tapes in the midsagittal (top row) and axial plane (bottom row). The IVS is difficult to detect in the sagittal, but generally easier to see in the axial plane. (From Dietz HP, Barry C, Lim Y, Rane A. 2D and 3D Ultrasound Imaging of suburethral slings. Ultrasound in Obstetrics and Gynaecology 2005;26:175–179, with permission.)

a frozen bladder neck and very thin urethra. If there is significant hypermobility, even a tape inserted loosely is likely to work well, whereas it is much more difficult to get the tension right (i.e., avoid both stress recurrence and voiding dysfunction) in someone with intrinsic sphincter deficiency after an anatomically successful colposuspension.[8]

In some instances, postoperative ultrasound shows an obviously obstructive tape, e.g., a tape that assumes a tight c shape at rest and is close to the urethra. Such a finding will help with the decision whether to divide the tape. On the other hand, a tape that appears very flat even on Valsalva and is more than 2 cm posterior to the central urethra in the midsagittal plane does easily explain recurrent stress incontinence. However, it is often impossible to judge outcome by ultrasound appearances alone because of the impact of the above-mentioned confounders.

Implants Used in Pelvic Reconstructive Surgery

There is a worldwide trend toward mesh implantation, especially for recurrent prolapse, and complications such as failure and mesh erosion are not uncommon.[20,21] Imaging will undoubtedly be useful in determining functional outcome and location of such implants (see Figure 7.7). Both traditional materials such as Marlex and Mersilene as well as the now obsolete Goretex implants (see Figure 4.15) are highly echogenic, as are the more modern materials such as Prolene and combination meshes such as Vypro.

Figure 7.7. Rendered volume (maximal Valsalva, axial plane) of the most dependent part of a recurrent cystocele after mesh implantation. The mesh is detached from its anchoring on one side, with its edge being clearly visible (arrow). (From Dietz HP Ultrasound Imaging of the Pelvic Floor: 3D aspects. Ultrasound Obstet Gynecol 2004;23(6):615–625, with permission.)

In the past, the main problem with mesh techniques has been fixation. This is not an issue for vault suspension, for which the sacral promontory with the anterior longitudinal ligament of the spine allows reliable mesh anchoring. However, until recently, there were no demonstrably successful techniques for anchoring meshes used for cystocele or rectocele repair. Figure 7.7 shows an anterior compartment mesh repair that has failed, at least partly because of ineffective anchoring of the mesh on the left pelvic sidewall.

The latest transobturator and pararectal techniques such as the posterior IVS, Perigee (Figures 7.8 and 7.9, and Case 13 of the Appendix), and Apogee (Figure 7.8 and 7.10–7.11 and Case 11 of the Appendix) are of particular interest at present, precisely because they provide for anchoring of mesh by extensions that are placed through the obturator foramen in the case of the Perigee, and through the pararectal space and levator ani in the case of the Apogee. Anterior vaginal wall mesh repair techniques that use the obturator foramen for anchoring may be particularly useful in women with levator avulsion injuries who seem more prone to recurrence after anterior repair.[22] Figure 7.9 demonstrates that the mesh and its anchoring arms are situated precisely at the site of bilateral levator trauma (see also Case 13 of the Appendix).

We have recently been able to show that 3D pelvic floor ultrasound is a useful method in auditing transobturator mesh repair for large and/or recurrent cystocele.[23] The implant was visible in all 48 women at an average follow-up of 11 months. In five patients, there was cystocele recurrence dorsal to the mesh, and in four there was significant descent ventral to the mesh. In five women, the mesh axis changed markedly on Valsalva with more than 90° of rotation of the cranial margin in a ventrocaudal direction, implying dislodgment of the superior anchoring arms, a phenomenon that had not been observed before. In one woman, this was accompanied by the development of an anterior enterocele. Clearly, ultrasound will have a major role in assessing and optimizing these new surgical techniques.

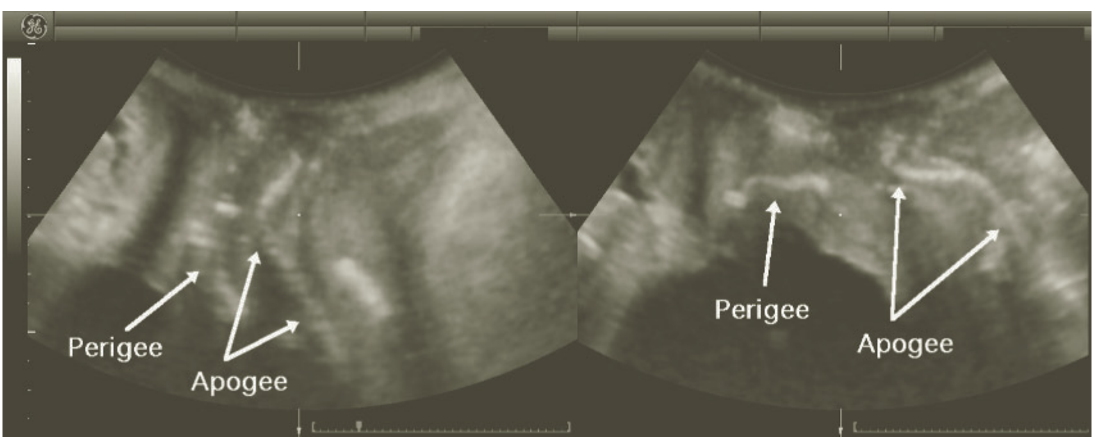

Figure 7.8. Successful anterior ("Perigee") and posterior ("Apogee") vaginal wall mesh repair: midsagittal view at rest (left) and maximal Valsalva (right).

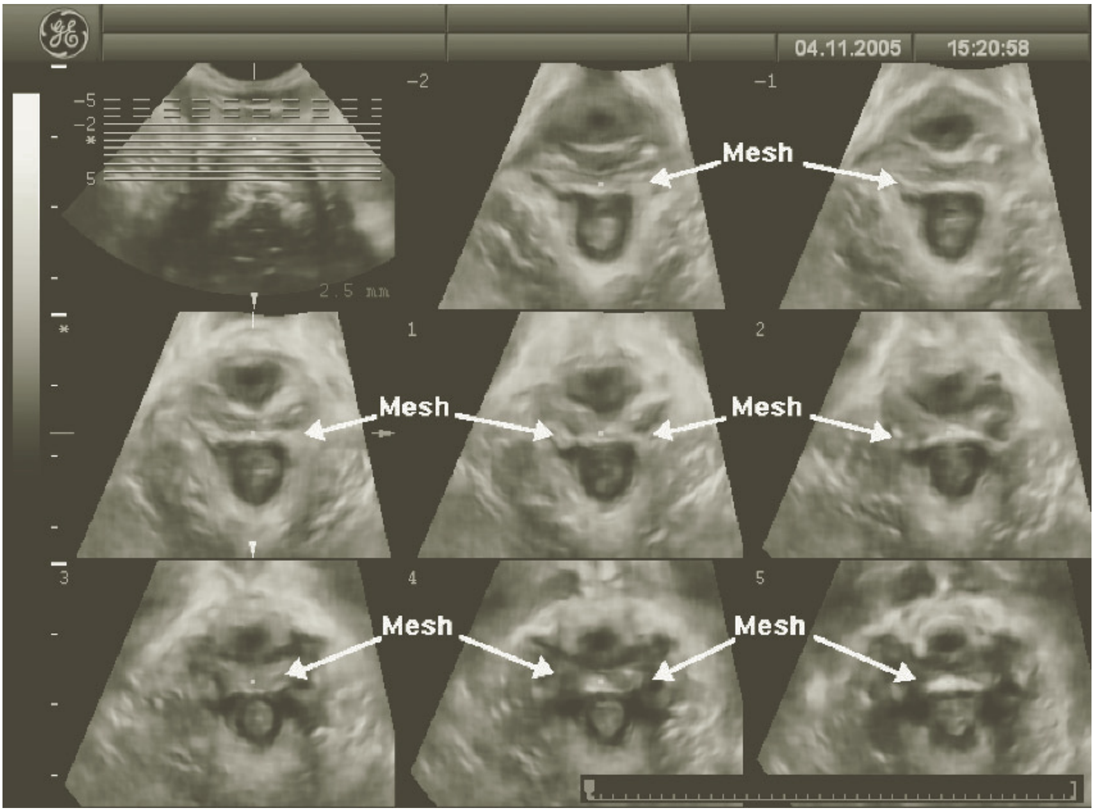

Figure 7.9. Tomographic imaging, axial plane, of a Perigee implant in a patient with bilateral avulsion of the pubovisceral muscle. It is evident that the implant traverses the hiatus at the site of the avulsion injuries.

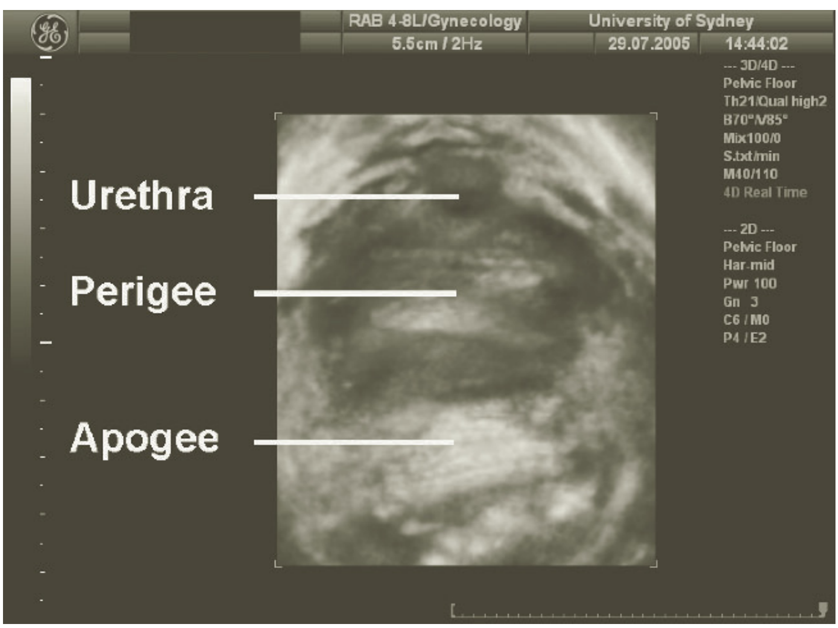

Figure 7.10. Axial plane rendered volume, maximal Valsalva. There is marked ballooning of the hiatus to about 50 cm^2, with the two implants forming bars across the hiatus. The mesh has not reduced ballooning which generally is very similar to preoperative findings.

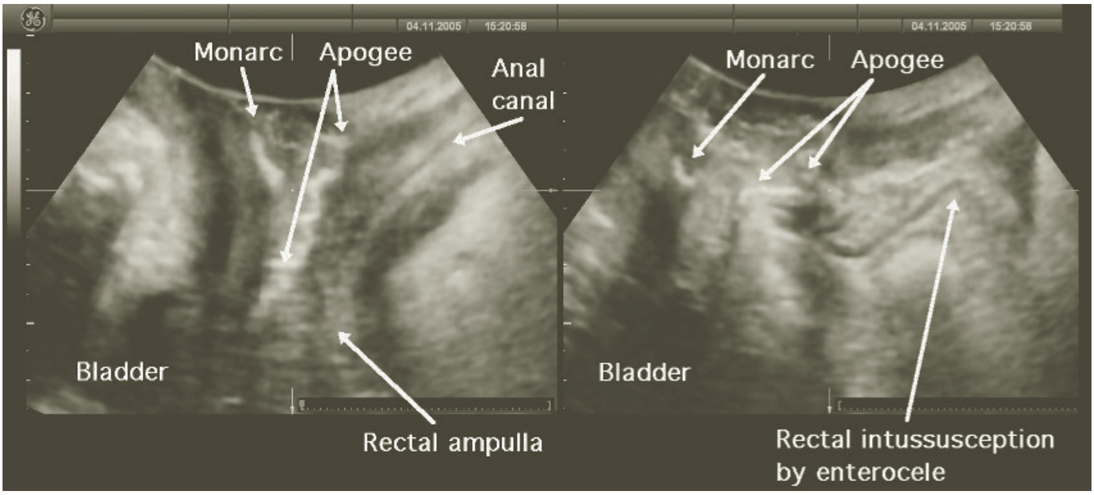

Figure 7.11. Enterocele developing posterior to an Apogee mesh as seen in the midsagittal plane, causing a rectal intussusception or internal rectal prolapse (left image at rest, right image on maximal Valsalva). Clearly, the vaginal prolapse has been cured, only to be replaced by an incipient (and, so far, occult) rectal prolapse in a patient with a very large hiatus and levator damage.

Figure 7.10 shows that an Apogee-type implant seems to bridge the hiatus at its widest portion. Initially, it was hoped that such techniques, by virtue of the anchoring arms perforating the levator ani muscle, may effect a minimally invasive levatorplasty. If true, one would expect a marked reduction in levator ballooning after Apogee. Unfortunately, this is not the case as shown in Figures 7.10 and 7.11 (see also Case 11 of the Appendix), probably because the lateral extensions of an Apogee-type repair traverse the iliococcygeus muscle, not the more substantial lower aspects of the levator ani. Further modifications of pararectal techniques may be necessary in order to provide for permanent narrowing of the hiatus.

Figure 7.10 demonstrates findings in a patient with three-compartment prolapse after Apogee/Perigee mesh insertion and an excellent clinical result. In the axial plane, it is evident that the underlying problem, i.e., massive levator ballooning, has not been addressed. The pelvic organs are prevented from entering the vagina by two bars of mesh that traverse the hiatus, and clinically this seems to be entirely sufficient to prevent recurrence of vaginal prolapse.

Unfortunately, there remains an alternative route for prolapse to develop in women predisposed to this condition – via the anal canal. Figure 7.11 (and Case 11 of the Appendix) shows an enterocele beginning to invaginate the rectal wall in another patient after “gynecologically successful” posterior vaginal wall mesh repair for posthysterectomy vault prolase. The patient had de novo symptoms of dyschezia and obstructed defecation 4 months after the procedure and was found to have an internal rectal prolapse on colorectal assessment. This rectal prolapse had not been apparent on preoperative imaging.

Finally, several of the injectables used in anti-incontinence surgery are also highly echogenic. Macroplastique, for example, can be visualized as a hyperechoic donut shape surrounding the urethra (see Figure 7.12). Unfortunately, there seems to be little correlation between imaging findings and treatment success.

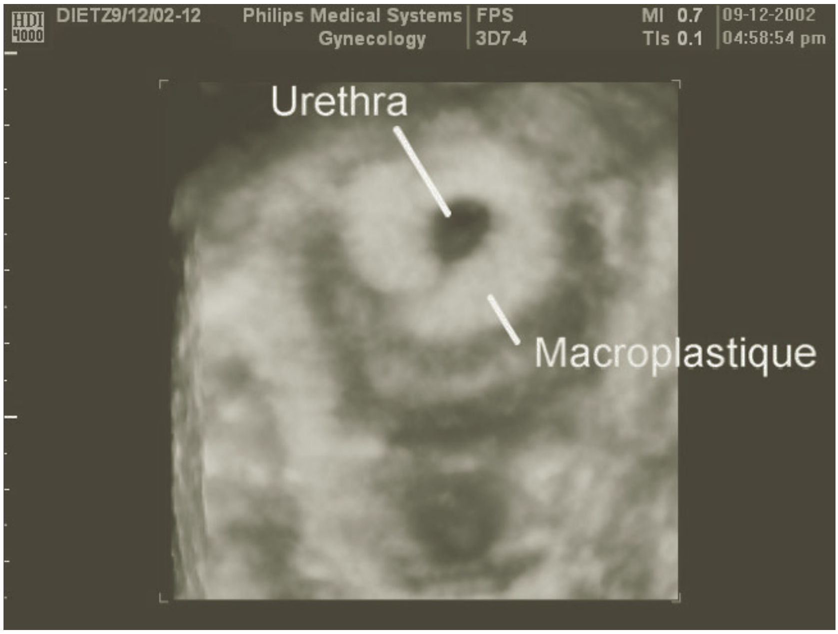

Figure 7.12. Findings 6 months after Macroplastique injection for recurrent stress incontinence. In the axial plane, the silicone macroparticles are evident as a highly echogenic area surrounding the urethra in the shape of a doughnut. (From Dietz HP Ultrasound Imaging of the Pelvic Floor: 3D aspects. Ultrasound Obstet Gynecol 2004;23(6):615–625, with permission.)

References

1. Schuettoff S, Beyersdorff D, Gauruder-Burmester A, Tunn R. Visibility of the polypropylene tape after tension-free vaginal tape (TVT) procedure in women with stress urinary incontinence: comparison of introital ultrasound and magnetic resonance imaging in vitro and in patients. Ultrasound Obstet Gynecol 2006;27(6):687–692.
2. Kaum HJ, Wolff F. TVT: on midurethral tape positioning and its influence on continence. Int Urogynecol J 2002;13(2):110–115.
3. Halaska M, Otcenasek M, Martan A, Masata J, Voigt R, Seifert M. Pelvic anatomy changes after TVT procedure assessed by MRI. Int Urogynecol J 1999;10(S1): S87–S88.
4. Ulmsten U, Henriksson L, Johnson P, Varhos G. An ambulatory surgical procedure under local anesthesia for treatment of female urinary incontinence. Int Urogynecol J 1996;7(2):81–85; discussion 85–86.
5. Ulmsten U, Falconer C, Johnson P, et al. A multicenter study of tension-free vaginal tape (TVT) for surgical treatment of stress urinary incontinence. Int Urogynecol J 1998;9(4):210–213.
6. Nilsson CG, Rezapour M, Falconer C. 7 years followup of the tension-free vaginal tape (TVT) procedure. Int Urogynecol J 2003;14(S1):S35.
7. Delorme E, Droupy S, de Tayrac R, Delmas V. Transobturator tape (Uratape): a new minimally-invasive procedure to treat female urinary incontinence. Eur Urol 2004;45(2):203–207.
8. Dietz HP, Wilson PD. The "iris effect": how two-dimensional and three-dimensional ultrasound can help us understand anti-incontinence procedures. Ultrasound Obstet Gynecol 2004;23(3):267–271.

9. Greenland HP, Dietz H, Barry C, Rane A. An independent assessment of the location of the transobturator tape (Monarc) in relation to the levator ani muscle using 3 dimensional scanning techniques. Int Urogynecol J 2005;16(S2): S59.
10. Baessler K, Hewson AD, Tunn R, Schuessler B, Maher C. Severe mesh complications following intravaginal slingplasty. Obstet Gynecol 2005;106(4):713–716.
11. Dietz HP, Foote AJ, Mak HL, Wilson PD. TVT and Sparc suburethral slings: a case-control series. Int Urogynecol J 2004;15(2):129–131.
12. Lo TS, Horng SG, Liang CC, Lee SJ, Soong YK. Ultrasound assessment of mid-urethra tape at three-year follow-up after tension-free vaginal tape procedure. Urology 2004;63(4):671–675.
13. Dietz HP, Mouritsen L, Ellis G, Wilson PD. Does the tension-free vaginal tape stay where you put it? Am J Obstet Gynecol 2003;188(4):950–953.
14. Ng CC, Lee LC, Han WH. Use of three-dimensional ultrasound scan to assess the clinical importance of midurethral placement of the tension-free vaginal tape (TVT) for treatment of incontinence. Int Urogynecol J 2005;16(3):220–225.
15. Dietz HP, Mouritsen L, Ellis G, Wilson PD. How important is TVT location? Acta Obstet Gynecol Scand 2004;83(10):904–908.
16. Dietz HP, Wilson PD, Gillies K, Vancaillie TG. How does the TVT achieve continence? Neurourol Urodyn 2000;19(4):393–394.
17. Dietz HP, Vancaillie P, Svehla M, Walsh W, Steensma AB, Vancaillie TG. Mechanical properties of implant materials used in incontinence surgery. Neurourol Urodyn 2001;20(4):530–532.
18. Lim YN, Muller R, Corstiaans A, Dietz HP, Barry C, Rane A. Suburethral slingplasty evaluation study in North Queensland, Australia: the SUSPEND trial. Aust N Z J Obstet Gynaecol 2005;45(1):52–59.
19. Fritel X, Zabak K, Pigne A, Demaria F, Benifla JL. Predictive value of urethral mobility before suburethral tape procedure for urinary stress incontinence in women. J Urol 2002;168(6):2472–2475.
20. Iglesia CB, Fenner DE, Brubaker L. The use of mesh in gynecologic surgery. Int Urogynecol J 1997;8(2):105–115.
21. Achtari C, O'Reilly B, Schierlitz L, Dwyer P. Mesh erosion following vaginal repair: is it avoidable? Int Urogynecol J 2003;14(S1):S65.
22. Adekanmi OA, Freeman R, Puckett M, Jackson S. Cystocele: does anterior repair fail because we fail to correct the fascial defects? A clinical and radiological study. Int Urogynecol J 2005;16(S2):S73.
23. Shek K, Dietz HP, Rane A. Transobturator mesh anchoring for the repair of large or recurrent cystocele. ICS Annual Scientific Meeting 2006, Christchurch, New Zealand. Abstract.

8

Outlook

Hans Peter Dietz

Ultrasound imaging, and in particular translabial or transperineal ultrasound, has become the new diagnostic standard in urogynecology. Several factors are contributing to its acceptance, the most important being the availability of suitable equipment. Developments such as the assessment of levator activity and prolapse, but also the use of color Doppler to document urine leakage, enhance the clinical usefulness of the method. With 3D/4D imaging, the technique has finally reached resolutions comparable to magnetic resonance in all three planes, while providing clearly superior temporal resolution – by at least one order of magnitude.

The convenience with which pre- and posttreatment imaging data can now be obtained and archived will simplify outcome studies after prolapse and incontinence surgery. Ultrasound imaging may be able to significantly enhance our understanding of the different mechanisms by which conservative and surgical methods achieve – or fail to achieve – continence or cure of prolapse. It is now possible to identify distinct fascial (such as defects of the rectovaginal septum in true rectoceles) and muscular (such as levator avulsion) defects, which should open up new surgical possibilities.

Regardless of which methodology is used to determine descent of pelvic organs, it is evident that there is a wide variation in pelvic organ mobility even in young nulliparous women. This variation is likely to be at least partly genetic in origin. Ultrasound imaging now allows quantification of the phenotype of pelvic organ prolapse, which will facilitate molecular and population genetic approaches to evaluate the etiology of pelvic floor and bladder dysfunction.

However, there is no doubt that childbirth causes significant alterations of pelvic organ support and levator structure and function, and that there is some relationship between the prior state of pelvic organ supports and labor outcome. It is highly likely that pelvic floor ultrasound will help us identify women at high risk of operative delivery and/or significant pelvic floor damage. It remains to be seen, however, whether such information can have a positive effect on clinical outcomes in what is no doubt a highly politicized environment.

Three-dimensional volume ultrasound adds not one, but several dimensions to pelvic floor imaging, in particular in its most recent incarnations

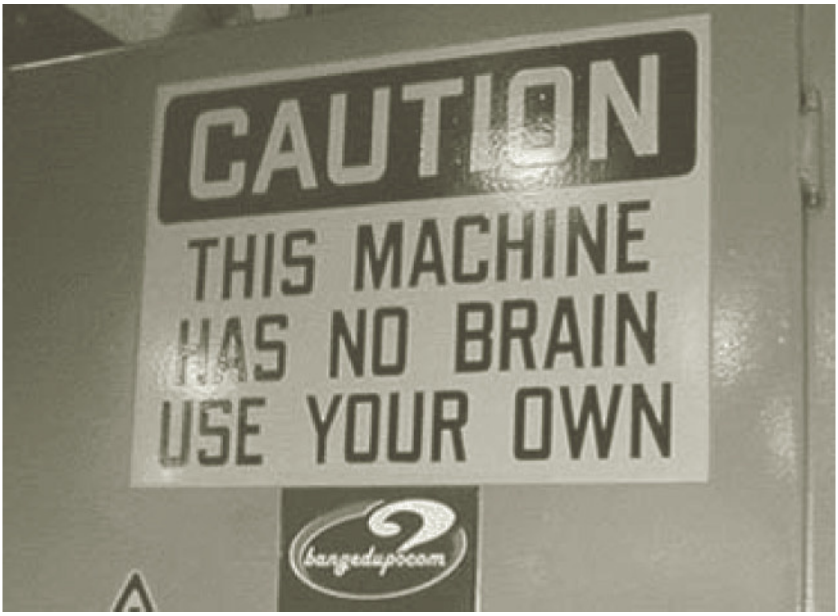

Figure 8.1. To remind us all of the operator-dependent nature of diagnostic ultrasound!

using automatic volume acquisition and 4D cine volume ultrasound. Software-based enhancements, using rendering techniques to improve resolution in all planes, and tomographic or multislice imaging continue to improve capabilities. Three- and four-dimensional technology opens up entirely new possibilities for observing functional anatomy and examining muscular and fascial structures of the pelvic floor. Data acquisition and storage will be simplified and research capabilities enhanced, and surgical audit in this field will undergo significant change.

Whether the new method will be used primarily by clinicians or imaging specialists will depend on local conditions and demand. It will likely be many years before the potential for true progress inherent in this technology is fully realized. The speed with which this development occurs will, to a large degree, depend on the level of cooperation and understanding between those who have access to the most up to date equipment – i.e., imaging specialists – and those who see patients with symptoms of pelvic floor dysfunction, that is, their clinical colleagues.

Another determinant of the uptake of any new diagnostic method is undoubledly the availability of teaching resources. This volume and the accompanying DVD should contribute significantly in this area. Hopefully, there will be regular imaging courses at scientific meetings dedicated to pelvic floor dysfunction to provide a more personal form of skills transfer. Diagnostic ultrasound is highly operator dependent (see Figure 8.1), and this implies that teaching is of paramount importance to ensure appropriate and effective use of technology.

9

An Introduction to 4D View^{TM} (Version 5.0)

Hans Peter Dietz

This book includes a DVD that contains a version of the software 4D View (version 5.0), courtesy of GE Medical, Kretz Ultrasound, Zipf, Austria. To allow you to practice with this software, we have included 16 de-identified volume datasets. This chapter will give an overview of the functionality of this software and take first-time users through the basic steps of performing an analysis in patients with lower urinary tract symptoms and/or pelvic floor dysfunction.

After installation on a PC running Windows 2000 or XP/XP Professional, preferably a Pentium IV, a screen showing the program version becomes visible. Click on this screen. Via the File pulldown menu on the left (see Figure 9.1, long arrow), any GE Kretz compatible volume data file can be opened. Incidentally, the file menu also allows for export of bitmaps ("Export graphic") and AVI videoclips ("Export 4D Img. Cine Sequence"). Most options in the "File" menu are also accessible via a vertical bar of icons on the far left of the screen (short arrow).

The datasets included on the DVD should be visible on clicking "Open." Please open Case 1 in the folder "De-identified volume data." It is a single static volume dataset of about 5 MB, obtained at rest. This should result in appearances similar to Figure 9.1.

The black workspace shows the three orthogonal planes A (midsagittal, top left), B (coronal, top right), and C (axial, bottom left) plus a rendered volume (bottom right). The rendered volume shows a semitransparent representation of all "voxels" (volume pixels) in the "region of interest" or "ROI," i.e., the box visible in the orthogonal planes (thin arrows). The green line at the top of the box represents the rendering direction, i.e., the direction in which the rendering algorithm analyzes the volume data. This function is accessible via the "Settings" pulldown menu ("ROI direction") in case you want to explore the effect of altering the rendering direction.

We'll start with some simple two-dimensional (2D) measurements. To optimize for this, please click on the "Sectional Planes" button (Figure 9.2, arrow) in the "Visualization" menu on the far right. This should make the rendered volume and the region of interest box disappear (see Figure 9.2).

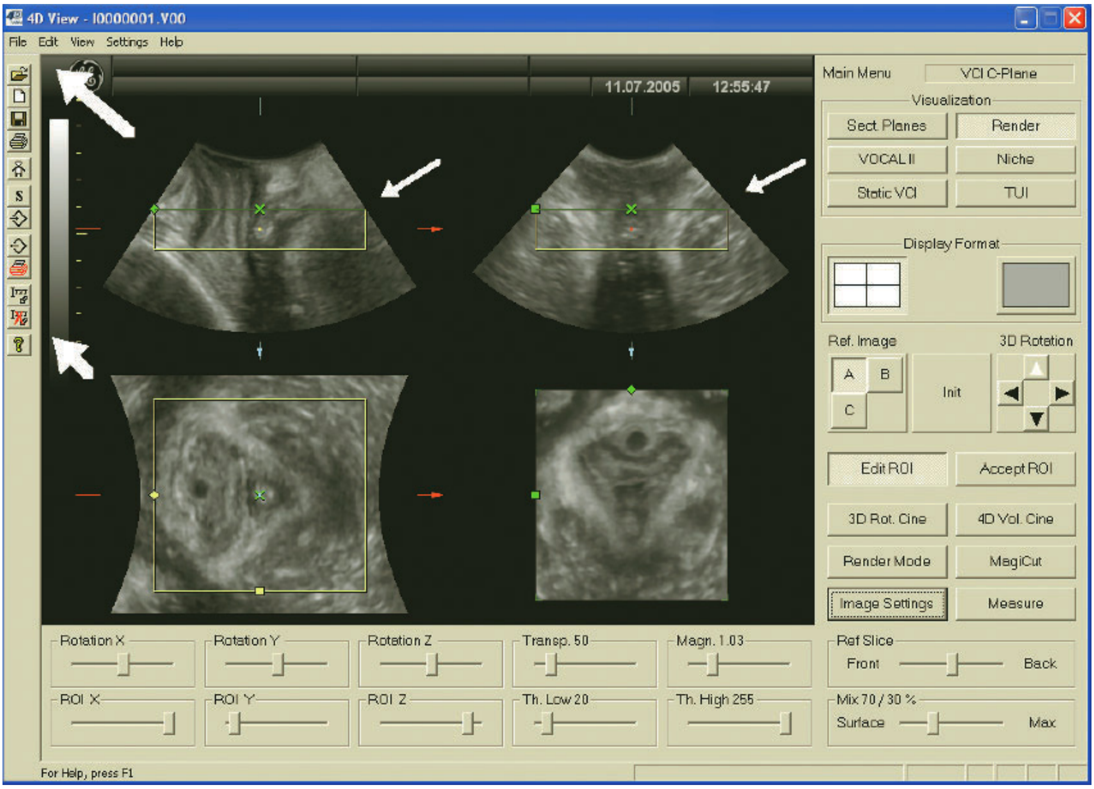

Figure 9.1. Standard orthogonal views on 4D View.

You can manipulate all three planes arbitrarily – either by clicking on the image itself (e.g., the A plane), or by using the three control sliders immediately below the workspace ("Rotation X," "Rotation Y," "Rotation Z"). Moving the mouse cursor over the A plane and left clicking changes your arrow into a small icon. This icon will vary depending on how close to the center of the image (identified by a small yellow dot in the plane that's currently active) you are. Please try and drag this icon and observe the effect on your screen. Rotating the A plane image may result in appearances such as in Figure 9.3, or (more likely) something a lot more confusing.

Once you are well and truly lost, please click the "Init" button (Figure 9.3, long arrow) to revert to the appearances in Figure 9.2. The three buttons to the left of "Init," incidentally, allow you to select the active plane without clicking on the plane in question. (Tip: The "Init" option will come in handy whenever appearances on your screen deviate markedly from the figures given in this chapter – which is likely to happen many times. However, if you'd rather not lose whatever you've done until that point in time – e.g., altered image settings – the "Orient. Help" button (small arrow) under "Init" may be more useful, giving you a graph of the location of your currently selected plane in the entire volume.)

To perform some basic measurements in the A plane, let's enlarge the top left hand part of the workspace. Please click on the right-hand button

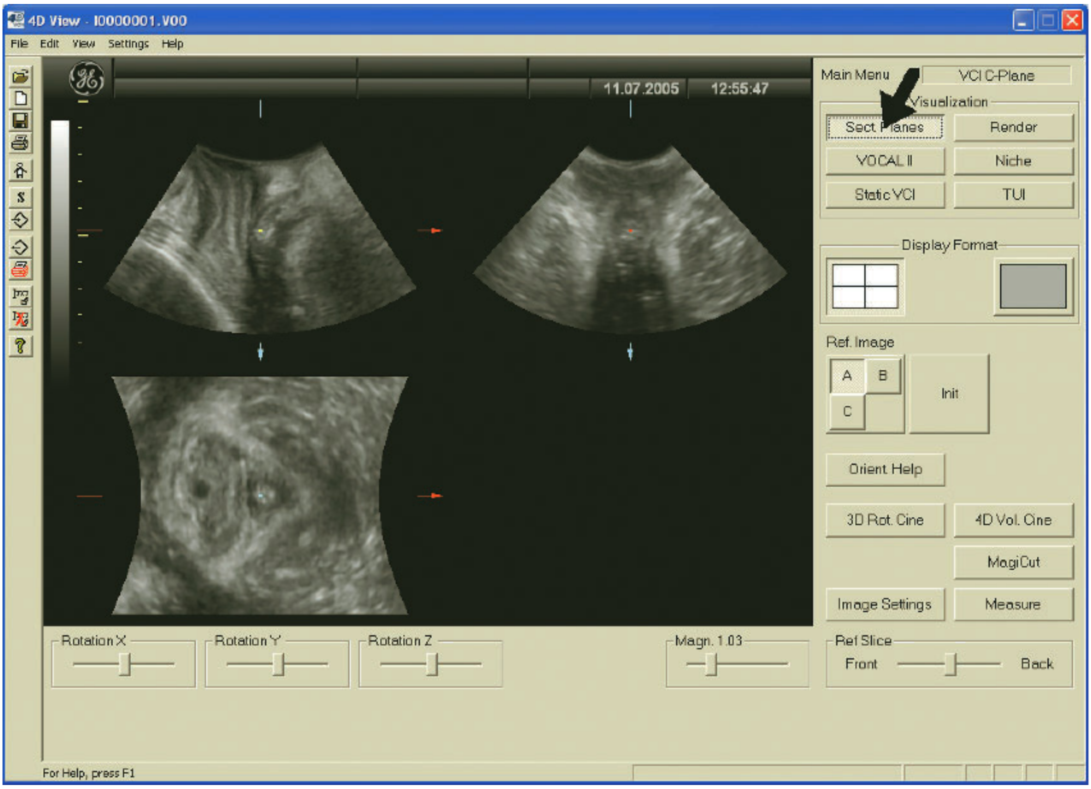

Figure 9.2. Sectional planes.

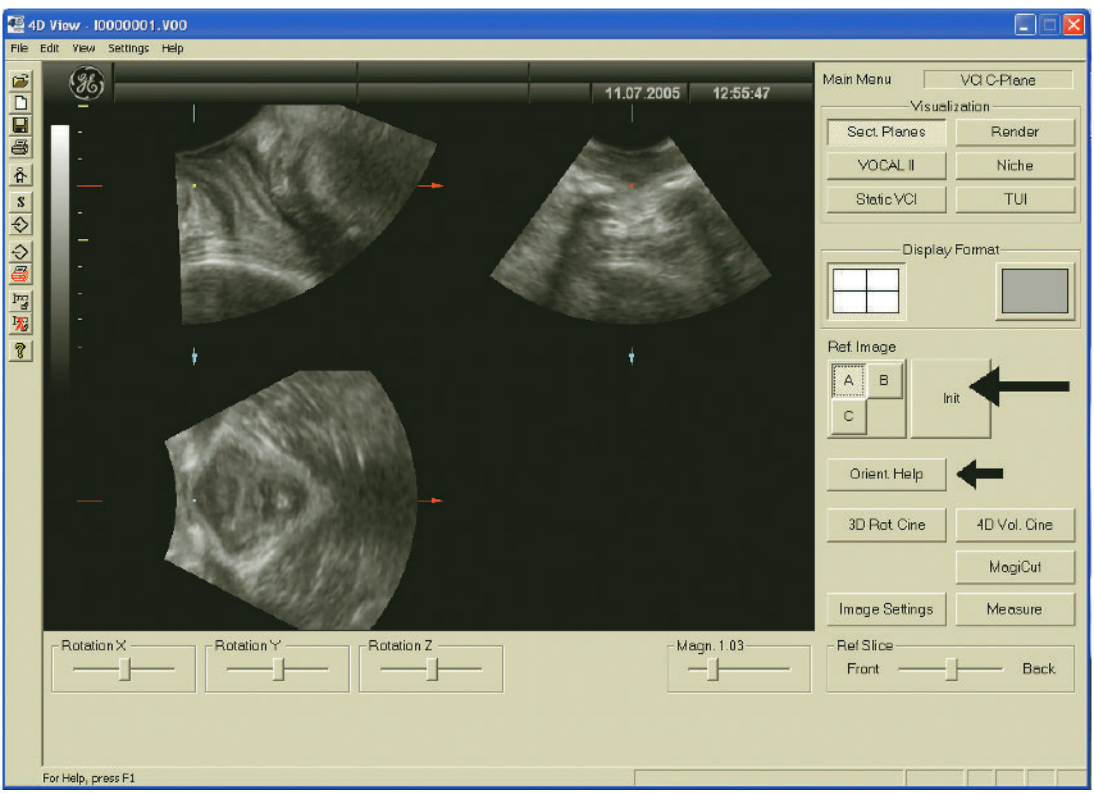

Figure 9.3. Rotating the A plane.

under “Display Format” which allows the currently active plane (which should be the A plane) to fill the workspace. The screen should now look like Figure 9.4.

If your image should not be exactly centered (i.e., if the A plane does not show the urethra well), use the “Ref slice” control for adjustment (short arrow in Figure 9.4).

Once you’re happy with the appearance of your A plane, please click on “Measure” (Figure 9.4, long arrow). The 4D View measurement package will take some seconds to load. Because there currently is no application “Pelvic Floor” yet, we’ll use the “Generic” menu. This should give you the appearance shown in Figure 9.5.

By clicking on “Generic Dist” (Figure 9.5, long arrow) and “Dist 2 point” (short arrow), you should be able to measure, e.g., bladder neck position relative to the symphysis pubis (see Figure 9.5) and detrusor wall thickness (not that easy here because the bladder is completely empty). By clicking on “Generic angle” and “Angle 2 line” you should be able to measure any angle you may want to determine, e.g., retrovesical angle or the levator plate angle.

To perform measurements in the C plane, you need to click “Main Menu” (bottom right corner) and the left button under “Display Format.” Rotating the A plane (see Figure 9.3) will change the appearances of the C plane until the C plane represents the minimal dimensions of the hiatus. Experiment

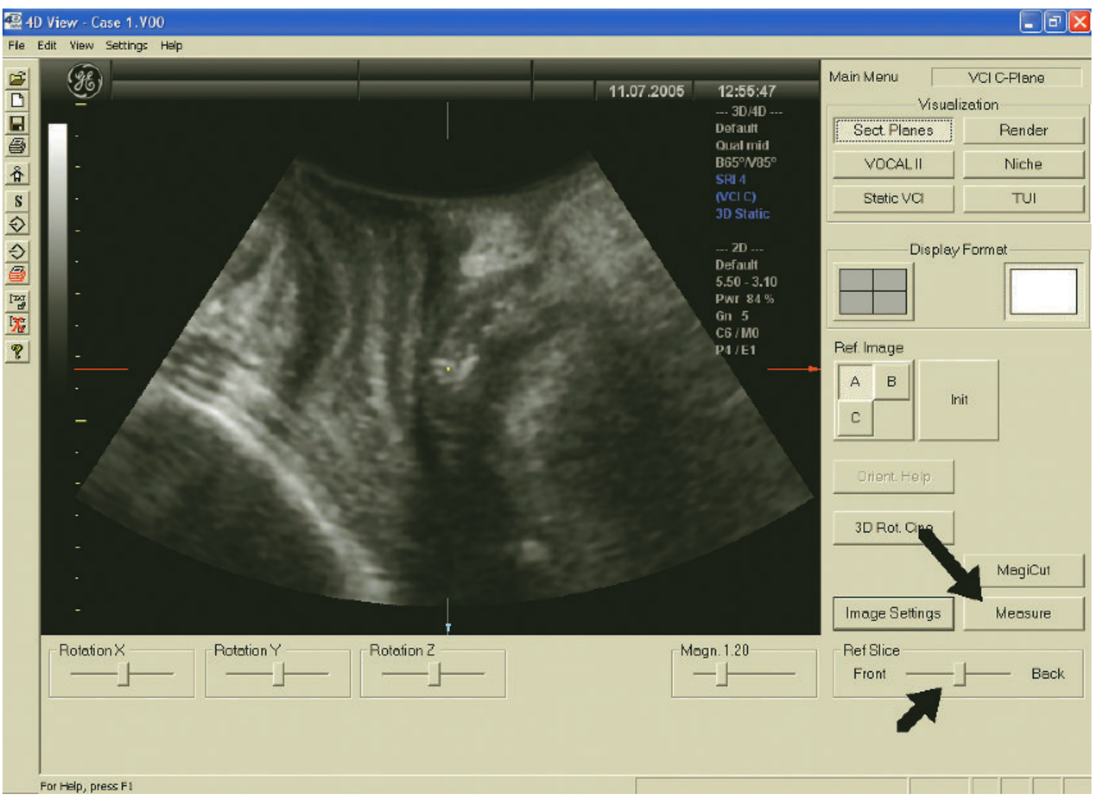

Figure 9.4. Measurements.

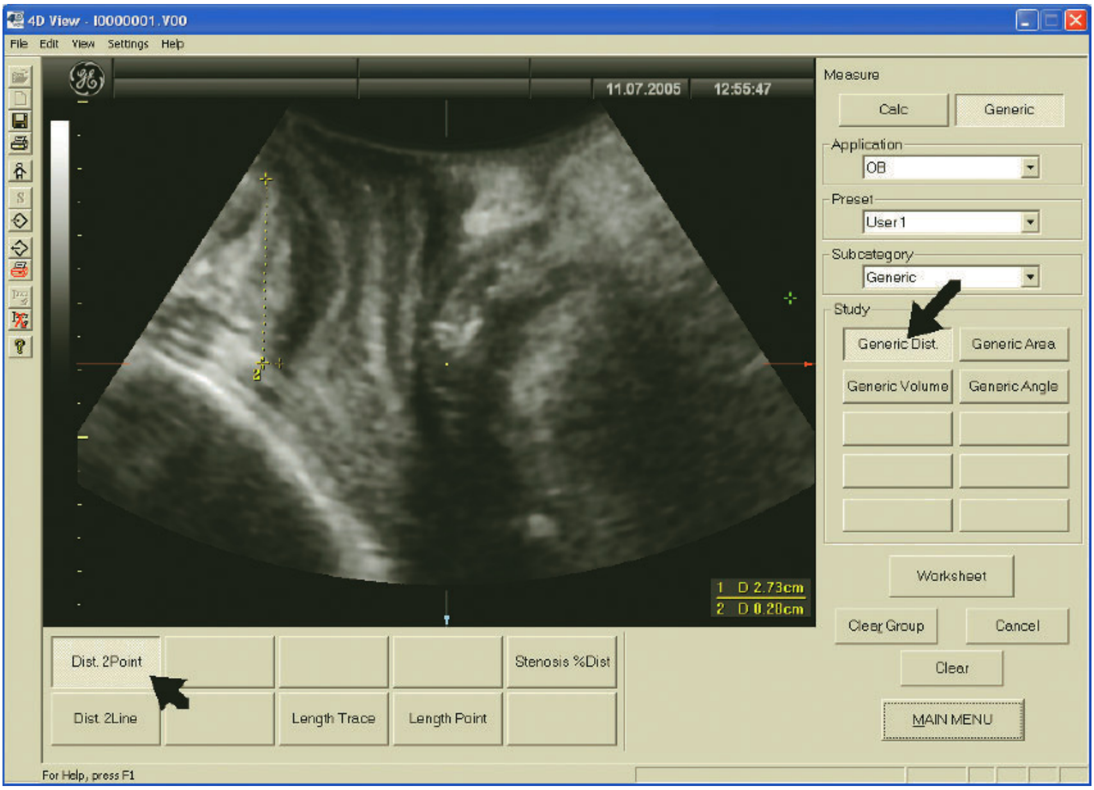

Figure 9.5. Measuring distances.

with moving the central marker in the A plane up/down and left/right before rotating. (Tip: If a small double-sided arrow comes up instead of the bulls-eye, you've clicked on the image too far from the central marker.) Remember the "Init" button: it will likely take several attempts until you have appearances similar to Figure 9.3. Once this is the case, select the C plane and click the right-hand button under "Display Format" to enlarge the C plane. Then rotate the C plane by clicking on it about 1–2 cm from the central marker, and drag the image until the hiatus assumes appearances as in 9.6. You may also drag the control "Magn." under the right-hand corner of the work area in order to make sure that the feature you want to measure fills the screen. (Tip: If you can't see the "Magn." control, you're probably not in the Main Menu. You can always get there by clicking the "Main Menu" button. If you can't see that button, you're already there.)

Once you're back in the "Measure" menu you should see an image similar to Figure 9.6. Now you should try and measure an area, e.g., the hiatal area as in Figure 9.6, by clicking "Generic Area" and "Area Trace." (Tip: At this stage, you're probably cursing your track-pad or mouse, and searching frantically for a decent mouse pad. A graphic tablet, if available, is likely to give superior results.)

At this stage, let's try and optimize image quality a bit further. This is likely to be necessary for many (if not all) of the volume datasets included on the DVD. Please click "Main Menu" in the bottom right-hand corner and select "Image settings" next to the "Measure" button. This should give you the appearances shown in Figure 9.7.

Please experiment by dragging the controls "Bias" and "Pos" until you're happy with the image (Figure 9.7, long arrow). There also is an option "SRI" (see Chapter 3) which improves resolution by speckle reduction (short arrow). SRI comes in six steps; the author usually selects steps 4 or 5. (Tip: SRI may result in irritating whorl-like artifacts, especially when processing volumes obtained by older systems. It's a matter of trial and error.)

While we're in the C plane, let's also try another recent innovation, "Tomographic Ultrasound Imaging." In the Main Menu, you'll find a button "TUI," situated in the "Visualisation" submenu on the right (Figure 9.8, long arrow). Clicking on this button will give you the standard TUI screen, containing a reference plane in the top left-hand corner and seven axial slices at predetermined intervals filling the rest of the workspace. It should look approximately like Figure 9.8. These intervals can be adjusted with the "TUI distance" control (short arrow). You may also want to increase the number of slices via "Slices: –, +" and change which ones are shown in the workspace by using "TUI slices," "Prev," and "Next" in the bottom right corner.

Now let's do some dynamic measurements and start using the 4D capabilities of 4D View. For this purpose, please go back to the File menu and load Case 5. This is a cineloop of dozens of volumes and therefore much larger in size, about 142 MB. Older PCs will require some time to upload

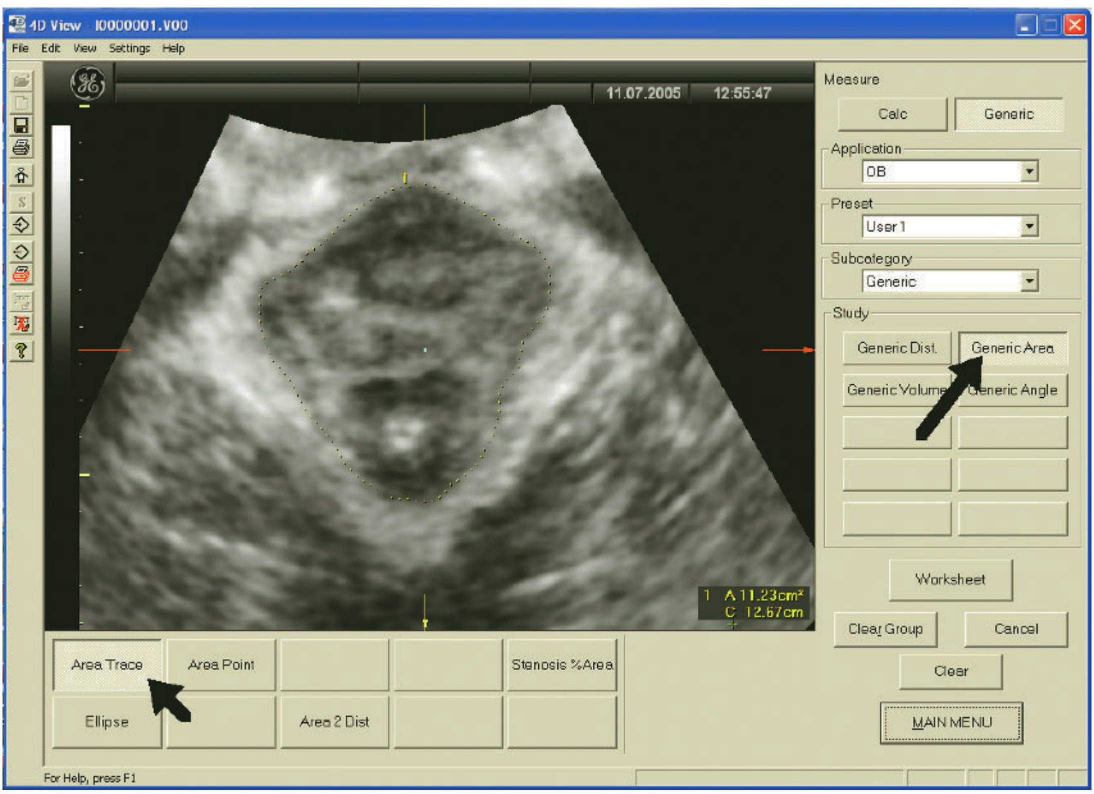

Figure 9.6. Measuring angles.

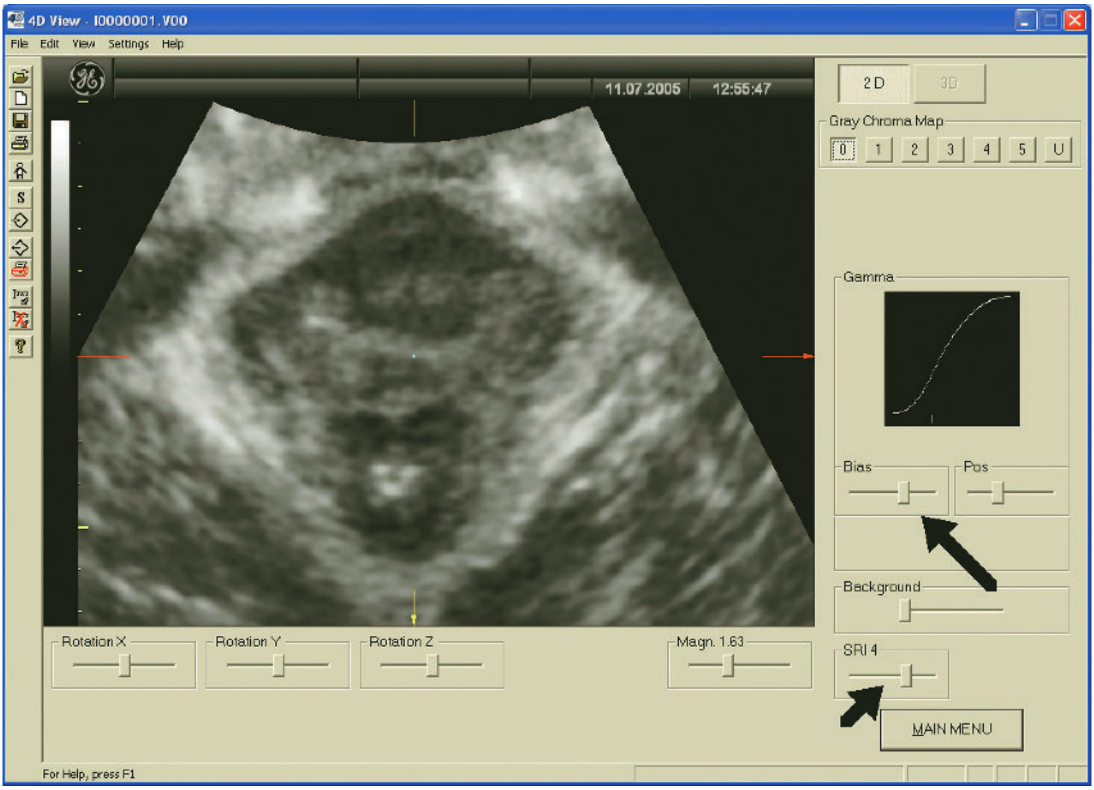

Figure 9.7. Optimizing image quality.

Figure 9.8. Tomographic ultrasound imaging.

this dataset. It may be necessary to copy the files to your computer's hard disk before starting work.

The resulting image should look much like Figure 9.9, once you've clicked on "Sect. Planes" to get rid of the rendered volume. Please feel free to optimize appearances by using "Magn.," "Ref slice," and "Image settings."

You'll notice that there is a sliding bar in the bottom right-hand corner of the workspace (Figure 9.9, long arrow). Please click on the bar and move it by dragging the indicator (short arrow). (Tip: If the image suddenly seems independent of what you're doing, i.e., it's moving of its own accord, then you haven't clicked on the right spot. Clicking anywhere on the bar activates the cineloop. Stop it by clicking again, then click and hold the indicator.) This lets you replay the whole cineloop of volumes, in this case a Valsalva maneuver.

Please stop the cineloop (by clicking anywhere on the bar, or by letting go of the sliding control if you're dragging it) near the start of the cineloop. Select the A plane and go through the steps illustrated above (Figures 9.4 and 9.5) in order to obtain the vertical distance between inferior symphyseal margin and the bladder neck – similar to Measurement 1 in Figure 9.5. The vertical distance between inferoposterior symphyseal margin and bladder neck should be about 28–30 mm.

Now go back to "Main Menu." Drag the cineloop control until there is maximal displacement of the bladder neck (see Figure 9.10) and measure

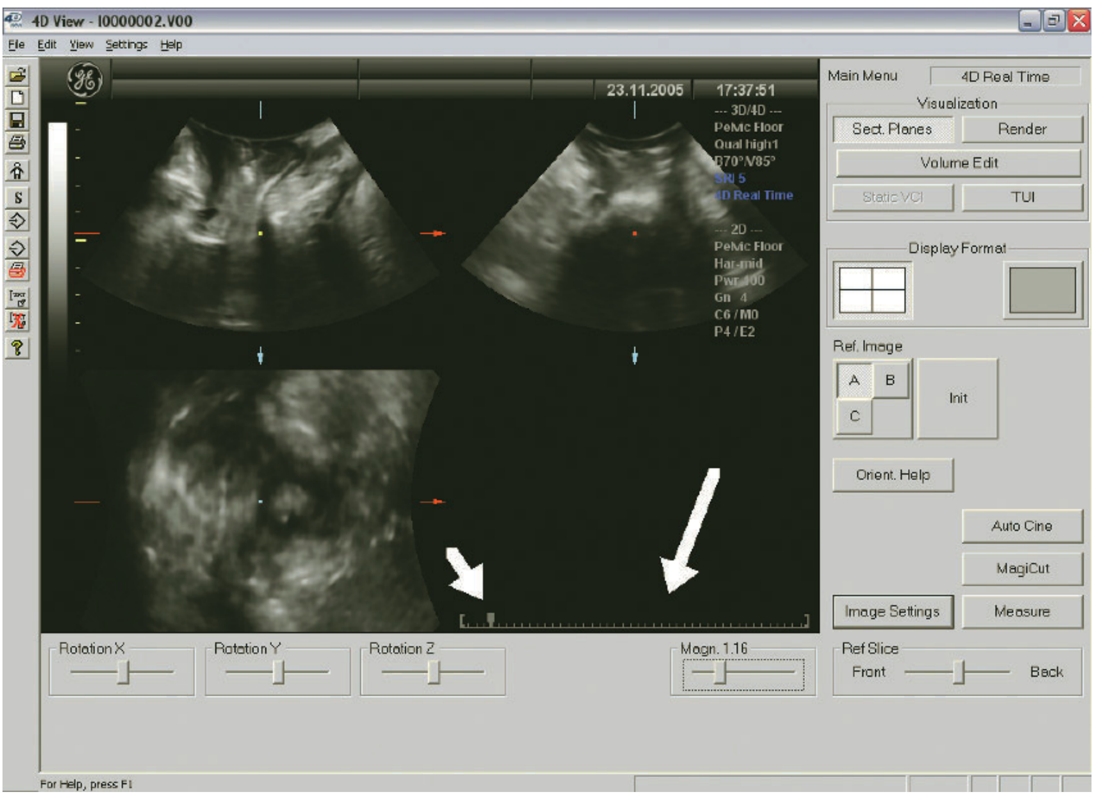

Figure 9.9. The cineloop control bar.

again. Do make sure you're able to identify the inferoposterior margin of the symphysis pubis on the frames you select for measuring – it's very close to the edge of the image in this volume. Once you have identified a frame that shows a maximal Valsalva (before you select the "Measure" menu), you'll have to use the "Ref slice" control in order to visualize the bladder neck – it has moved somewhat laterally of the reference plane. There is some funneling although it's not very clear because of artifact in the near field (see Figure 9.10, white arrow).

This should give you a measurement of about 8–10 mm for the position of the bladder neck on maximal Valsalva, which is negative because the bladder neck is now caudal to the symphyseal margin. On deducting this second measurement from the first, you arrive at approximately 29 – (–9) = 38 mm of bladder neck descent on Valsalva. And while we're at it, you could also measure maximal descent of the bladder, uterus (Figure 9.11, long arrow), and rectal ampulla (short arrow) against the inferior symphyseal margin (see also Chapter 4). The uterus remains 3.9 mm above the reference line, the rectal ampulla descends to 11.4 mm below. The lowest point of the bladder is virtually at the level of the bladder neck, and the measurement for maximal bladder descent, 8.5 mm below the symphysis, is therefore very close to the measurement obtained in Figure 9.10.

Let's see what else we can do with this cine volume dataset. By all means, have a look at the axial (C) plane – it's definitively not normal. In this case,

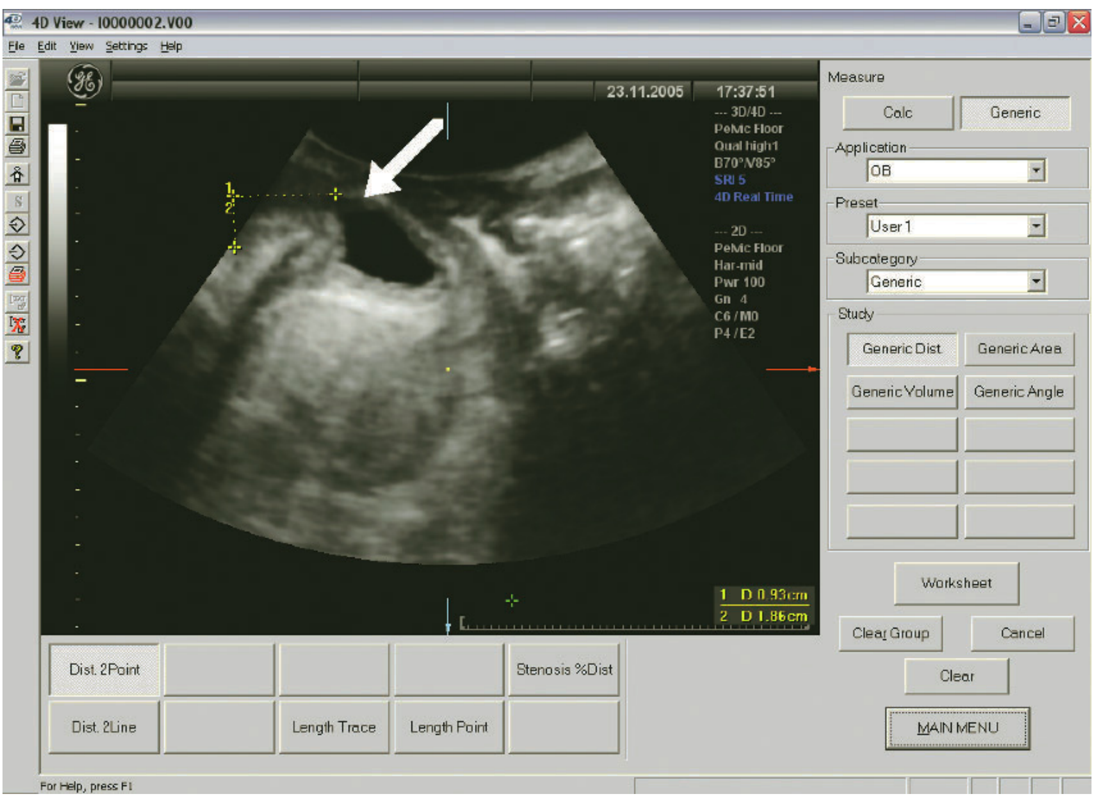

Figure 9.10. Measuring bladder neck descent.

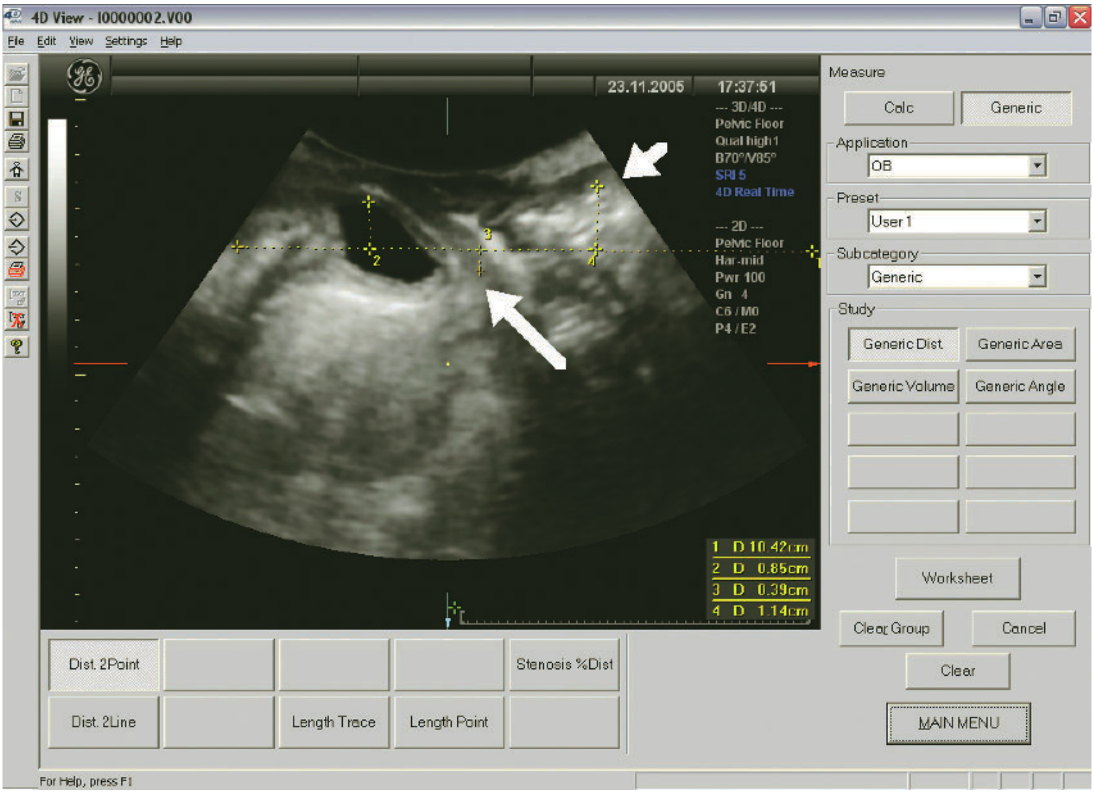

Figure 9.11. Measuring pelvic organ descent.

the abnormality is best seen on a rendered volume though. Click "Init" in the main menu, click "Render," then optimize image settings. You can change image settings separately for cross-sectional planes A, B, C ("2D"), and the rendered volume (3D) by selecting one or the other at the top right, once you're in the "Image Settings" menu. The result should be something close to Figure 9.12.

Please select "Main Menu" and then click on the "box," i.e., the perimeter of the region of interest (ROI) in the A plane (long arrow), and try and manipulate it. You can shrink or enlarge the box, even change the course of the green line by clicking directly on it. Most of those effects can also be achieved by using the controls "ROI X," "ROI Y," and "ROI Z" on the bottom left (short arrows). To shift the region of interest up or down, please go to Main Menu, select the C plane, and use the "Ref slice" control on the bottom left. Click the right button under "Display Format" to enlarge the rendered volume. The result should look approximately like Figure 9.13, which shows a small left-sided defect of the pubovisceral muscle (long arrow).

Use the cineloop control (short arrow) to observe how the levator hiatus enlarges on Valsalva ("ballooning"). You may want to select "Measure" and determine the area of the hiatus on Valsalva, which should be in the order of 36–38 cm^2 (see Figure 9.14). Incidentally, you may have noticed that this small defect becomes virtually invisible on Valsalva (arrow) as the area of interest gets flattened against the pelvic sidewall (see Chapter 6).

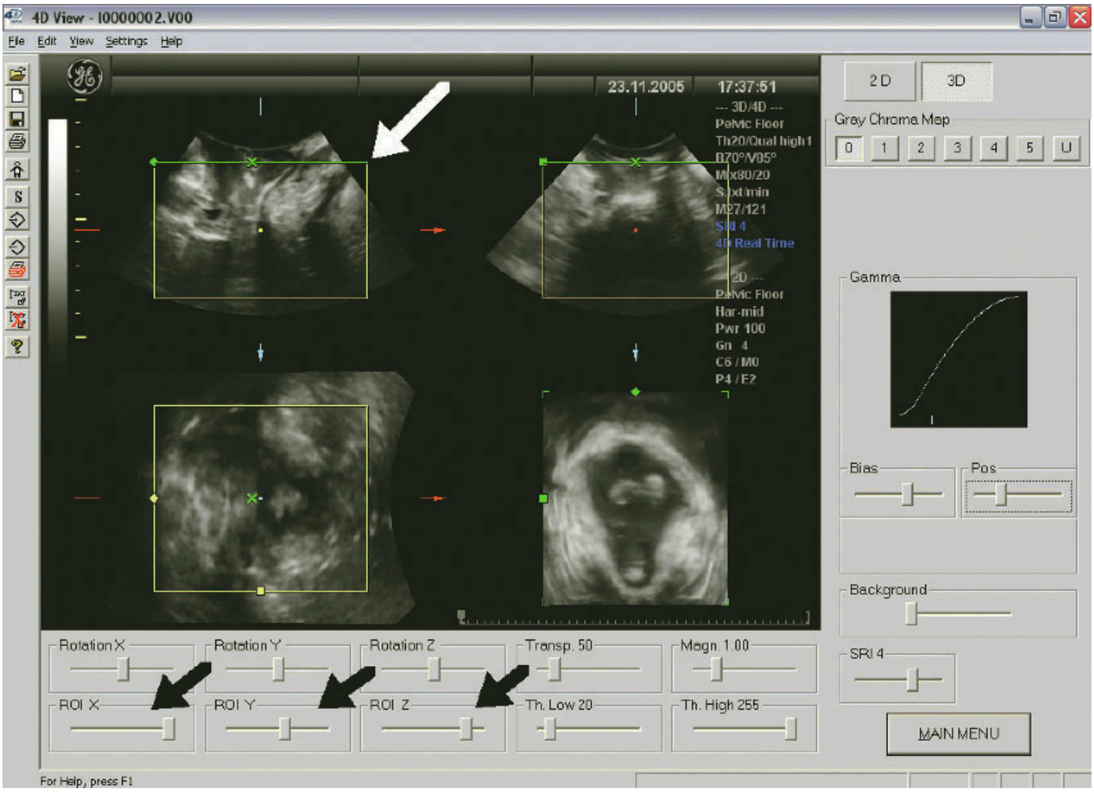

Figure 9.12. Region of interest controls.

Figure 9.13. Left-sided avulsion in a rendered volume.

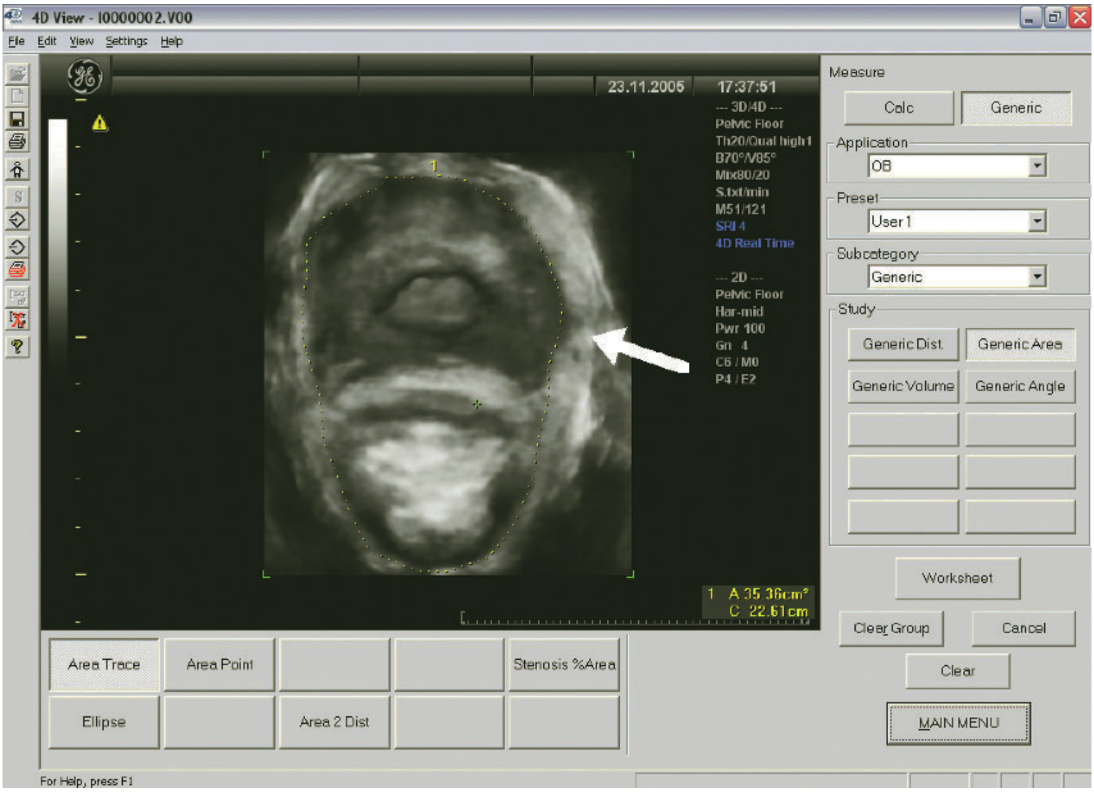

Figure 9.14. Levator ballooning in a rendered volume.

Congratulations for reaching the end of this short course!

You should now be able to analyze all 16 volume datasets on 15 "virtual patients" included on the DVD. The first and fifth you've already encountered. Usually, a full examination will include volumes obtained on levator contraction in order to be able to assess pelvic floor muscle function. To simplify matters, I've given two datasets only in Case 2 in order to demonstrate the effect of levator activation. In all other cases (4–15), there is only one cine volume dataset, comprising volumes from resting to maximal Valsalva. The settings have been optimized for brightness, contrast, magnification, and speckle reduction, but of course you're welcome to change these settings as you see fit.

In the Appendix, I've added (hypothetical) reports describing those "virtual patients" in order for you to be able to check your findings against mine. As regards numerical measurements, I'd suggest that you recheck your methodology if your figures differ by more than 20% from those given in the reports. You're welcome to e-mail me with specific questions or comments at hpdietz@bigpond.com.

Good luck!

H.P. Dietz
Sydney, December 2006

Appendix

Cases for "Virtual Scanning" Using 4D View

Hans Peter Dietz

Case 1: Static Volume at Rest, Normal Anatomy

Dear Colleague,

I saw your above patient yesterday for a pelvic floor ultrasound. As you know, she has been getting recurrent urinary tract infections, about five over the last year.

She was examined supine and after voiding, using a GE Kretz Voluson 730 expert system with 8–4 MHz volume transducer. Unfortunately, our system crashed halfway through the examination, leaving me with just the static volume ultrasound, which is what I can report to you today.

Findings:

There was no postvoid residual. The urethra and vagina appeared normal, in particular there was no evidence of a urethral diverticulum or stenosis. Detrusor wall thickness was normal at 2.9 mm. The levator ani muscle and hiatus were completely normal, measuring about 12 cm^2 at rest. Because of the absence of volumes on Vasalva, I'm unable to comment on pelvic organ descent or prolapse.

Interpretation: Normal anatomy at rest.

I hope to have been of assistance.

Case 2: Normal Anatomy (2a), Pelvic Floor Contraction (2b)

Dear Colleague,

Thanks for referring this 21-year-old primigravid woman at 30 weeks' gestation who is presenting with a sensation of prolapse, or laxity, without there being, as I understand from your referral, any clinical findings. I gather that she is a women's health physiotherapist who wants to know whether her pelvic floor is normal.

2D and 3D pelvic floor ultrasound was performed using a GE Kretz Voluson 730 Expert system.

Findings:

2D: There was no postvoid residual. The urethra appeared normal. The bladder neck descended only 9 mm, with 10° of urethral rotation and no funneling. There was no other evidence of pelvic organ descent. The rectovaginal septum was intact. Detrusor wall thickness was normal at 3.1 mm.

3D: The pubovisceral muscle was intact bilaterally and invariably activated whenever the patient increased intraabdominal pressure. The hiatus on Valsalva measured only 11 cm^2. The patient was able to perform a symmetrical pelvic floor contraction which reduced the hiatus by 7 mm in the midsagittal diameter, and to about 8 cm^2 in the axial plane.

Interpretation: Normal pelvic floor anatomy and function.

Case 3: Cystocele I, Elevated Detrusor Wall Thickness

Dear Colleague,

Thanks for referring this 25-year-old woman who is presenting with symptoms of irritable bladder. There is urgency, urge incontinence, frequency, and nocturia, as well as occasional stress incontinence. She is mother of two children born by normal vaginal delivery.

2D and 3D pelvic floor ultrasound was performed using a GE Kretz Voluson 730 Expert system.

Findings:

2D: There was no postvoid residual. The urethra appeared normal. The bladder neck descended by about 30 mm, with 80° of urethral rotation but no funneling. There was no other evidence of pelvic organ descent. Detrusor wall thickness was abnormal at 6.1 mm.

3D: The pubovisceral muscle was intact bilaterally and appeared to be rather substantial, especially on the left. The hiatus opened to 21 cm^2 on Valsalva, which is normal.

Interpretation: Mild cystourethrocele with urethral rotation and opening of the retrovesical angle, but no funneling. Elevated detrusor wall thickness which is associated with detrusor overactivity. Otherwise normal pelvic floor anatomy.

Case 4: Cystocele I, Funneling, Stress Incontinence

Dear Colleague,

Thanks for referring this lady who is presenting with symptoms of severe stress incontinence. There are no other symptoms of bladder or bowel dysfunction.

2D and 3D pelvic floor ultrasound was performed using a GE Kretz Voluson 730 Expert system.

Findings:

2D: There was no postvoid residual. The urethra was normal. The bladder neck descended 27 mm on Valsalva, with 50° of urethral rotation, an open retrovesical angle (180°), and marked funneling. No cystocele. Detrusor wall thickness was normal at 2.6 mm. No central or posterior compartment descent.

3D: The pubovisceral muscle was intact bilaterally, and there was no ballooning, with the hiatus measuring less than 20 cm^2 on Valsalva. There was normal paravaginal tenting bilaterally.

Interpretation: Mild bladder neck descent with marked urethral funneling, indicative of a low-pressure urethra and likely to be associated with urodynamic stress incontinence. No prolapse. Good levator and hiatal anatomy.

Case 5: Cystocele II, Uterine Prolapse I, Right-sided Levator Avulsion

Dear Colleague,

As you're aware, this 32-year-old woman has noticed a "lump downbelow" after the delivery of her first child some 4 months ago. There are no symptoms of bladder or bowel dysfunction.

2D and 3D pelvic floor ultrasound was performed using a GE Kretz Voluson 730 Expert system.

Findings:

2D: There was no postvoid residual. The urethra appeared normal. We saw 36 mm of bladder neck descent on Valsalva, with the retrovesical angle opening to 180°, 90° of urethral rotation, and some funneling. A cystocele descended to about 8 mm below the symphysis, the uterus to 4 mm above, and the rectal ampulla to 12 mm below. There was no "true" rectocele or defect of the rectovaginal septum, but possibly a minor degree of rectal intussusception or internal rectal prolapse. Detrusor wall thickness was abnormal at 5.4 mm.

3D: There was some asymmetry of the pubovisceral muscle with a moderate-sized defect of the entire pubovisceral muscle on the left. On Valsalva, there was moderate ballooning of the hiatus to 36 cm^2.

Interpretation: Mild–moderate cystocele with open retrovesicle angle and funneling. Minor degree of uterine prolapse. Perineal hypermobility but no true rectocele. Left-sided avulsion defect of the pubovisceral muscle and moderate ballooning. Significant risk of prolapse recurrence after reconstructive surgery.

Case 6: Rectocele II

Dear Colleague,

Thanks for referring this 72-year-old woman who is presenting with symptoms of prolapse, incomplete bowel emptying and straining at stool, as well as occasional fecal incontinence. There are no urinary symptoms apart from mild frequency and nocturia.

2D and 3D pelvic floor ultrasound was performed using a GE Kretz Voluson 730 Expert system.

Findings:

2D: There was a postvoid residual of less than 30 mL. The urethra was normal. The bladder neck was obscured by a fairly large rectocele on Valsalva but did not seem to descend more than 2 cm on Valsalva, with about 30° of rotation. No cystocele. Detrusor wall thickness was normal at 3.9 mm. The main finding was a large rectocele, reaching to about 28 mm below the symphysis pubis, of a depth of 30 mm on Valsalva. A transverse defect of the rectovaginal septum was evident even at rest, at the level of the anorectal junction. No rectal prolapse or intussusception. The internal and external anal sphincters were intact.

3D: The pubovisceral muscle seemed intact bilaterally, and the hiatus enlarged to only 25 cm^2 on Valsalva, which is normal.

Interpretation: Large rectocele caused by a transverse defect of the rectovaginal septum at the level of the anorectal junction. No major morphologic abnormality of the levator ani; no ballooning of the hiatus.

Case 7: Previous Burch Colposuspension, Rectoenterocele II, Severe Ballooning

Dear Colleague,

Thanks for referring this 68-year-old woman who is presenting with symptoms of prolapse about 5 years after a Burch colposuspension. There also is incomplete bowel emptying and straining at stool, and she has had several urinary tract infections (UTI) over the last year.

2D and 3D pelvic floor ultrasound was performed using a GE Kretz Voluson 730 Expert system.

Findings:

2D: There was a postvoid residual of approximately 40 mL. The urethra showed the obvious distortional effects of a colposuspension. There may be some urethral stenosis as a result. The bladder neck was well elevated, with only 4 mm of bladder neck descent on Valsalva and an intact retrovesical angle. No cystocele. Detrusor wall thickness was normal at 4.5 mm. The main finding was a moderate rectoenterocele, with the enterocele dominant and reaching about 18 mm below the symphysis pubis. The rectocele reached to 14 mm below and measured at a depth of 18 mm.

3D: The pubovisceral muscle seemed intact bilaterally, if somewhat thin, more so on the left. However, there was marked ballooning of the hiatus to 42 cm^2.

Interpretation: Well-supported bladder neck after Burch colposuspension which may be slightly on the tight side. Moderate rectoenterocele, with the enterocele present at rest and clearly the dominant feature. No major morphologic abnormality of the levator ani, but marked ballooning of the hiatus.

Case 8: Cystocele III after Burch and Zacharin Procedure, Voiding Dysfunction

Dear Colleague,

Thank you kindly for referring this 62-year-old woman who is presenting with symptoms of recurrent prolapse after a vaginal hysterectomy and anterior/posterior (A/P) repairs in 1980, a Burch colposuspension 12 years ago, and a Zacharin abdominoperineal levatorplasty plus sacrocolpopexy in 2002. She describes urge incontinence, hesitancy and recurrent urinary tract infections, as well as symptoms of chronic constipation and prolapse.

2D and 3D pelvic floor ultrasound was performed using a GE Kretz Voluson 730 Expert system.

Findings:

2D: There was a postvoid residual of 120 mL. The urethra and bladder neck showed the effects of a colposuspension but were otherwise normal. We measured 13 mm of bladder neck descent, with intact retrovesical angle and no funneling. There was a large "high cystocele" to 26 mm below the symphysis pubis but no other evidence of prolapse. The cul-de-sac remained about 2 cm above the symphysis pubis, and there was no rectocele. Detrusor wall thickness was normal at 3 mm although this finding should be regarded with caution because of the high residual.

3D: The pubovisceral muscle seemed intact. Typical for a Zacharin levatorplasty, there was a thick scar plate anterior to the rectum, linking the lateral aspects of the pubovisceral muscle. This scar plate extended over at least 2.5 cm in a craniocaudal direction, ventral to the anorectal junction. However, there still was some ballooning of the hiatus to 33 cm^2.

Interpretation: Well-supported bladder neck after Burch colposuspension. Moderate high cystocele. Good vault and posterior compartment support. Intact levator ani with evidence of effective Zacharin levatorplasty. There may be a degree of stenosis at the level of the anorectal junction. Mild hiatal ballooning. Likely mild to moderate voiding dysfyunction.

Case 9: Gartner Cysts

Dear Colleague,

As you're aware, this 30-year-old woman recently had a transvaginal ultrasound during which cystic structures were noted in the anterior vaginal wall. She is mother of one child born by normal vaginal delivery. There are no symptoms of bladder or bowel dysfunction.

2D and 3D pelvic floor ultrasound was performed using a GE Kretz Voluson 730 Expert system.

Findings:

2D: There was a small postvoid residual of 60 mL. The urethra appeared normal. We saw 13 mm of bladder neck descent on Valsalva, with the retrovesical angle on Valsalva at 130°, 40° of urethral rotation, and no funneling. No pelvic organ prolapse. Detrusor wall thickness was normal at 2.7 mm. There were multiple cystic structures in the anterior vaginal wall without obvious connection to the urethra, and no internal echoes. They extended close to the ureteric orifices but again appeared separate from those structures.

3D: There was no asymmetry of the pubovisceral muscle, no evidence of defects. On Valsalva, there was only very minor opening of the hiatus to 17 cm^2.

Interpretation: Multiple cystic structures situated in the anterior vaginal wall, up to 2 × 3 cm in diameter. No obvious connection to lower or upper urinary tract, but the cysts extend close to the ureters bilaterally and surround the urethra, especially on the left. These structures are very likely to be attributable to Gartner duct cysts and best left alone unless clearly symptomatic.

Case 10: Cystocele II, Uterine Prolapse II, Bilateral Avulsion

Dear Colleague,

I've had the honor of seeing your above patient for a pelvic floor ultrasound. As you're aware, this 37-year-old woman had her first child by rotational forceps, about 9 months ago. She says that she hasn't been the same since. There is urgency, urge incontinence, and a sensation of prolapse as well as incomplete bowel emptying.

2D and 3D pelvic floor ultrasound was performed using a GE Kretz Voluson 730 Expert system.

Findings:

2D: There was a postvoid residual of approximately 70 mL. The urethra appeared normal. We saw 44 mm of bladder neck descent on Valsalva, with the retrovesical angle opening to 180°, 80° of urethral rotation, but no funneling. A cystocele descended to about 15 mm below the symphysis; the uterus to 13 mm below. Detrusor wall thickness was normal at 3.5 mm. There was no defect of the rectovaginal septum.

3D: There was a major bilateral avulsion injury of the pubovisceral muscle, worse on the right, with complete loss of paravaginal tenting. The hiatus measured more than 6 cm in the coronal plane, and the defects measured almost 3 cm in width. Although dimensions in the sagittal plane remained reasonable, the severe damage to levator insertions bilaterally caused marked ballooning of the hiatus to 43 cm^2.

Interpretation: Moderate cystocele with open retrovesicle angle (RVA) but no funneling. Moderate uterine prolapse. Normal posterior compartment. Major bilateral avulsion defect of the pubovisceral muscle and severe ballooning. Marked risk of prolapse recurrence after reconstructive surgery. Her anterior compartment prolapse is probably incurable unless one uses mesh interposition. Anorectal function may require further investigation.

Case 11: Rectal Prolapse after Monarc, Apogee Procedures

Dear Colleague,

Thanks for referring this woman who is presenting with symptoms of obstructive defecation and dyschezia 4 months after an apparently successful repair of a posthysterectomy vault prolapse by "Apogee" mesh. As you're aware, she has had multiple anti-incontinence and prolapse procedures in the past. There is no incontinence.

2D and 3D pelvic floor ultrasound was performed using a GE Kretz Voluson 730 Expert system.

Findings:

2D: There was a postvoid residual of approximately 40 mL. The urethra was normal. There was a transobturator suburethral sling in a typical midurethral position. It seemed under moderate tension, as evidenced by its c shape on Valsalva, but not unduly obstructive because there still was a gap of 13 mm between tape and symphysis pubis on Valsalva. The bladder neck descended by 17 mm on Valsalva, without significant rotation. No cystocele. Detrusor wall thickness was normal at 4.5 mm. The main finding was an enterocele reaching about 10 mm below the symphysis pubis. It seemed to develop posterior to the Apogee mesh and was starting to invaginate the rectum, causing an internal rectal prolapse.

3D: The pubovisceral muscle showed marked asymmetry. Whereas there was no evidence of an avulsion injury, the left pubovisceral muscle appeared deficient, especially in its more cranial aspects, resulting in marked asymmetrical ballooning to about 40 cm^2. The enterocele developed mainly on the left as a consequence.

Interpretation: Both Monarc and Apogee mesh are in their typical locations. There is no evidence of vaginal prolapse recurrence. As preoperatively, there is ballooning of the hiatus to 40 cm^2, and evidence of left-sided impairment of the pubovisceral muscle. The previously visible enterocele is still present and now seems to develop posterior to the mesh, into the anal canal, resulting in an incipient rectal prolapse. A colorectal assessment is recommended.

Case 12: Cystocele II, Rectocele II, Voiding Dysfunction

Dear Colleague,

Thanks for referring this 64-year-old woman who is presenting with symptoms of prolapse and recurrent urinary tract infections. There are no other symptoms of bladder or bowel dysfunction. She is mother of three children born by normal vaginal delivery and had a vaginal hysterectomy about 20 years ago.

2D and 3D pelvic floor ultrasound was performed using a GE Kretz Voluson 730 Expert system.

Findings:
2D: There was a postvoid residual of 90 mL. The urethra showed several hyperechogenic foci which are of uncertain significance. The bladder neck descended 37 mm on Valsalva, with 120° of urethral rotation, a retrovesical angle that remained at 130°, and no funneling. There was marked urethral kinking of 90°, with the proximal urethra closely tethered to the pubis. The cystocele reached to 20 mm; a rectocele to 15 mm below the symphysis. Its depth was measured at 13 mm only. Detrusor wall thickness was normal at 4 mm.

3D: There was a left-sided pubovisceral muscle avulsion injury of up to 17 mm in width at the level of the hiatus and extending cranially for at least 25 mm. The upper aspects of the left puborectalis muscle seemed to be almost completely absent, with the defect measuring up to 35 mm at this level. These was mild ballooning to 31 cm^2 on Valsalva.

Interpretation: Moderate cystocele with intact retrovesical angle and significant urethral kinking. Likely mild–moderate voiding dysfunction. Small rectocele. Marked left-sided pubovisceral muscle injury, mild ballooning. This woman seems to be at increased risk of prolapse recurrence in case surgery is undertaken. Prolapse correction may result in better voiding, but may also unmask potential occult stress incontinence.

Case 13: Bilateral Avulsions, Perigee Procedure

Dear Colleague,

Thanks for referring this 37-year-old woman who had a Perigee anterior vaginal wall repair about 3 months ago for anterior and central-compartment prolapse. She is currently completely asymptomatic and very happy with the outcome.

2D and 3D pelvic floor ultrasound was performed using a GE Kretz Voluson 730 Expert system.

Findings:

2D: There was no postvoid residual. The urethra was normal. The bladder neck was well elevated, with only 8 mm of bladder neck descent on Valsalva and a retrovesical angle of 140°. No cystocele. The Perigee was situated between urethra and cervix and in a typical, functional position. The uterus descended to about the symphysis pubis, and the posterior compartment was well elevated. Detrusor wall thickness was normal at 4 mm.

3D: There was a major bilateral avulsion injury to the pubovisceral muscle measuring 26 mm in width and extending over at least 2 cm in a craniocaudal direction. On Valsalva, the hiatus measured about 8 cm in the coronal plane which is unusually wide. The Perigee implant seemed to traverse these defects. There was moderate ballooning of the hiatus to 36 cm^2.

Interpretation: Well-supported anterior and posterior compartment after Perigee mesh which is in a typical position and traverses a major bilateral avulsion injury. Mild uterine descent. Moderate ballooning.

Case 14: Mixed Incontinence after Tensionless Vaginal Tape (TVT) and Burch Colposuspension

Dear Colleague,

Thanks for referring this 59-year-old woman who is presenting with symptoms of urgency and urge incontinence as well as recurrent stress incontinence. There are no other symptoms of bladder or bowel dysfunction. She is mother of two children born vaginally. In 1989 she had a total abdominal hysterectomy (TAH) and colposuspension, and you performed a TVT for recurrent stress incontinence a few years ago.

2D and 3D pelvic floor ultrasound was performed using a GE Kretz Voluson 730 Expert system.

Findings:

2D: There was a postvoid residual of about 20 mL. The urethra was normal, but the bladder neck was massively distorted because of the colposuspension. The bladder neck descended about 15 mm on Valsalva. There was no urethral rotation but marked funneling. There was a small high cystocele which remained 6 mm above the symphysis. The vault was well supported as was the posterior compartment. The TVT was in a typical midurethral position and did not seem to be particularly tight, with a minimum gap of 13 mm between tape and symphysis. Detrusor wall thickness was normal at 2.8 mm.

3D: The levator ani muscle and hiatus appeared normal. There was no ballooning and the hiatus measured about 20 cm^2 on Valsalva.

Interpretation: Previous Burch colposuspension still in evidence, small high cystocele. Midurethral TVT which is not unduly obstructive. Marked funneling indicative of a low-pressure urethra. Good central and posterior compartment support; normal levator muscle and hiatus.

Case 15: Urethral Diverticulum

Dear Colleague,

As you're aware, this 34-year-old woman has had symptoms of voiding difficulty and dyspareunia for several years. There are no symptoms of bladder or bowel dysfunction apart from the sensation of a lump in the vagina. This frequently is tender on intercourse. She has had no urinary tract infections (UTI) but was investigated by urologic colleagues, with two cystoscopies in 2002 and 2005 reported as normal.

2D and 3D pelvic floor ultrasound was performed using a GE Kretz Voluson 730 Expert system.

Findings:

2D: There was no postvoid residual. We saw 28 mm of bladder neck descent on Valsalva, with the retrovesical angle opening to 180°, 40° of urethral rotation, and minor funneling. No cystocele, no rectocele. There was a thick-walled (about 3 mm) multicystic complex structure measuring approximately $2 \times 3 \times 2$ cm surrounding the proximal urethra almost symmetrically in a horseshoe-shaped configuration. It was situated ventral to the proximal urethra and bladder neck. Detrusor wall thickness was normal at 2.5 mm.

3D: There was no major asymmetry of the pubovisceral muscle, although the upper aspects of the left puborectalis muscle seemed thin. On Valsalva, the hiatus reached 26 cm^2 which is normal.

Interpretation: Atypical urethral diverticulum ventral and lateral to the proximal urethra, measuring about 2 cm in maximal diameter. There seems to be a diverticular neck about 2.5 cm from the external meatus and 1.5 cm from the internal meatus at about 12 o'clock. Mild rotatory descent of the bladder neck with opening of the RVA and funneling. There is an increased likelihood of stress incontinence after removal of the diverticulum, which would best be approached through the space of Retzius. No prolapse; no major abnormality of the levator ani.

Index

On the DVD

Case Collection

Case 1: Static Volume at rest, normal anatomy
Case 2: Normal anatomy (2a), Pelvic Floor contraction (2b)
Case 3: Cystocele I, elevated detrusor wall thickness
Case 4: Cystocele I, funneling, stress incontinence
Case 5: Cystocele I, Uterine prolapse I, right sided levator avulsion
Case 6: Rectocele II
Case 7: Previous Burch Colposuspension, Rectoenterocele II, severe ballooning
Case 8: Cystocele III after Burch and Zacharin Procedure, voiding dysfunction
Case 9: Gartner cysts
Case 10: Cystocele II, Uterine prolapse II, bilateral avulsion
Case 11: Rectal prolapse after Monarc, Apogee procedures
Case 12: Cystocele II, Rectocele II, Voiding dysfunction
Case 13: Bilateral levator avulsions, Perigee procedure
Case 14: Incontinence after TVT and Burch Colposuspension
Case 15: Urethral diverticulum

Cases courtesy of Hans Peter Dietz, MD. Ph.D. e-mail: hpdietz@bigpond.com

Getting Started

If a previous version of 4D View is installed, please use the setup from this 4D View disk for uninstalling the previous version and installing this version. Data collected with a previous version can be preserved.

Before installing the software on the PC be sure to be logged in as the user who will use 4D View on the system. Be sure that the system is running in resolution 1024 × 768 or higher. Select "High Color" or "True Color" display mode to get best results. (True Color is recommended.)

4D View is distributed on DVD. Put this DVD into the DVD drive and execute the program 4DviewSetup.exe by double-clicking.

Safety Regulations

The software package 4D View has been developed for the use on a PC under the operating system Microsoft® Windows 2000®.

Installation Requirements

In order to install 4D View on a PC correctly, ensure that the requirements as listed below are met:

Component	Required
Processor:	Pentium™ 4 or higher recommended
RAM:	256 MB minimum, 512 MB recommended
Graphic Card:	2 MB minimum, 4 MB recommended
DVD Drive:	installed
Free disk space:	100 MB minimum (200 MB with DICOM server function)
Operating system:	Microsoft® Windows 2000®
USB connector:	installed

Optional Component	Used for
DVD-Writer:	Backup
Removable Disk:	Backup
Soundcard:	Voice annotation
Microphone:	Voice annotation

To use a network connection following components are needed:

Component	Required
Networking card:	installed
TCP/IP Protocol:	must be running